

# Master of Science in Advanced Mathematics and Mathematical Engineering

---

**Title: Existence of Invariant Tori in Skew-Product Systems:  
A Computer Assisted Approach**

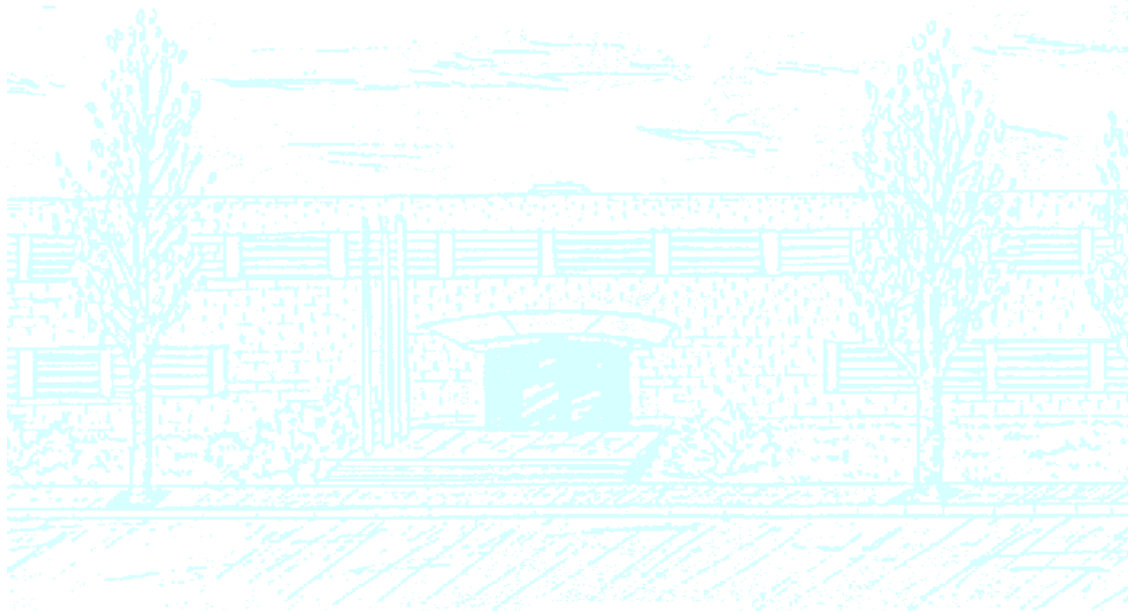
**Author: Eric Sandín Vidal**

**Advisor: Dr. Alex Haro Provinciale**

**Tutor: Dr. José Tomás Lázaro Ochoa**

**Department: Departament de Matemàtiques i Informàtica UB**

**Academic year: 2019-2020**





Master's Degree Thesis  
Facultat de Matemàtiques i Estadística

---

---

EXISTENCE OF INVARIANT TORI  
IN SKEW-PRODUCT SYSTEMS:  
A COMPUTER-ASSISTED  
APPROACH

---

---

Author: Eric Sandín Vidal

Supervisor: Dr. Alex Haro Provinciale

Tutor: Dr. Jose Tomás Lázaro Ochoa



UNIVERSITAT POLITÈCNICA  
DE CATALUNYA  
BARCELONATECH

MAMME

January 8, 2020



# Contents

<b>Abstract</b>	<b>iii</b>
<b>Acknowledgements</b>	<b>v</b>
<b>Introduction</b>	<b>vii</b>
<b>1 Quasi-Periodic Skew-Product Systems</b>	<b>1</b>
1.1 Introductory Definitions . . . . .	1
1.1.1 Bundles . . . . .	1
1.1.2 Skew-Product Dynamical Systems . . . . .	4
1.2 Quasi-Periodic Maps and Invariant Tori . . . . .	5
1.2.1 Spaces of Analytic Functions . . . . .	5
1.2.2 Quasi-Periodic Maps . . . . .	6
1.2.3 Reducibility and Hyperbolicity . . . . .	7
<b>2 The Validation Theorem</b>	<b>9</b>
2.1 Preparatory Results . . . . .	9
2.2 The Validation Theorem . . . . .	13
<b>3 Fourier Series</b>	<b>27</b>
3.1 The FT and the DFT . . . . .	27
3.2 Error Estimates on Approximations . . . . .	29
3.2.1 Analytic Periodic Functions . . . . .	29
3.2.2 Matrices of Periodic Functions . . . . .	33
3.3 The FFT . . . . .	34
<b>4 Computer Assisted Proof</b>	<b>37</b>
4.1 Computation of Error Bounds . . . . .	38
4.1.1 The Invariance Error Bound . . . . .	38
4.1.2 The Reducibility Error Bound . . . . .	40
4.1.3 The Invertibility Error Bound . . . . .	43
4.1.4 Norm of a Bilinear Form . . . . .	43
4.2 Intervalar Arithmetics . . . . .	44
4.2.1 Basic Operations . . . . .	45

4.3	Computer Validation . . . . .	46
4.3.1	Study Case: The Standard Map . . . . .	48
4.3.2	Results . . . . .	48
	<b>Appendix: Whiskers</b>	<b>55</b>
	<b>Conclusions</b>	<b>61</b>
	<b>Annex</b>	<b>63</b>
	<b>Bibliography</b>	<b>95</b>

# Abstract

The field of dynamical systems is very broad, and one shall find all sorts of objects and structures contained within its secrets. This is the case of quasi-periodically forced maps, maps in which a quasi-periodic rotation has been applied over the torus of a skew-product dynamical system. Such systems can be studied from several points of view, such as the study of the dynamics of its subbundles, the reducibility into simpler dynamics, or, as it is our interest, the validation of invariant tori given approximately invariant tori. The main theoretical result of this work is a validation theorem that ensures the existence of an invariant torus should certain conditions be fulfilled. But given this matter has already been addressed by several authors, we will follow the next step and validate the torus computationally using computer assisted proofs. For that we will require the aid of validated numerics and the use of the necessary computational tools built for said purpose, such as the MPFI package. Those tools can be so as multi-precision numerics and intervalar arithmetics. However, the validation will also require some theoretical tools for dealing with mathematical objects. Fourier transforms and Fourier series will become the pillar over which the validation algorithm is sustained. For that, a much needed chapter of Fourier analysis results will be provided to make of this project a self-contained work.



# Acknowledgements

It is such an honor to dive and learn from this fascinating topic and, of course, this work wouldn't have been possible without the inestimable help of a lot of people. First and foremost, I would like to thank my professors, Dr. José Tomás Lázaro for giving me the chance of writing a work in a more unconventional way, supporting me and revising all the work I sent to him, and Dr. Álex Haro for supervising my work and having the never ending patience to go through the theory and the coding process with me even at late hours in the night and making of this, even though at times painful, a great and fruitful experience. I would also like to thank my friend, pal, and colleague Sergio Gor for spending way too many hours helping me with software issues for the computer validation. And at last but not least, my family, for enduring the tough times that this work has brought and supporting me with all their love.



# Introduction

The study of dynamical systems has proved to be of great use when it comes to solving a certain kind of problems. They allow us to predict natural and artificial phenomenon, study the most hidden properties of intricate systems or just provide helpful tools for the development of other areas of science or engineering. The case we present in this work is no different.

In the pages ahead, we will focus our attention towards a special kind of dynamical systems, the so called skew-product dynamical systems. Skew-products are systems based on a torus and its fiber, allowing us to define our map of interest over such structure, which we will refer as fiber bundle. Moreover, our interest will lie on quasi-periodically forced skew-product systems, that is, systems in which the dynamics on the torus is quasi-periodic. Amongst all the things we could study from such systems, we will deal with the problem of the existence of invariant torus under our map, providing a good result that ensures the existence of an invariant torus under our map given an approximately invariant one that fulfills certain conditions. This result is what we call the validation theorem, since it validates an invariant torus. Besides proving the validation theorem, we will also implement it on a computer in the form of a computer assisted proof.

Computer assisted proofs have been on the rise in the last years, given that they are a very powerful tool for validating objects or simply proving theorems by computing great amounts of information. In our case, we implement a computer assisted proof that will calculate the error bounds and the constants that appear in our validation theorem and check the conditions that such result requires in order to yield a satisfactory response. To do so, we will also need other tools of a more theoretical nature, so we can quickly compute terms that could require more resources than we would like to. Such tools are Fourier series.

Fourier analysis is a very interesting field which basically deals with periodic functions. The famous Fourier Transform is a very powerful tool that allows the user to find the frequency values given only amplitude values of a signal. These Fourier coefficients make up Fourier series, which are trigonometric polynomials that are capable of rebuilding almost any function. These transforms will be of great use to us since they will allow the computer to perform quick calculations by simply moving our grid-evaluated objects onto Fourier space, where exponential operations can be easily done. With the necessary results to bound the error committed when moving from one space to another, we will be able to rigorously calculate

the error bounds and the constants needed to apply our theorem and therefore validate a torus.

In addition to this theory and implementation, we will provide in the Appendix an out-of-scope brief introduction to whiskers, which are invariant manifolds attached to a torus. There we will settle the bases for a future proof of existence and an algorithm for a validation of such manifolds using similar tools to the ones used for the validation theorem.

# Chapter 1

## Quasi-Periodic Skew-Product Systems

In this very first chapter, we are going to introduce the basic notions of what quasi-periodic systems are, as well as some other useful properties and definitions that will be used further ahead in the project. Beyond that, we will give a motivation on the expansion of the real domain into a complex domain in order to be able to deal with real-analytic functions, such as real-analytic torus, as the pinnacle of regularity properties. But before diving directly in, we will need some general notions about the structures that will determine our working spaces, such as bundles, fiber bundles and other concepts in order to fully understand the particular case that a skew-product system is.

### 1.1 Introductory Definitions

#### 1.1.1 Bundles

We present here very general definitions that can be found almost in any geometry or topology book. In our case, we will take [6] as reference.

**Definition 1.1.** *A bundle is a triple  $(E, \pi, B)$  where  $E$  is a set called the total space,  $B$  is a set called the base space of the bundle and  $\pi : E \rightarrow B$  is the projection map. In addition, for each  $b \in B$ ,  $\pi^{-1}(b)$  is the fiber of the bundle over  $b$  and a bundle  $(E^*, \pi^*, B^*)$  is a subbundle of  $(E, \pi, B)$  if  $B^* \subset B$ ,  $E^* \subset E$  and  $\pi^* = \pi|_{E^*}$ .*

This definition of a bundle is very general but also very useful to construct the needed definition of our future working space. Even though it is now defined for general sets, we will take soon such sets as topological spaces. More restrictive conditions on regularity or set structure will be further ahead given.

**Definition 1.2.** *Let  $(E_1, \pi_1, B)$  and  $(E_2, \pi_2, B)$  be bundles and  $f : B_1 \rightarrow B_2$  a map. Then a bundle map  $F : E_1 \rightarrow E_2$  covering  $f$  is a continuous map such that  $\pi_2 \circ F = f \circ \pi_1$ , that is*

$$\begin{array}{ccc} E_1 & \xrightarrow{F} & E_2 \\ \pi_1 \downarrow & & \downarrow \pi_2 \\ B_1 & \xrightarrow{f} & B_2 \end{array}$$

**Definition 1.3.** Let  $(E_1, \pi_1, B_1)$  and  $(E_2, \pi_2, B_2)$  be bundles and  $F : E_1 \rightarrow E_2$  be a bundle map covering  $f : B_1 \rightarrow B_2$ . If  $B_1 = B_2$  and  $f = id$ , then  $F$  is a bundle map over  $B = B_1 = B_2$  such that  $\pi_2 \circ F = \pi_1$ . That is, the following diagram should commute

$$\begin{array}{ccc} E_1 & \xrightarrow{F} & E_2 \\ \pi_1 \downarrow & \swarrow \pi_2 & \\ B & & \end{array}$$

Equivalently, for any point  $x \in B$ ,  $F$  maps the fiber  $E_{1_x} = \pi_1^{-1}(\{x\})$  of  $E_1$  over  $x$  to the fiber  $E_{2_x} = \pi_2^{-1}(\{x\})$  of  $E_2$  over  $x$ .

**Definition 1.4.** Let  $(E, \pi, B)$  be a bundle, then a section of that bundle is a continuous map  $\sigma : B \rightarrow E$  such that  $\pi(\sigma(x)) = x$  for all  $x \in B$ . That is,  $\pi \circ \sigma = id$  which means that the following diagram commutes

$$\begin{array}{ccc} E & \xrightarrow{\pi} & B \\ \sigma \uparrow & \nearrow id & \\ B & & \end{array}$$

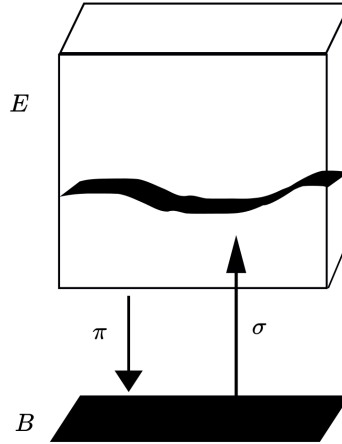


Figure 1.1: A section  $\sigma$  of a bundle  $\pi : E \rightarrow B$ . A section  $\sigma$  allows the base space  $B$  to be identified with a subspace  $\sigma(B)$  of  $E$  [12].

**Definition 1.5.** A fiber bundle is a structure  $(E, \pi, B, P)$ , where  $E$ ,  $B$  and  $P$  are topological spaces and  $\pi : E \rightarrow B$  is a continuous surjection. The space  $B$  is connected and is called the base space of the bundle,  $E$  the total space, and  $P$  the fiber. The map  $\pi$  is called the projection map (or bundle projection). Such structure must satisfy the following condition.

We require that for every  $x \in E$ , there is an open neighborhood  $U \subset B$  of  $\pi(x)$  (which will be called a trivializing neighborhood) such that there is a homeomorphism  $\varphi : \pi^{-1}(U) \rightarrow U \times P$  (where  $U \times P$  is the product space) in such a way that  $\pi$  agrees with the projection onto the

first factor. That is, the following diagram should commute

$$\begin{array}{ccc}
 \pi^{-1}(U) & \xrightarrow{\varphi} & U \times P \\
 \pi \downarrow & \swarrow \text{proj}_1 & \\
 U & & 
 \end{array}$$

where  $\text{proj}_1 : U \times P \rightarrow U$  is the natural projection and  $\varphi : \pi^{-1}(U) \rightarrow U \times P$  is a homeomorphism. The set of all  $\{(U_i, \varphi_i)\}$  is called a local trivialization of the bundle.

Thus for any  $y \in B$ , the preimage  $\pi^{-1}(\{y\})$  is homeomorphic to  $P$  (since  $\text{proj}_1^{-1}(\{y\})$  clearly is) and is called the fiber over  $y$ . Every (fiber bundle) projection  $\pi : E \rightarrow B$  is an open map (maps open subsets with open subsets), since projections of products are open maps. Therefore  $B$  carries the quotient topology determined by the map  $\pi$ .

For a better understanding of the fiber bundle concept, one shall see  $E$  locally like the product  $B \times P$ , except that the fibers  $\pi(x)^{-1}$  for  $x \in B$  may be a bit "twisted" [6]. Notice that a bundle is a generalization of a fiber bundle but with the sets lacking of a topology, which makes the condition of a local product structure drop.

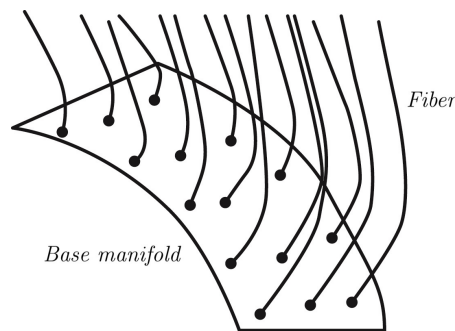


Figure 1.2: A fiber bundle [9].

**Remark 1.6.** Let  $E = B \times P$  and let  $\pi : E \rightarrow B$  be the projection onto the first factor. Then we will say that  $E$  is a fiber bundle (of  $P$ ) over  $B$ . Here  $E$  is not just locally a product but globally one. Any such fiber bundle is called a trivial bundle [6].

We will see in the following section that the space with which we will work is a trivial bundle over a torus, thus the importance of properly building up the definition of fiber bundle and more specifically, of trivial bundle.

**Definition 1.7.** A real vector bundle consists of a fiber bundle  $(E, \pi, B, P)$  with  $P = \mathbb{R}^k$ , where the compatibility condition is satisfied, that is,  $\forall p \in B$ , there is an open neighborhood  $U \subseteq B$ , and a homeomorphism  $\varphi : U \times \mathbb{R}^k \rightarrow \pi^{-1}(U)$ , such that  $\forall x \in U$ ;

1.  $(\pi \circ \varphi)(x, v) = x \quad \forall v \in \mathbb{R}^k$ .
2. The map  $v \mapsto \varphi(x, v)$  is a linear isomorphism between the vector spaces  $\mathbb{R}^k$  and  $\pi^{-1}(\{x\})$ .

**Remark 1.8.** The open neighborhood  $U$  together with the homeomorphism  $\varphi$  is called a local trivialization of the vector bundle. The local trivialization shows that, locally, the map  $\pi$  looks like the projection of  $U \times \mathbb{R}^k$  on  $U$  [10].

**Definition 1.9.** Let  $(E, \pi, B)$  be a bundle, given a bundle map  $F : E \rightarrow E$  covering  $f : B \rightarrow B$ , an  $F$ -invariant section is a section that satisfies that  $F \circ \sigma = \sigma \circ f$ , which means the following diagram commutes

$$\begin{array}{ccc} E & \xrightarrow{F} & E \\ \sigma \uparrow & & \uparrow \sigma \\ B & \xrightarrow{f} & B \end{array}$$

This last definition is very important since the main objects we will be working with are invariant sections of the map  $F$ , which will be presented in the following section.

### 1.1.2 Skew-Product Dynamical Systems

In this work we will deal with a particular type of fiber bundles, the aforementioned trivial bundles. Specifically, we will work with  $\mathbb{R}^n \times \mathbb{T}^d$  as a trivial bundle over  $\mathbb{T}^d$  with  $\pi : \mathbb{R}^n \times \mathbb{T}^d \rightarrow \mathbb{T}^d$  as the corresponding bundle projection. We consider in  $\mathbb{R}^n \times \mathbb{T}^d$  the product topology, so that the bundle projection is continuous. With our space defined, we can proceed to determine the norms we are going to use on them as well as the basic map over which the whole work will revolve around.

**Definition 1.10.** Let  $\mathbb{R}^n \times \mathbb{T}^d$  be a trivial fiber bundle with projection  $\pi : \mathbb{R}^n \times \mathbb{T}^d \rightarrow \mathbb{T}^d$ . A Finsler norm in the bundle is a continuous map

$$\begin{aligned} |\cdot| : \mathbb{R}^n \times \mathbb{T}^d &\longrightarrow \mathbb{R}_+ \\ (x, \theta) &\longrightarrow |(x, \theta)| = |x|_\theta \end{aligned}$$

such that, for each  $\theta \in \mathbb{T}^d$ ,  $|\cdot|_\theta : \mathbb{R}^n \rightarrow \mathbb{R}_+$  is a norm.

In simpler terms, a Finsler norm in  $\mathbb{R}^n \times \mathbb{T}^d$  is a norm  $|\cdot|_\theta$  on each fiber  $\mathbb{R}^n \times \{\theta\}$  that depends continuously on  $\theta$ . Examples of Finsler norms are the constant Finsler norm  $|\cdot|$ , independent of  $\theta$ , or given a norm  $|\cdot|$  on  $\mathbb{R}^n$ , and a continuous matrix map  $P : \mathbb{T}^d \rightarrow GL(\mathbb{R}^n)$ , the Finsler norm  $|x|_\theta = |P(\theta)x|$ . We will usually omit the explicit dependence on  $\theta$  of  $|\cdot|_\theta$  when it is clear from the context.

Once we have the space and the norm, it is time to introduce the map that will define our dynamical system. These are called *Skew-product Dynamical Systems*.

**Definition 1.11. (Skew-product Dynamical System)** Let  $f : \mathbb{T}^d \rightarrow \mathbb{T}^d$  be a homeomorphism. A skew-product dynamical system in  $\mathbb{R}^n$  over  $f$  is a bundle map

$$\begin{aligned} \hat{F} = (F, f) : \mathbb{R}^n \times \mathbb{T}^d &\longrightarrow \mathbb{R}^n \times \mathbb{T}^d \\ (x, \theta) &\longrightarrow (F(x, \theta), f(\theta)) \end{aligned}$$

where for each fixed  $\theta$ ,  $F(\cdot, \theta)$  is a diffeomorphism of  $\mathbb{R}^n$ .

From now on, we will refer to a continuous torus as a continuous section on the bundle  $\mathbb{R}^n \times \mathbb{T}^d$ , that is, a continuous map of the form  $(K, id) : \mathbb{T}^d \rightarrow \mathbb{R}^n \times \mathbb{T}^d$ , where  $K : \mathbb{T}^d \rightarrow \mathbb{R}^n$  is continuous [4]. Analogously, we will refer to an analytic torus when the map  $K : \mathbb{T}^d \rightarrow \mathbb{R}^n$  is real-analytic. The main goal of this work will be finding invariant tori, that is, invariant sections  $\sigma = (K, id)$  such that  $F \circ \sigma = \sigma \circ f$ , which translates to  $F(K(\theta), \theta) = K(f(\theta))$ . From now on, we will omit the identity map of the section  $(K, id)$  when we refer to a torus, so we can directly say that a torus is a map  $K : \mathbb{T}^d \rightarrow \mathbb{R}^n$ .

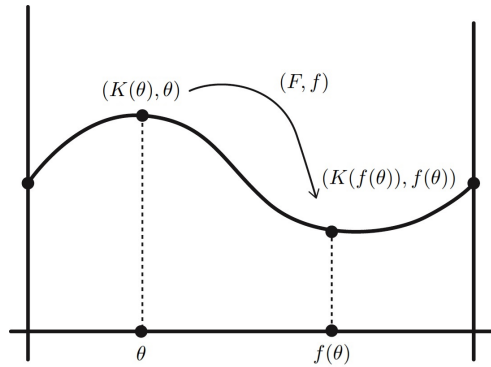


Figure 1.3: A continuous torus.

Moreover, we will work with a particular case of skew-products systems, quasi-periodic systems. Such systems are skew-product systems over rotations and will be properly defined in the following section. For now, in our particular case, we will denote our rotation  $f(\theta) = R_\omega(\theta) = \theta + \omega$ , with  $\omega \in \mathbb{R}^d$ , turning the previous invariance equation into  $F(K(\theta), \theta) = K(\theta + \omega)$ .

## 1.2 Quasi-Periodic Maps and Invariant Tori

Clearly, before going deep into the study of our system, it is necessary that we define the proper spaces and their respective norms we will be dealing with when it comes to real-analytic functions.

### 1.2.1 Spaces of Analytic Functions

As said, our goal is to easily manipulate real-analytic functions, or, in our case, tori. For that, we will have to put in our toolbox some basic concepts on spaces of analytic functions, such as their domain or a tailored norm that allows us to properly measure their images.

Let  $\mathbb{T}^d = (\mathbb{R}/\mathbb{T})^d$  be the real torus, and  $\mathbb{T}_{\mathbb{C}}^d = \mathbb{T}^d + i\mathbb{R}^d$  be the complex torus. We denote a complex strip (in  $\mathbb{T}_{\mathbb{C}}^d$ ) of width  $\rho > 0$  by

$$\mathbb{T}_{\rho}^d = \{\theta \in \mathbb{T}_{\mathbb{C}}^d : \text{Im } |\theta_i| < \rho, i = 1, \dots, d\}.$$

Thus, we denote by  $C^0(\bar{\mathbb{T}}_\rho^d, \mathbb{C}^m)$  the Banach space of continuous functions  $f : \bar{\mathbb{T}}_\rho^d \rightarrow \mathbb{C}^m$  such that  $f(\mathbb{T}^d) \subset \mathbb{R}^n$ , endowed with the norm

$$\|f\|_\rho = \sup_{\theta \in \mathbb{T}_\rho^d} |f(\theta)|,$$

where  $|\cdot|$  is the supremum norm in  $\mathbb{C}^m$ . We denote by  $C^a(\bar{\mathbb{T}}_\rho^d, \mathbb{C}^m)$  the Banach space of continuous functions  $f : \bar{\mathbb{T}}_\rho^d \rightarrow \mathbb{C}^m$ , holomorphic on  $\mathbb{T}_\rho^d$  and such that  $f(\mathbb{T}^d) \subset \mathbb{R}^n$ , that is,  $f$  is real-analytic (just analytic from now on), endowed with the supremum norm.

Consider the phase space an annulus  $\mathcal{A}$  in  $\mathbb{R}^n \times \mathbb{T}^d$ , that is, an open set  $\mathcal{A} \subset \mathbb{R}^n \times \mathbb{T}^d = \{z = (x, \theta) : x \in \mathbb{R}^n, \theta \in \mathbb{T}^d\}$  homotopic to  $\mathcal{V} \times \mathbb{T}^d$ , where  $\mathcal{V} \subset \mathbb{R}^n$  is open. Let  $\mathcal{B} \subset \mathbb{C}^n \times \mathbb{T}_\rho^d$  be a complex neighborhood of the annulus  $\mathcal{A}$ .

We denote by  $C^a(\bar{\mathcal{B}}, \mathbb{C}^m)$  the Banach space of continuous functions  $f : \bar{\mathcal{B}} \rightarrow \mathbb{C}^m$ , holomorphic on  $\mathcal{B}$  and such that  $f(\mathcal{A}) \subset \mathbb{R}^m$  (so  $f$  is analytic), endowed with the norm [1]

$$\|f\|_{\mathcal{B}} = \sup_{z \in \bar{\mathcal{B}}} |f(z)|.$$

### 1.2.2 Quasi-Periodic Maps

With the motivation of working with analytic functions, we can now extend the space of our skew-product system to the complex field, at the same time that we stretch our torus into a complex band of width  $\rho$ . Thus, we can finally provide the space in which this work will be focused, and that is  $\mathbb{C}^n \times \mathbb{T}_\rho^d$ .

Once we know this, we can turn our attention towards systems in which the dynamics on the torus is quasi-periodic, defined by the aforementioned irrational rotation  $R_\omega(\theta) = \theta + \omega$ , with  $\omega \in \mathbb{R}^d$ . This means that we will be working with quasi-periodic skew-products  $\hat{F} : \mathbb{C}^n \times \mathbb{T}_\rho^d \rightarrow \mathbb{C}^n \times \mathbb{T}_\rho^d$  of the form:

$$\begin{pmatrix} x \\ \theta \end{pmatrix} \xrightarrow{\hat{F}} \begin{pmatrix} F(x, \theta) \\ \theta + \omega \end{pmatrix}. \quad (1.1)$$

Also, we will study invariant tori by looking for parameterizations in which the motion is given by the rotation stated previously. That is, we seek those maps  $K : \mathbb{T}_\rho^d \rightarrow \mathbb{C}^n$  in such a way that

$$F(K(\theta), \theta) = K(\theta + \omega). \quad (1.2)$$

If we consider the graph of  $K$

$$\mathcal{K} = \{(K(\theta), \theta) \mid \theta \in \mathbb{T}_\rho^d\},$$

we observe that (1.2) is equivalent to saying that  $\mathcal{K}$  is invariant under the skew-product (1.1). It will be convenient to think of (1.2) as an equation for the zeroes of the operator  $\mathcal{F}$  defined

by:

$$\mathcal{F}[K](\theta) = F(K(\theta - \omega), \theta - \omega) - K(\theta). \quad (1.3)$$

We note that if  $F$  is  $C^{r+l}$ , then,  $\mathcal{F}$  is an  $l$  times differentiable operator from  $C^r$  to  $C^r$ . Hence the application of Newton method in function spaces is justified if  $F$  is differentiable enough. We also note that it is clear (and it can be justified under regularity assumptions on  $F$ ) that the differential of the operator  $\mathcal{F}$  in a torus  $K$  evaluated on a section  $\xi : \bar{\mathbb{T}}_\rho^d \rightarrow \mathbb{C}^n$  of the bundle  $\mathbb{C}^n \times \mathbb{T}_\rho^d$  is given by

$$D\mathcal{F}[K]\xi(\theta) = D_x F(K(\theta - \omega), \theta - \omega)\xi(\theta - \omega) - \xi(\theta). \quad (1.4)$$

The first term of  $D\mathcal{F}$  is called the transfer operator and we will denote it by  $\mathcal{M}_\omega$ . Recall that given a torus by  $K : \mathbb{T}_\rho^d \rightarrow \mathbb{C}^n$ , the matrix  $M(\theta) = D_x F(K(\theta), \theta)$  defines a linear skew product (or cocycle) by

$$\begin{pmatrix} v \\ \theta \end{pmatrix} \xrightarrow{\hat{M}} \begin{pmatrix} M(\theta)v \\ \theta + \omega \end{pmatrix}, \quad (1.5)$$

where (in an abuse of notation)  $M(\theta) : E_\theta \rightarrow E_{\theta+\omega}$  takes a  $v$  in the fiber at position  $\theta$  and takes it to the fiber in position  $\theta + \omega$ .

Now we can explicit the norm of the operator  $\mathcal{M}_\omega$  when acting on analytic sections

$$\begin{aligned} \|\mathcal{M}_\omega\|_\rho &= \sup_{\|v\|_\rho=1} \|\mathcal{M}_\omega v\|_\rho = \sup_{\|v\|_\rho=1} \sup_{\theta \in \bar{\mathbb{T}}_\rho^d} |\mathcal{M}(\theta)v(\theta)|_{\theta+\omega} \leq \sup_{\|v\|_\rho=1} \sup_{\theta \in \bar{\mathbb{T}}_\rho^d} |M(\theta)|_\theta \cdot |v(\theta)|_\theta \\ &\leq \sup_{\theta \in \bar{\mathbb{T}}_\rho^d} |M(\theta)|_\theta = \sup_{\theta \in \bar{\mathbb{T}}_\rho^d} \sup_{v \in \mathbb{C}^n, |v|_\theta=1} |M(\theta)v|_{\theta+\omega} = \|M\|_\rho, \end{aligned}$$

where  $|\cdot|_\theta$  is a given Finsler norm. The operator  $\mathcal{M}_\omega$  is clearly related to the derivative of the operator  $\mathcal{F}$  since  $D\mathcal{F}[K] = \mathcal{M}_\omega - Id$ . When using a Newton method to find a zero for  $\mathcal{F}$ , it is quite important to know whether 0 is in the spectrum of  $D\mathcal{F}$  or equivalently, whether 1 is in the spectrum of  $\mathcal{M}_\omega$  [5].

### 1.2.3 Reducibility and Hyperbolicity

Going back to linear dynamics, it is worth explaining the concept of reducibility, a concept that may come handy when dealing with cocycles to manipulate them in a simpler way.

If the torus is invariant, the cocycle represents the linearization of the dynamics around the torus. If we think of  $v$  as an infinitesimal perturbation of the initial condition,  $M(\theta)v$  describes how the disturbance propagates [5].

We will seek matrix maps  $P : \mathbb{T}^d \rightarrow M_{n \times n}$ , and  $\Lambda : \mathbb{T}^d \rightarrow M_{n \times n}$  such that

$$P(\theta + \omega)^{-1}M(\theta)P(\theta) - \Lambda(\theta) = 0, \quad (1.6)$$

where  $P$  is an adapted frame for the torus and  $\Lambda$  represents the linearized dynamics. The idea of this transformation on  $M$  is to express the linearized dynamics in a simple way, that is as a triangular, constant or block-diagonal matrix. An important case, and the one we are treating here, is the case where  $P$  parametrizes two complementary invariant subbundles  $E_1, E_2$  with rank  $n_1, n_2$  respectively and  $\Lambda$  is a block-diagonal matrix.

In this work we will assume that our objects are fiberwise hyperbolic, this means that the linear dynamics can be decomposed into stable and unstable subbundles. In such context we can say that the matrix  $P$  parametrizes a stable subbundle (now  $E_s$ , of rank  $n_s$ ) in its first  $n_s$  columns and an unstable subbundle (now  $E_u$ , of rank  $n_u$ ) in its last  $n_u$  columns. Therefore our matrix  $\Lambda$  will look like the following

$$\Lambda(\theta) = \begin{pmatrix} \Lambda^s(\theta) & 0 \\ 0 & \Lambda^u(\theta) \end{pmatrix}$$

where  $\Lambda^s(\theta) \in M_{n_s \times n_s}$  represents the linearized stable dynamics, which are assumed to be uniformly contracting, and  $\Lambda^u(\theta) \in M_{n_u \times n_u}$  represents the linearized unstable dynamics, which are assumed to be uniformly expanding. This means that  $|\Lambda^s(\theta)| < 1$  and  $|(\Lambda^u(\theta))^{-1}| < 1$  for a given Finsler norm  $|\cdot|_\theta$ .

**Remark 1.12.** When there exists a matrix  $\Lambda$  such that equation (1.6) is satisfied, we say that the system is hyperbolically reducible. Notice that not all bundles admit global frames, which is why we consider here the case where our bundles are trivial or easily trivializable. In that case it is safe to assume that there exist global frames.

**Remark 1.13.** If our  $\Lambda^s(\theta)$  is constant, we say that the system is reducible. We will see an example of this in the chapters ahead when we discuss rank-1 whiskers, where we will take  $n_s = 1$ .

## Chapter 2

# The Validation Theorem

In this chapter we will look at the main result of the work, and that is the validation theorem. Such theorem ensures the existence of an analytic invariant torus under an analytic quasi-periodic skew-product system given an approximately invariant analytic torus. Moreover, the theorem also states that such torus will be hyperbolic and gives a bound for the distance between the approximately invariant fibers of the initial torus and the actually invariant fibers of the newly found invariant torus.

As usual, we will require some introductory results before proving the theorem.

### 2.1 Preparatory Results

As we will have to deal with operators in the space of analytic functions, it will be useful to have some properties on the manipulation of such operators, and a very powerful tool is Neumann series. In addition, we will also need to understand the concept of resolvent.

**Definition 2.1.** *Let  $X$  be a Banach space and let  $T : X \rightarrow X$  be a bounded linear operator. Let  $Id$  be the identity operator on  $X$ . In this context, the resolvent set (or just resolvent) of the operator  $T$  over the space  $X$  is defined as*

$$\text{Res}(T, X) = \{z \in \mathbb{C} \mid T - zId \text{ is bijective} \},$$

*moreover, the spectrum is the complement of the resolvent set:*

$$\text{Spec}(T, X) = \mathbb{C} \setminus \text{Res}(T, X).$$

**Theorem 2.2. (Banach Open Mapping Theorem)** *If  $X$  and  $Y$  are Banach spaces and  $T : X \rightarrow Y$  is a surjective continuous linear operator, then  $T$  is an open map. If moreover,  $T : X \rightarrow Y$  is bijective, then  $T^{-1} : Y \rightarrow X$ .*

**Remark 2.3.** Banach's Open Mapping Theorem implies that the operator  $(T - zId)^{-1}$  is also bounded if  $z \in \text{Res}(T, X)$ .

With this, we can say that  $z \in \text{Res}(T, X) \iff \forall \eta \in X, \exists! \xi \in X$  such that  $T\xi - z\xi = \eta$ . In this context we will say that the operator  $T$  is hyperbolic if the unit circle is in the resolvent of  $T$ , that is  $\text{Spec}(T, X) \cap S_1 = \emptyset$ , where  $S_1 = \{z \in \mathbb{C} \mid |z| = 1\}$ .

Let's proceed now with some Neumann series results.

**Definition 2.4.** *A Neumann series is a series of the form*

$$\sum_{k=0}^{\infty} T^k,$$

where  $T$  is an operator and  $T^k = T^{k-1} \circ T$  is the  $k$  times repeated application, with  $T^0 = Id$ , being  $Id$  the identity operator.

**Proposition 2.5.** *Let  $T$  be a bounded linear operator over  $X$ . If the Neumann series converges in the operator norm, then  $Id - T$  is invertible and*

$$(Id - T)^{-1} = \sum_{k=0}^{\infty} T^k.$$

*Proof.* Working with partial sums we obtain

$$\begin{aligned} (Id - T) \lim_{n \rightarrow \infty} \sum_{k=0}^n T^k &= \lim_{n \rightarrow \infty} (Id - T) \sum_{k=0}^n T^k = \lim_{n \rightarrow \infty} \left( \sum_{k=0}^n T^k - \sum_{k=0}^n T^{k+1} \right) \\ &= \lim_{n \rightarrow \infty} (Id - T^{n+1}) = Id. \end{aligned}$$

where the result is given because of the series' convergence [13]. □

**Lemma 2.6.** *Let  $P, T$  be bounded linear operators over a space  $X$  such that  $Id - PT = E$ , where  $\|E\| < \tau < 1$  for a small  $\tau$  and any given norm  $\|\cdot\|$ . Then  $P$  is invertible.*

*Proof.* Manipulating the matrices as their associated operators we have

$$Id - PT = E \iff Id - E = PT.$$

Since  $\|E\| < 1$ , its Neumann series converges, and by Proposition 2.5 (which from now on will be called the Neumann series argument), we have that  $(Id - E)$  is invertible, which means that  $PT$  is also invertible, resulting in  $P^{-1} = T(Id - E)^{-1}$ . □

In addition, we can see that  $\|P^{-1} - T\| \leq \|T\| \frac{\tau}{1-\tau}$ :

$$\begin{aligned} \|P^{-1} - T\| &= \|T(Id - E)^{-1} - T\| \leq \|T\| \cdot \|(Id - E)^{-1} - Id\| \\ &= \|T\| \cdot \|(Id - E)^{-1}[Id - (Id - E)]\| \leq \|T\| \cdot \|(Id - E)^{-1}\| \cdot \|E\| \\ &\leq \|T\| \cdot \sum_{k=0}^{\infty} \|E\|^k \cdot \|E\| \leq \|T\| \frac{\tau}{1-\tau}. \end{aligned}$$

It will also be useful to give a couple of fixed point theorems to properly understand the path we will be taking in order to prove the validation theorem.

**Definition 2.7.** *Let  $(X, d)$  be a complete metric space. Then a map  $T : X \rightarrow X$  is called a contraction mapping (or a map that satisfies the contraction principle) on  $X$  if there exists  $L \in [0, 1)$  such that*

$$d(T(x), T(y)) \leq L d(x, y) \quad \forall x, y \in X.$$

**Theorem 2.8. (Banach Fixed Point Theorem)** *Let  $(X, d)$  be a complete metric space and  $f : X \rightarrow X$  a contractive map with contraction factor  $L \in [0, 1)$ , then exists a unique  $x_* \in X$  such that  $f(x_*) = x_*$ .*

*Proof.* Start by taking a  $x_0 \in X$ , and then defining the sequence  $(x_n)_n$  as  $x_n = f^n(x_0)$ . Since our metric space is complete, it suffices to prove that our sequence is a Cauchy one.  $\forall n$  and  $\forall p \geq 0$

$$\begin{aligned} d(x_{n+p}, x_n) &\leq d(x_{n+p}, x_{n+p-1}) + \dots + d(x_{n+1}, x_n) \\ &\leq (L^{n+p-1} + L^{n+p-2} + \dots + L^n)d(x_1, x_0) \\ &\leq L^n(1 + L + \dots + L^{p-1})d(x_1, x_0) \leq \frac{L^n}{1-L}d(x_1, x_0). \end{aligned}$$

Where, in the third step, we have applied that

$$d(x_{m+1}, x_m) \leq L d(x_m, x_{m-1}) \leq \dots \leq L^m d(x_1, x_0)$$

using the contractive property and a geometric sum in the last step. From the inequality we obtain  $\lim_{n \rightarrow \infty} \sup_{p \geq 0} d(x_{n+p}, x_n) = 0$ , since  $\sup_{p \geq 0} d(x_{n+p}, x_n) \leq \frac{L^n}{1-L}d(x_1, x_0)$ , hence it is a Cauchy sequence and therefore  $(x_n)_n$  converges to a certain  $x_*$ . Thus  $x_{n+1} = f(x_n) \xrightarrow{n \rightarrow \infty} x_* = f(x_*)$  and  $x_*$  is a fixed point of  $f$ .

The uniqueness is easily proved by assuming there are two different fixed points,  $x_*$ ,  $y_*$ , and therefore

$$0 < d(x_*, y_*) = d(f(x_*), f(y_*)) \leq L d(x_*, y_*) \rightarrow d(x_*, y_*) \leq L d(x_*, y_*)$$

which is a contradiction since  $L \in [0, 1)$ . □

Notice that, in addition,  $d(x_*, x_0) \leq \frac{d(x_1, x_0)}{1-L}$ .

**Theorem 2.9. (Radial Fixed Point Theorem)** *Let  $(X, d)$  be a complete metric space and let  $x_0 \in X$ . Let now  $T : B_R(x_0) \subset X \rightarrow X$  be a map in the open set  $B_R(x_0)$  such that  $\forall r \in (0, R)$ ,  $T|_{\bar{B}_r(x_0)}$  is Lipschitz, where  $\bar{B}_r(x_0) = \{x \in X : d(x, x_0) \leq r\}$  and*

$$L : (0, R) \longrightarrow \mathbb{R}_+$$

$$r \longmapsto L(r) = \sup_{\substack{x_1, x_2 \in \bar{B}_r(x_0) \\ x_1 \neq x_2}} \frac{d(T(x_2), T(x_1))}{d(x_2, x_1)}.$$

*Notice that  $L$  is an increasing function.*

*Assume that  $d(T(x_0), x_0) \leq \varepsilon$ , where  $\varepsilon > 0$  is the error bound of the fixed point condition, and take  $r \in (\varepsilon, R)$ . Then if  $\frac{\varepsilon}{r} + L(r) - 1 \leq 0$ , there exists a unique  $x_* \in \bar{B}_r(x_0)$  such that  $T(x_*) = x_*$ .*

*Proof.* Since  $X$  is a Banach space, and therefore a complete space, Theorem 2.8 allows us to reduce the proof to the following two steps:

1.  $T(\bar{B}_r(x_0)) \subseteq \bar{B}_r(x_0)$ , so the image of the ball won't escape the ball itself.
2.  $T|_{\bar{B}_r(x_0)}$  is contractive.

For the first step we pick  $x \in \bar{B}_r(x_0)$  and we see

$$\begin{aligned} d(T(x), x_0) &\leq d(T(x), T(x_0)) + d(T(x_0), x_0) \leq L(r)d(x, x_0) + \varepsilon \\ &\leq L(r)r + \varepsilon = r \left( L(r) + \frac{\varepsilon}{r} \right) \leq r \end{aligned}$$

which means that  $T(x)$  is in  $\bar{B}_r(x_0)$ .

Since our function  $T$  is already Lipschitz, we only need to see if the Lipschitz constant  $L(r)$  dwells in the  $(0, 1)$  interval. By hypothesis,  $\frac{\varepsilon}{r} + L(r) - 1 \leq 0$  which leads to  $L(r) \leq 1 - \frac{\varepsilon}{r} < 1$ . □

**Remark 2.10.** Notice that the estimation that  $x_* \in \bar{B}_r(x_0)$  cannot be further refined, given that using the formula obtained before and the inequality hypothesis of the theorem,  $d(x_*, x_0) \leq \frac{d(x_1, x_0)}{1-L(r)} \leq \frac{\varepsilon}{r(1-L(r))} = r$ . Keep in mind that the best estimation is taken for the smallest  $r$  that satisfies the conditions.

## 2.2 The Validation Theorem

Once we have all the needed definitions and results, it is time to state and prove the most important result of the work, the theorem that proves the existence of a hyperbolic invariant torus given an approximately invariant torus under quasi-periodic dynamics.

**Theorem 2.11.** *Let  $\mathcal{U} \subset \mathbb{C}^n \times \mathbb{T}_{\mathbb{C}}^d$  be an open set and  $F : \mathcal{U} \subset \mathbb{C}^n \times \mathbb{T}_{\mathbb{C}}^d \rightarrow \mathbb{C}^n$  be an analytic map (of class  $C^a$ ) with respect to the  $x$  variables, defining a skew-product over the irrational rotation  $\omega \in \mathbb{R}^d$ . Assume that given a  $\rho > 0$  we have an analytic torus  $K_0 : \bar{\mathbb{T}}_{\rho}^d \rightarrow \mathbb{C}^n$  (that is, continuous in  $\bar{\mathbb{T}}_{\rho}^d$  and analytic in  $\mathbb{T}_{\rho}^d$ ) satisfying  $\mathcal{K}_0 = \text{graph}(K_0) = \{(K_0(\theta), \theta) \mid \theta \in \mathbb{T}_{\rho}^d\} \subset \mathcal{U}$  and also that there exist:*

- 1) *Two analytic matrix-valued maps  $P_1, P_2 : \bar{\mathbb{T}}_{\rho}^d \rightarrow M_n(\mathbb{C})$ , where  $P_1$  represents a vector bundle map (over the identity) giving the change of variables to an adapted frame, and  $P_2$  is its approximate inverse (see condition 5.3);*
- 2) *An analytic block-diagonal matrix-valued map*

$$\Lambda_0(\theta) = \begin{pmatrix} \Lambda_0^s(\theta) & 0 \\ 0 & \Lambda_0^u(\theta) \end{pmatrix}$$

*where  $\Lambda_0^s : \bar{\mathbb{T}}_{\rho}^d \rightarrow M_{n_s}(\mathbb{C})$  and  $\Lambda_0^u : \bar{\mathbb{T}}_{\rho}^d \rightarrow M_{n_u}(\mathbb{C})$ , with  $n = n_s + n_u$ ;*

- 3) *An (adapted) Finsler metric  $|\cdot|_{\theta}$ , of the form  $|\hat{v}|_{\theta} = |\hat{v}^s|_{\theta} + |\hat{v}^u|_{\theta}$  for  $\hat{v} = (\hat{v}^s, 0) + (0, \hat{v}^u) \in \mathbb{C}^n = \mathbb{C}^{n_s} \times \mathbb{C}^{n_u}$ , and the induced norm on analytic sections and vector bundle maps is denoted by  $\|\cdot\|_{\rho}$ ;*
- 4) *Positive constants  $\varepsilon, \sigma, \tau, \lambda, R, r, b$  with  $\lambda + \sigma + \tau < 1$ ;*

*such that*

- 5.1)  *$E(\theta) = P_2(\theta)(F(K_0(\theta - \omega), \theta - \omega) - K_0(\theta))$  satisfies  $\|E\|_{\rho} \leq \varepsilon$  (as a section);*
- 5.2)  *$E_{red}(\theta) = P_2(\theta + \omega)D_x F(K_0(\theta), \theta)P_1(\theta) - \Lambda_0(\theta)$  satisfies  $\|E_{red}\|_{\rho} \leq \sigma$  (as a vector bundle map over the rotation  $\omega$ );*
- 5.3)  *$E_{inv}(\theta) = P_2(\theta)P_1(\theta) - Id$  satisfies  $\|E_{inv}\|_{\rho} \leq \tau$  (as a vector bundle map over the identity);*
- 5.4)  *$\Lambda_0^s(\theta)$  and  $\Lambda_0^u(\theta)$  satisfy  $\|\Lambda_0^s\|_{\rho} \leq \lambda$  and  $\|(\Lambda_0^u)^{-1}\|_{\rho} \leq \lambda$  (as vector bundle maps over the rotation  $\omega$  in  $\mathbb{C}^{n_s} \times \mathbb{T}^d$  and  $\mathbb{C}^{n_u} \times \mathbb{T}^d$ , respectively);*
- 5.5) *For all points  $(x, \theta)$  in the strip*

$$\bar{D}_{\rho}(K_0, R) = \{(x, \theta) \in \mathbb{C}^n \times \bar{\mathbb{T}}_{\rho}^d \mid x = K_0(\theta) + P_1(\theta)\xi, \xi \in \mathbb{C}^n, |\xi|_{\theta} \leq R\} \subset \mathcal{U},$$

*the bilinear maps over the rotation  $\omega$*

$$B(x, \theta) = P_2(\theta + \omega) D_x^2 F(x, \theta) [P_1(\theta) \cdot, P_1(\theta) \cdot]$$

satisfy  $\|B(x, \theta)\| \leq b$  as a norm of a bilinear form.

The norm of such a bilinear form can be defined as

$$\|B(x, \theta)\| = \sup_{(x, \theta) \in \bar{D}(K_0, \bar{r})} \sup_{|\xi_1|, |\xi_2| \neq 1} |P_2(\theta + \omega) D_x^2 F(x, \theta) [P_1(\theta) \xi_1, P_1(\theta) \xi_2]|_{\theta + \omega}.$$

We now define the constants

$$\hat{\varepsilon} = \frac{\varepsilon}{1 - (\lambda + \sigma + \tau)}, \quad \beta = \frac{b}{1 - (\lambda + \sigma + \tau)}, \quad h = \beta \hat{\varepsilon}.$$

Assume

$$6) \quad h < \frac{1}{2};$$

$$7) \quad r_0 = \frac{1 - \sqrt{1 - 2h}}{h} \cdot \hat{\varepsilon} \leq r \leq \min\{r_1, R\}, \quad \text{where } r_1 = \frac{1 + \sqrt{1 - 2h}}{h} \cdot \hat{\varepsilon}.$$

Under the hypotheses 1-7:

- a)  $P_1(\theta)$  is invertible and there exists an analytic invariant torus  $K_* : \mathbb{T}_\rho^d \rightarrow \mathbb{C}^n$  to which the Newton method converges from the initial approximation  $K_0$  and

$$\|P_1(\theta)^{-1}(K_*(\theta) - K_0(\theta))\|_\rho \leq r_0 < 2\hat{\varepsilon}.$$

But also

$$\|P_1(\theta)^{-1}(K_*(\theta) - K_0(\theta))\|_\rho \leq \min\{r_1, R\}.$$

This means that  $K_*$  is unique within a radius  $r_1$  and that, more precisely, it is contained within a radius  $r_0$ .

- b) The torus  $K_*$  is normally hyperbolic, that is, the transfer operator  $\mathcal{M}_\omega$  is hyperbolic.

Let  $\hat{\lambda} = \|\Lambda_0\|_\rho$ . Define the constant

$$\mu = \frac{\lambda}{1 - \lambda^2} \frac{1}{1 - \tau} (br_0 + \sigma + \hat{\lambda}\tau)$$

and suppose that, moreover, it suffices;

$$8) \quad \mu < \frac{1}{2 + 2\sqrt{2}}.$$

Then:

- c) The stable and unstable bundles differ from the initial approximate invariant bundles in a distance smaller than  $\frac{2\mu}{(1-2\mu) + \sqrt{-4\mu^2 - 4\mu + 1}}$ , and can be computed using the contraction principle.

**Remark 2.12.** We can actually dispose of the analytic regularity of the torus, since the Bootstrap Theorem ensures the torus to be at least as regular as the map  $F$ .

*Proof.* The approach we are going to take is similar to the application of a Newton-Kantorovich method (a method that given enough regularity on the map and suitable bounds, ensures the quadratic convergence of a Newton method), but using also fixed point methods. This will suffice to prove the convergence of our method.

Lastly, and in order to provide more clarity to a proof of such length, it will be convenient to separate it in subsections dedicated to each of the statements that need to be proven.

### Invariant Torus

First of all, using condition 5.3) and Lemma 2.6, we see that  $P_1$  is invertible. Let us denote  $P_1^{-1}$  its inverse. By using  $P_1$  as a change of coordinates on the bundle  $\mathbb{C}^n \times \mathbb{T}_\rho^d$ , we write  $\hat{K} = P_1^{-1}K$ , so the approximate invariant torus in the new coordinates is  $\hat{K}_0 = P_1^{-1}K_0$ . The functional on  $C^a(\mathbb{T}_\rho^d, \mathbb{C}^n)$  we will consider is

$$\hat{\mathcal{F}}[\hat{K}](\theta) = P_2(\theta)(F(P_1(\theta - \omega)\hat{K}(\theta - \omega), \theta - \omega) - P_1(\theta)\hat{K}(\theta)).$$

From the regularity properties of the composition operator that can be found in [2], we can say that  $\hat{\mathcal{F}}$  is (at least)  $C^2$  when acting on analytic functions (which is enough regularity for our purpose as we will see further ahead).

Clearly, in order to find a solution to our problem, which is finding an invariant  $K$ , we will have to solve  $\hat{\mathcal{F}}[\hat{K}] = 0$ . For that, we can use a Newton method, which is defined as follows.

$$\hat{N}[\hat{K}] = \hat{K} - (D\hat{\mathcal{F}}[\hat{K}])^{-1}\hat{\mathcal{F}}[\hat{K}].$$

But in order to simplify, we will apply a quasi-Newton method, which does not update  $(D\hat{\mathcal{F}}[\hat{K}_i])^{-1}$  for every new found tori  $K_i$ , but instead fixes it to the first one we calculate, which is  $(D\hat{\mathcal{F}}[\hat{K}_0])^{-1}$ . The downside of such method is that the quadratic speed of convergence (once convergence is proven) will drop, but that is not a problem for us since we only want to see convergence. Hence, our new iterative method is defined as

$$\hat{N}_0[\hat{K}] = \hat{K} - (D\hat{\mathcal{F}}[\hat{K}_0])^{-1}\hat{\mathcal{F}}[\hat{K}].$$

So, in order to prove that the method converges, we want to apply Theorem 2.9, a fixed point theorem.

Let us define the domain of the operator  $\hat{N}_0[\hat{K}]$  as

$$\bar{B}_\rho(\hat{K}_0, r) = \{\hat{K} \in C^a(\mathbb{T}_\rho^d, \mathbb{C}^n) \mid \|\hat{K} - \hat{K}_0\|_\rho \leq r\},$$

which implies that if a torus  $\hat{K}$  is in  $\bar{B}_\rho(\hat{K}_0, r)$ , then the torus  $K(\theta) = K_0(\theta) + P_1(\theta)(\hat{K}(\theta) - \hat{K}_0(\theta))$  is also in the tube  $\bar{D}_\rho(K_0, R)$ .

Recalling Theorem 2.9, in order to ensure the existence of a fixed point in our operator, we need to find

$$\|\hat{N}_0[\hat{K}_0] - \hat{K}_0\|_\rho = \|\hat{K}_0 - (\mathcal{D}\hat{\mathcal{F}}[\hat{K}_0])^{-1}\hat{\mathcal{F}}[\hat{K}_0] - \hat{K}_0\|_\rho$$

and  $L(r)$  for which

$$\|\hat{N}_0[\hat{K}_2] - \hat{N}_0[\hat{K}_1]\|_\rho \leq L(r) \|\hat{K}_2 - \hat{K}_1\|_\rho$$

such that

$$\frac{\|\hat{N}_0[\hat{K}_0] - \hat{K}_0\|_\rho}{r} + L(r) - 1 \leq 0.$$

Notice that  $\|\hat{K}_0 - (\mathcal{D}\hat{\mathcal{F}}[\hat{K}_0])^{-1}\hat{\mathcal{F}}[\hat{K}_0] - \hat{K}_0\|_\rho \leq \|(\mathcal{D}\hat{\mathcal{F}}[\hat{K}_0])^{-1}\|_\rho \|\hat{\mathcal{F}}[\hat{K}_0]\|_\rho$ . It is clear that we have to find bounds for  $\|(\mathcal{D}\hat{\mathcal{F}}[\hat{K}_0])^{-1}\|_\rho$  and  $\|\hat{\mathcal{F}}[\hat{K}_0]\|_\rho$ , but recall that

$$\hat{\mathcal{F}}[\hat{K}](\theta) = P_2(\theta)(F(P_1(\theta - \omega)\hat{K}(\theta - \omega), \theta - \omega) - P_1(\theta)\hat{K}(\theta)),$$

which means that  $\|\hat{\mathcal{F}}[\hat{K}_0]\|_\rho$  is the invariance error, which, by condition 5.1), satisfies  $\|\hat{\mathcal{F}}[\hat{K}_0]\|_\rho = \|E\|_\rho \leq \varepsilon$ . Let's compute now the bound for  $\|(\mathcal{D}\hat{\mathcal{F}}[\hat{K}_0])^{-1}\|_\rho$ . First, we have to calculate  $\mathcal{D}\hat{\mathcal{F}}[\hat{K}_0]$ . The differential of  $\hat{\mathcal{F}}$  is defined by

$$\begin{aligned} (\mathcal{D}\hat{\mathcal{F}}[\hat{K}_0]\hat{\xi})(\theta) &= P_2(\theta)\mathcal{D}_x F(P_1(\theta - \omega)\hat{K}_0(\theta - \omega), \theta - \omega)P_1(\theta - \omega)\hat{\xi}(\theta - \omega) - P_2(\theta)P_1(\theta)\hat{\xi}(\theta) \\ &= (\Lambda_0(\theta - \omega) + E_{red}(\theta - \omega))\hat{\xi}(\theta - \omega) - \hat{\xi}(\theta) - E_{inv}(\theta)\hat{\xi}(\theta), \end{aligned}$$

where  $\hat{\xi}: \bar{\mathbb{T}}_\rho^d \rightarrow \mathbb{C}^n$  is analytic. Denoting  $\mathcal{L}_\omega$ ,  $\mathcal{E}_{red,\omega}$  the transfer operators associated to  $\Lambda_0(\theta)$  and  $E_{red}(\theta)$  respectively (over the rotation by  $\omega$ ), and  $\mathcal{E}_{inv}$  the transfer operator associated to  $E_{inv}(\theta)$  (over the identity), that is,

- $\mathcal{L}_\omega \hat{\xi}(\theta) = \Lambda_0(\theta - \omega) \hat{\xi}(\theta - \omega)$
- $\mathcal{E}_{red,\omega} \hat{\xi}(\theta) = E_{red}(\theta - \omega) \hat{\xi}(\theta - \omega)$
- $\mathcal{E}_{inv} \hat{\xi}(\theta) = E_{inv}(\theta) \hat{\xi}(\theta)$ ,

we can write

$$\mathcal{D}\hat{\mathcal{F}}[\hat{K}_0] = \mathcal{L}_\omega + \mathcal{E}_{red,\omega} - Id - \mathcal{E}_{inv} = (\mathcal{L}_\omega - Id) + \mathcal{E}_{red,\omega} - \mathcal{E}_{inv}$$

Notice that, from condition 5.4) and using a Neumann series argument, by decomposing  $\mathcal{L}_\omega$  into its stable and unstable blocks (given that  $\hat{K}_0$  is hyperbolic) and the fact that each operator  $\mathcal{L}_\omega^{s,u}$  is bounded, we can say that  $Id - \mathcal{L}_\omega^{s,u}$  are invertible. This means that  $(Id - \mathcal{L}_\omega^{s,u})^{-1} = -(\mathcal{L}_\omega^{s,u} - Id)^{-1}$ . Separating the stable and unstable cases we can calculate for the stable bundle

$$(\mathcal{L}_\omega^s - Id)^{-1} = -(Id - \mathcal{L}_\omega^s)^{-1} = -\sum_{k=0}^{\infty} (\mathcal{L}_\omega^s)^k.$$

Taking norms and using, again, 5.4)

$$\|(\mathcal{L}_\omega^s - Id)^{-1}\|_\rho = \left\| - \sum_{k=0}^{\infty} (\mathcal{L}_\omega^s)^k \right\|_\rho \leq \sum_{k=0}^{\infty} \|(\mathcal{L}_\omega^s)^k\|_\rho \leq \sum_{k=0}^{\infty} \|\mathcal{L}_\omega^s\|_\rho^k \leq \sum_{k=0}^{\infty} \lambda^k = \frac{1}{1-\lambda}, \quad (2.1)$$

given that  $\lambda < 1$ . The process for the unstable bundle is analogous, one only has to notice that

$$(\mathcal{L}_\omega^u - Id) = \mathcal{L}_\omega^u \cdot (Id - (\mathcal{L}_\omega^u)^{-1}) \longrightarrow (\mathcal{L}_\omega^u - Id)^{-1} = (Id - (\mathcal{L}_\omega^u)^{-1})^{-1} \cdot (\mathcal{L}_\omega^u)^{-1}$$

and therefore

$$\|(\mathcal{L}_\omega^u - Id)^{-1}\|_\rho \leq \|(Id - (\mathcal{L}_\omega^u)^{-1})^{-1}\|_\rho \cdot \|(\mathcal{L}_\omega^u)^{-1}\|_\rho \leq \sum_{k=0}^{\infty} \|(\mathcal{L}_\omega^u)^{-1}\|_\rho^k \cdot \lambda \leq \sum_{k=0}^{\infty} \lambda^k \cdot \lambda = \frac{\lambda}{1-\lambda}.$$

Obtaining thus

$$\|(\mathcal{L}_\omega^s - Id)^{-1}\|_\rho \leq \frac{1}{1-\lambda}, \quad \|(\mathcal{L}_\omega^u - Id)^{-1}\|_\rho \leq \frac{\lambda}{1-\lambda}.$$

Then,  $\mathcal{L}_\omega - Id$  is also invertible and using the norm defined in 3) (taking the maximum norm between both blocks), we have

$$\|(\mathcal{L}_\omega - Id)^{-1}\|_\rho \leq \frac{1}{1-\lambda}.$$

Notice that for a  $z \in \mathbb{C}^n$  such that  $|z| = 1$ ,  $\|(\mathcal{L}_\omega - Id)^{-1}\|_\rho = \|(\mathcal{L}_\omega - zId)^{-1}\|_\rho$ .

By rewriting the expression of the differential of  $\hat{\mathcal{F}}$  such as

$$D\hat{\mathcal{F}}[\hat{K}_0] = (\mathcal{L}_\omega - Id) + \mathcal{E}_{red,\omega} - \mathcal{E}_{inv} = (\mathcal{L}_\omega - Id) \cdot (Id + (\mathcal{L}_\omega - Id)^{-1}(\mathcal{E}_{red,\omega} - \mathcal{E}_{inv})),$$

we can find an expression for its inverse,

$$(D\hat{\mathcal{F}}[\hat{K}_0])^{-1} = (Id + (\mathcal{L}_\omega - Id)^{-1}(\mathcal{E}_{red,\omega} - \mathcal{E}_{inv}))^{-1}(\mathcal{L}_\omega - Id)^{-1}.$$

From 5.2) and 5.3), and provided that  $\|(\mathcal{L}_\omega - Id)^{-1}(\mathcal{E}_{red,\omega} - \mathcal{E}_{inv})\|_\rho \leq \frac{1}{1-\lambda}(\sigma + \tau) < 1$ , using Neumann series we have the estimate

$$\|(D\hat{\mathcal{F}}[\hat{K}_0])^{-1}\|_\rho \leq \frac{1}{1 - \frac{\sigma + \tau}{1-\lambda}} \frac{1}{1-\lambda}.$$

Notice that from condition 4) we have that  $\lambda + \sigma + \tau < 1$ , so finally

$$\|(D\hat{\mathcal{F}}[\hat{K}_0])^{-1}\|_\rho \leq \frac{1}{1 - (\lambda + \sigma + \tau)}.$$

With those estimates, we can lastly compute

$$\|\hat{K}_0 - (\mathbf{D}\hat{\mathcal{F}}[\hat{K}_0])^{-1}\hat{\mathcal{F}}[\hat{K}_0] - \hat{K}_0\|_\rho \leq \|(\mathbf{D}\hat{\mathcal{F}}[\hat{K}_0])^{-1}\|_\rho \|\hat{\mathcal{F}}[\hat{K}_0]\|_\rho \leq \frac{\varepsilon}{1 - (\lambda + \sigma + \tau)} = \hat{\varepsilon}.$$

The next step is to find the  $L(r)$  term. For that, we proceed as usual, by checking that

$$\|\hat{N}_0[\hat{K}_2] - \hat{N}_0[\hat{K}_1]\|_\rho \leq L(r) \|\hat{K}_2 - \hat{K}_1\|_\rho.$$

We can start by expressing  $\hat{\mathcal{F}}[\hat{K}_2]$  in terms of its Taylor approximation plus the residue in its integral form around  $\hat{K}_1$ .

$$\hat{\mathcal{F}}[\hat{K}_2] = \hat{\mathcal{F}}[\hat{K}_1] + \int_0^1 \mathbf{D}\hat{\mathcal{F}}[\hat{K}_1 + t(\hat{K}_2 - \hat{K}_1)] dt (\hat{K}_2 - \hat{K}_1).$$

Then,

$$\begin{aligned} \hat{N}_0[\hat{K}_2] - \hat{N}_0[\hat{K}_1] &= \hat{K}_2 - (\mathbf{D}\hat{\mathcal{F}}[\hat{K}_0])^{-1}\hat{\mathcal{F}}[\hat{K}_2] - \hat{K}_1 + (\mathbf{D}\hat{\mathcal{F}}[\hat{K}_0])^{-1}\hat{\mathcal{F}}[\hat{K}_1] \\ &= \hat{K}_2 - (\mathbf{D}\hat{\mathcal{F}}[\hat{K}_0])^{-1} \left( \hat{\mathcal{F}}[\hat{K}_1] + \int_0^1 \mathbf{D}\hat{\mathcal{F}}[\hat{K}_1 + t(\hat{K}_2 - \hat{K}_1)] dt (\hat{K}_2 - \hat{K}_1) \right) \\ &\quad - \hat{K}_1 + (\mathbf{D}\hat{\mathcal{F}}[\hat{K}_0])^{-1}\hat{\mathcal{F}}[\hat{K}_1]. \end{aligned}$$

Before continuing, let's find another expression for  $\mathbf{D}\hat{\mathcal{F}}[\hat{K}_1 + t(\hat{K}_2 - \hat{K}_1)]$ .

$$\begin{aligned} \mathbf{D}\hat{\mathcal{F}}[\hat{K}_1 + t(\hat{K}_2 - \hat{K}_1)] &= \mathbf{D}\hat{\mathcal{F}}[\hat{K}_0] + \int_0^1 \frac{d}{ds} \left( \mathbf{D}\hat{\mathcal{F}} \left[ \hat{K}_0 + s(\hat{K}_1 + t(\hat{K}_2 - \hat{K}_1) - \hat{K}_0) \right] \right) ds \\ &= \mathbf{D}\hat{\mathcal{F}}[\hat{K}_0] + \int_0^1 \mathbf{D}^2\hat{\mathcal{F}} \left[ \hat{K}_0 + s((\hat{K}_1 - \hat{K}_0) + t(\hat{K}_2 - \hat{K}_1)) \right] ds \cdot \\ &\quad \cdot \left( (\hat{K}_1 - \hat{K}_0) + t(\hat{K}_2 - \hat{K}_1) \right). \end{aligned}$$

Notice that we can transform

$$\begin{aligned} (\hat{K}_1 - \hat{K}_0) + t(\hat{K}_2 - \hat{K}_1) &= (\hat{K}_1 - \hat{K}_0) + t(\hat{K}_2 - \hat{K}_1) - t\hat{K}_0 + t\hat{K}_0 \\ &= (\hat{K}_1 - \hat{K}_0) + t(\hat{K}_2 - \hat{K}_0) - t(\hat{K}_1 - \hat{K}_0) \\ &= (1 - t)(\hat{K}_1 - \hat{K}_0) + t(\hat{K}_2 - \hat{K}_0) \end{aligned}$$

and obtain

$$\begin{aligned} \hat{N}_0[\hat{K}_2] - \hat{N}_0[\hat{K}_1] &= \int_0^1 \int_0^1 (\mathbf{D}\hat{\mathcal{F}}[\hat{K}_0])^{-1} \mathbf{D}^2\hat{\mathcal{F}} \left[ \hat{K}_0 + s \left( (\hat{K}_1 - \hat{K}_0) + t(\hat{K}_2 - \hat{K}_1) \right) \right] ds \cdot \\ &\quad \cdot \left( (1 - t)(\hat{K}_1 - \hat{K}_0) + t(\hat{K}_2 - \hat{K}_0) \right) dt (\hat{K}_2 - \hat{K}_1). \end{aligned}$$

We estimate now the norm of  $D^2\hat{\mathcal{F}}$  on functions in  $\bar{B}_\rho(\hat{K}_0, r)$ . Recall that, since  $\|\hat{K}(\theta) - \hat{K}_0(\theta)\|_\rho \leq r \leq R$ , then  $(K(\theta), \theta) \in \bar{D}_\rho(K_0, R)$  for  $\theta \in \bar{\mathbb{T}}_\rho^d$ . With the second differential being

$$D^2\hat{\mathcal{F}}[\hat{K}][\hat{\xi}_1, \hat{\xi}_2](\theta) = P_2(\theta + \omega)D_x^2F(P_1(\theta)\hat{K}(\theta), \theta)[P_1(\theta)\hat{\xi}_1(\theta), P_1(\theta)\hat{\xi}_2(\theta)]$$

and applying condition 5.5) we obtain

$$\|D^2\hat{\mathcal{F}}[\hat{K}]\| \leq b$$

for any  $\hat{K} \in \bar{B}_\rho(\hat{K}_0, r)$ . This way, we can see that we can bound

$$\left\| (D\hat{\mathcal{F}}[\hat{K}_0])^{-1}D^2\hat{\mathcal{F}} \left[ \hat{K}_0 + s \left( (\hat{K}_1 - \hat{K}_0) + t(\hat{K}_2 - \hat{K}_1) \right) \right] \right\|_\rho \leq \frac{b}{1 - (\lambda + \sigma + \tau)} = \beta$$

and  $\|\hat{K}_2 - \hat{K}_1\|_\rho, \|\hat{K}_1 - \hat{K}_0\|_\rho \leq r$ . With this,

$$\|\hat{N}_0[\hat{K}_2] - \hat{N}_0[\hat{K}_1]\|_\rho \leq \frac{1}{2}\beta r \|\hat{K}_2 - \hat{K}_1\|_\rho,$$

so  $L(r) = \frac{1}{2}\beta r$ .

Once we have our estimates, we have to check the theorem's hypothesis, and that is  $\frac{\hat{\varepsilon}}{r} + \frac{1}{2}\beta r - 1 \leq 0$ , which is equivalent to  $\hat{\varepsilon} + \frac{1}{2}\beta r^2 - r \leq 0$ . By solving the inequation we find two values,

$$r_0 = \frac{1 - \sqrt{1 - 2h}}{\beta} = \frac{1 - \sqrt{1 - 2h}}{h} \hat{\varepsilon}, \quad r_1 = \frac{1 + \sqrt{1 - 2h}}{\beta} = \frac{1 + \sqrt{1 - 2h}}{h} \hat{\varepsilon}$$

for which  $r$  has to satisfy  $r_0 \leq r \leq \min\{r_1, R\}$  (since we have to remain inside the tube). Such condition is satisfied due to hypotheses 6) and 7), which implies the satisfaction of the hypothesis of Theorem 2.9 and therefore the existence of a fixed point in our quasi-Newton method and hence the existence of an invariant torus  $K_*$ . Notice that Theorem 2.9 also tells us that our Newton operator is contractive since  $L(r) < 1$ .

Recall that the estimates we just found mean that the newly found torus  $K_*$  will be contained within a radius  $r_0$  and that, furthermore, it will be unique in a radius  $r_1$ .

### Hyperbolicity

In order to prove the hyperbolicity of  $K_*$ , we will prove that, for any  $\hat{K}(\theta) \in \bar{B}_\rho(\hat{K}_0, r_0)$  (defined as before) the its transfer operator  $\mathcal{M}_\omega$  is hyperbolic. As we saw before, we have to check that the unit circle is in the resolvent of the transfer operator, that is,  $\forall z \in \mathbb{C}^n$  such that  $|z| = 1$ , we have to check that  $z \in \text{Res}(\mathcal{M}_\omega, C^a(\bar{\mathbb{T}}_\rho^d, \mathbb{C}^n))$ . This means that  $\forall \eta \in C^a(\bar{\mathbb{T}}_\rho^d, \mathbb{C}^n)$ ,  $\exists! \xi \in C^a(\bar{\mathbb{T}}_\rho^d, \mathbb{C}^n)$  such that  $\mathcal{M}_\omega \xi - z \xi = \eta$ .

Hence, for any  $z \in \mathbb{C}$  with  $|z| = 1$ , and given  $\eta \in C^a(\mathbb{T}_\rho^d, \mathbb{C}^n)$ , we have to solve the equation

$$\eta(\theta) = D_x F(K(\theta - \omega), \theta - \omega) \xi(\theta - \omega) - z \xi(\theta)$$

which is equivalent to

$$P_2(\theta) P_1(\theta) \hat{\eta}(\theta) = P_2(\theta) D_x F(K(\theta - \omega), \theta - \omega) P_1(\theta - \omega) \hat{\xi}(\theta - \omega) - z P_2(\theta) P_1(\theta) \hat{\xi}(\theta) \quad (2.2)$$

once we perform the change of variables giving rise  $\xi = P_1 \hat{\xi}$  and  $\eta = P_1 \hat{\eta}$ .

A first step is to compare the transfer operators associated to  $M(\theta) = D_x F(K(\theta), \theta)$  and  $M_0(\theta) = D_x F(K_0(\theta), \theta)$ . To do so, we consider the vector bundle map (over the rotation  $\omega$ ) defined by

$$B(\theta) = P_2(\theta) (D_x F(K(\theta - \omega), \theta - \omega) - D_x F(K_0(\theta - \omega), \theta - \omega)) P_1(\theta - \omega) \quad (2.3)$$

$$= \int_0^1 P_2(\theta) D_x^2 F(tK(\theta - \omega) + (1-t)K_0(\theta - \omega), \theta - \omega) \quad (2.4)$$

$$[P_1(\theta - \omega) (\hat{K}(\theta - \omega) - \hat{K}_0(\theta - \omega)), P_1(\theta - \omega) \cdot] dt. \quad (2.5)$$

The transfer operator for such map would be  $\mathcal{B}_\omega \hat{\xi}(\theta) = B(\theta - \omega) \hat{\xi}(\theta - \omega)$  and we see that  $\|\mathcal{B}_\omega\|_\rho \leq br_0$ . Then, we can manipulate equation (2.2) and get

$$\begin{aligned} P_2(\theta) P_1(\theta) \hat{\eta}(\theta) &= P_2(\theta) D_x F(K(\theta - \omega), \theta - \omega) P_1(\theta - \omega) \hat{\xi}(\theta - \omega) - z P_2(\theta) P_1(\theta) \hat{\xi}(\theta) \\ &= P_2(\theta) D_x F(K(\theta - \omega), \theta - \omega) P_1(\theta - \omega) \hat{\xi}(\theta - \omega) \\ &\quad - P_2(\theta) D_x F(K_0(\theta - \omega), \theta - \omega) P_1(\theta - \omega) \hat{\xi}(\theta - \omega) \\ &\quad + P_2(\theta) D_x F(K_0(\theta - \omega), \theta - \omega) P_1(\theta - \omega) \hat{\xi}(\theta - \omega) - z P_2(\theta) P_1(\theta) \hat{\xi}(\theta) \\ &= P_2(\theta) (D_x F(K(\theta), \theta) - D_x F(K_0(\theta), \theta)) P_1(\theta - \omega) \hat{\xi}(\theta - \omega) \\ &\quad + P_2(\theta) D_x F(K_0(\theta - \omega), \theta - \omega) P_1(\theta - \omega) \hat{\xi}(\theta - \omega) - z P_2(\theta) P_1(\theta) \hat{\xi}(\theta), \end{aligned} \quad (2.6)$$

which turns into

$$(Id + E_{inv}(\theta)) \hat{\eta}(\theta) = (\Lambda_0(\theta - \omega) + E_{red,\omega}(\theta - \omega) + B(\theta - \omega)) \hat{\xi}(\theta - \omega) - z (Id + E_{inv}(\theta)) \hat{\xi}(\theta).$$

Using transfer operator notation, the previous equation becomes

$$(Id + \mathcal{E}_{inv}) \hat{\eta} = ((\mathcal{L}_\omega - zId) + \mathcal{E}_{red,\omega} + \mathcal{B}_\omega - z\mathcal{E}_{inv}) \hat{\xi},$$

which can be expressed as a product as

$$(Id + \mathcal{E}_{inv}) \hat{\eta} = (\mathcal{L}_\omega - zId) (Id + (\mathcal{L}_\omega - zId)^{-1} (\mathcal{B}_\omega + \mathcal{E}_{red,\omega} - z\mathcal{E}_{inv})) \hat{\xi},$$

where the invertibility of  $(\mathcal{L}_\omega - zId)$  has been proven before. Following similar procedures, the solution of the previous equation is:

$$\hat{\xi} = (Id + (\mathcal{L}_\omega - zId)^{-1}(\mathcal{B}_\omega + \mathcal{E}_{red,\omega} - z\mathcal{E}_{inv}))^{-1}(\mathcal{L}_\omega - zId)^{-1}(Id + \mathcal{E}_{inv})\hat{\eta}.$$

Even though the existence (and therefore the hyperbolicity) is already proven, we can go a bit further and provide a bound for  $\|(\mathcal{M}_\omega - zId)^{-1}\|_\rho$ . Since  $\eta = (\mathcal{M}_\omega - zId)\xi$ , then  $\xi = (\mathcal{M}_\omega - zId)^{-1}\eta$ , so  $\|\xi\|_\rho = \|(\mathcal{M}_\omega - zId)^{-1}\|_\rho\|\eta\|_\rho$ . Recall that  $\eta = P_1\hat{\eta}$  and  $\xi = P_1\hat{\xi}$ , so with the last expression found for  $\hat{\xi}$ , we have

$$\xi = P_1(Id + (\mathcal{L}_\omega - zId)^{-1}(\mathcal{B}_\omega + \mathcal{E}_{red,\omega} - z\mathcal{E}_{inv}))^{-1}(\mathcal{L}_\omega - zId)^{-1}(Id + \mathcal{E}_{inv})P_1^{-1}\eta.$$

Since we can bound

$$\|(\mathcal{L}_\omega - zId)^{-1}(\mathcal{B}_\omega + \mathcal{E}_{red,\omega} - z\mathcal{E}_{inv})\|_\rho \leq \frac{br_0 + \sigma + \tau}{1 - \lambda},$$

by using Neumann series, one has

$$\|\hat{\xi}\|_\rho \leq \frac{1}{1 - \frac{\tau + br_0 + \sigma}{1 - \lambda}} \cdot \frac{1 + \tau}{1 - \lambda} \|\hat{\eta}\|_\rho = \frac{1 + \tau}{1 - (\lambda + \sigma + \tau + br_0)} \|\hat{\eta}\|_\rho.$$

Notice that  $\lambda + \sigma + \tau + br_0$  is a ‘‘dirtier’’ hyperbolicity constant than  $\lambda$ , therefore, if  $\lambda + \sigma + \tau + br_0 < 1$ , we can ensure that the operator is a contraction. In order to prove such bound, we have to check that  $br_0 < 1$  and that when added to  $\lambda + \sigma + \tau$ , the sum is still less than 1. For that we use hypothesis 6) and the fact that  $r_0 < 2\hat{\varepsilon}$  to obtain:

$$\frac{br_0}{1 - (\lambda + \sigma + \tau)} < 2\beta\hat{\varepsilon} = 2h < 1.$$

With that, we have

$$\|\xi\|_\rho \leq \|P_1\|_\rho \frac{1 + \tau}{1 - (\lambda + \sigma + \tau + br_0)} \|P_1^{-1}\|_\rho \|\eta\|_\rho,$$

which implies

$$\|(\mathcal{M}_\omega - zId)^{-1}\|_\rho \leq \|P_1\|_\rho \frac{1 + \tau}{1 - (\lambda + \sigma + \tau + br_0)} \|P_1^{-1}\|_\rho.$$

### Invariant Bundles

Once we have computed the invariant torus  $K_*$ , we are ready to compute its stable and unstable subbundles from the approximate invariant bundles.

The equation to be solved is

$$P(\theta + \omega)^{-1}D_x F(K_*(\theta), \theta)P(\theta) - \Lambda(\theta) = 0. \quad (2.7)$$

The unknowns in the previous equation are  $P$  and  $\Lambda = \text{blockdiag}(\Lambda^s, \Lambda^u)$ . Instead of using these unknowns, we will introduce new variables which take advantage of the fact that we have an approximate solution. Such variables will be  $Q, \Delta^s$  and  $\Delta^u$ , where

$$Q(\theta) = \begin{pmatrix} 0 & Q^{su}(\theta) \\ Q^{us}(\theta) & 0 \end{pmatrix}$$

with  $Q^{us}(\theta) : \bar{\mathbb{T}}_\rho^d \rightarrow \mathbb{C}^{n_s \times n_u}$ ,  $Q^{su}(\theta) : \bar{\mathbb{T}}_\rho^d \rightarrow \mathbb{C}^{n_u \times n_s}$  are analytic maps. In addition, we will have the  $\Delta^s$  and  $\Delta^u$  corrections, which will also be analytic maps  $\Delta^s(\theta) : \bar{\mathbb{T}}_\rho^d \rightarrow \mathbb{C}^{n_s \times n_s}$ ,  $\Delta^u(\theta) : \bar{\mathbb{T}}_\rho^d \rightarrow \mathbb{C}^{n_u \times n_u}$ .

The key idea of this is that we are looking for correction variables (the entries of the matrix  $Q$ ) such that when applied on the approximate fibers they will lead us to the invariant fibers. We can say that  $P_1$  is the matrix of the base of eigenvectors on the approximate subbundles split into stable and unstable eigenvectors (to be precise, the eigenvectors that generate the stable and unstable subbundles). And the same goes for  $P$  and  $K_*$  (we can affirm that such splitting exists for  $K_*$  because we just proved it is normally hyperbolic). Dropping the  $\theta$  dependence for a moment for the sake of the conceptual explanation and calling  $P_1 = (v_1^s | v_1^u)$  and  $P = (v^s | v^u)$ , we can write

$$\begin{cases} v^s = v_1^s + Q^{us}v_1^u \\ v^u = v_1^u + Q^{su}v_1^s \end{cases}$$

which is equivalent to

$$(v^s | v^u) = (v_1^s | v_1^u) + (v_1^s | v_1^u)Q,$$

or using matrices

$$P = P_1(Id + Q).$$

Hence,

$$P(\theta) = P_1(\theta) + P_1(\theta)Q(\theta), \quad \Lambda^s(\theta) = \Lambda_0^s(\theta) + \Delta^s(\theta), \quad \Lambda^u(\theta) = \Lambda_0^u(\theta) + \Delta^u(\theta). \quad (2.8)$$

We will use the contraction principle to analyze (2.7).

We take  $Q^{us} = 0$ ,  $Q^{su} = 0$ ,  $\Delta^s = 0$  and  $\Delta^u = 0$  as the first elements of the iteration. Then, by adding and subtracting the differential of  $K_0$  (more specifically  $\Lambda_0(\theta) + E_{red}(\theta)$ ), the error can be expressed as

$$\begin{aligned} \tilde{E}_{red}(\theta) &= P_1(\theta + \omega)^{-1} D_x F(K_*(\theta), \theta) P_1(\theta) - \Lambda_0(\theta) \\ &= (Id + E_{inv}(\theta + \omega))^{-1} (\Lambda_0(\theta) + E_{red}(\theta) + B(\theta + \omega)) - \Lambda_0(\theta) \\ &= ((Id + E_{inv}(\theta + \omega))^{-1} - Id) \Lambda_0(\theta) + (Id + E_{inv}(\theta + \omega))^{-1} (E_{red}(\theta) + B(\theta + \omega)), \end{aligned} \quad (2.9)$$

where  $B$  is defined as in (2.3) but taking  $K_*$  as  $K$ .

Notice that in the second equality we have applied the same reasoning as in (2.6). Notice that

$$\begin{aligned} ((Id + E_{inv}(\theta + \omega))^{-1} - Id) &= (Id + E_{inv}(\theta + \omega))^{-1}(Id - (Id + E_{inv}(\theta + \omega))) \\ &= (Id + E_{inv}(\theta + \omega))^{-1}(-E_{inv}(\theta + \omega)). \end{aligned}$$

Therefore, taking norms directly from the last expression in (2.9) we have

$$\|\tilde{E}_{red}\|_\rho \leq \frac{\tau}{1-\tau}\hat{\lambda} + \frac{1}{1-\tau}(\sigma + br_0) = \tilde{\sigma}, \quad (2.10)$$

where  $\hat{\lambda} = \|\Lambda_0\|_\rho$  (as defined in the hypotheses). Now equation (2.7) reads

$$\begin{aligned} 0 &= P_1(\theta + \omega)^{-1}D_x F(K_*(\theta), \theta)P_1(\theta)(Id + Q(\theta)) - (Id + Q(\theta + \omega))(\Lambda_0(\theta) + \Delta(\theta)) \\ &= (\tilde{E}_{red}(\theta) + \Lambda_0(\theta))(Id + Q(\theta)) - (Id + Q(\theta + \omega))(\Lambda_0(\theta) + \Delta(\theta)) \\ &= \Lambda_0(\theta)Q(\theta) - Q(\theta + \omega)\Lambda_0(\theta) - \Delta(\theta) + \tilde{E}_{red}(\theta)(Id + Q(\theta)) - Q(\theta + \omega)\Delta(\theta). \end{aligned} \quad (2.11)$$

We can write

$$\tilde{E}_{red}(\theta) = \begin{pmatrix} \tilde{E}_{red}^{ss}(\theta) & \tilde{E}_{red}^{su}(\theta) \\ \tilde{E}_{red}^{us}(\theta) & \tilde{E}_{red}^{uu}(\theta) \end{pmatrix}$$

so we can deal with (2.11) as a product of matrices and express the result block by block. The diagonal blocks result in

$$\begin{aligned} -\Delta^s(\theta) + \tilde{E}_{red}^{su}(\theta)Q^{us}(\theta) + \tilde{E}_{red}^{ss}(\theta) &= 0, \\ -\Delta^u(\theta) + \tilde{E}_{red}^{us}(\theta)Q^{su}(\theta) + \tilde{E}_{red}^{uu}(\theta) &= 0, \end{aligned}$$

which can be expressed as

$$\begin{aligned} \Delta^s(\theta) &= \tilde{E}_{red}^{su}(\theta)Q^{us}(\theta) + \tilde{E}_{red}^{ss}(\theta), \\ \Delta^u(\theta) &= \tilde{E}_{red}^{us}(\theta)Q^{su}(\theta) + \tilde{E}_{red}^{uu}(\theta). \end{aligned}$$

Using this expressions, we can write the results of the remaining blocks as

$$\begin{aligned} \Lambda_0^s(\theta)Q^{su}(\theta) - Q^{su}(\theta + \omega)\Lambda_0^u(\theta) &= -\left(\tilde{E}_{red}^{ss}(\theta)Q^{su}(\theta) - Q^{su}(\theta + \omega)\tilde{E}_{red}^{uu}(\theta)\right) + \\ &\quad Q^{su}(\theta + \omega)\tilde{E}_{red}^{us}(\theta)Q^{su}(\theta) - \tilde{E}_{red}^{su}(\theta), \end{aligned} \quad (2.12)$$

$$\begin{aligned} \Lambda_0^u(\theta)Q^{us}(\theta) - Q^{us}(\theta + \omega)\Lambda_0^s(\theta) &= -\left(\tilde{E}_{red}^{uu}(\theta)Q^{us}(\theta) - Q^{us}(\theta + \omega)\tilde{E}_{red}^{ss}(\theta)\right) + \\ &\quad Q^{us}(\theta + \omega)\tilde{E}_{red}^{su}(\theta)Q^{us}(\theta) - \tilde{E}_{red}^{us}(\theta). \end{aligned} \quad (2.13)$$

Hence, we just have to solve (2.12) and (2.13). We will make explicit the calculations for (2.12), since the ones for (2.13) can be obtained by applying the results from (2.12) to the inverse mapping.

Multiplying on both sides of the equation by  $(\Lambda_0^u)^{-1}$  and by defining the linear operator  $\mathcal{L}_\omega^{su}$

acting on analytic vector bundle maps (over the identity)  $Q^{su}(\theta) : \mathbb{R}^{n_u} \rightarrow \mathbb{R}^{n_s}$  as

$$\mathcal{L}_\omega^{su} Q^{su}(\theta) := \mathcal{L}_\omega^{su}[Q^{su}](\theta) = \Lambda_0^s(\theta - \omega) Q^{su}(\theta - \omega) (\Lambda_0^u(\theta - \omega))^{-1} \quad (2.14)$$

we can write equation (2.12) as

$$Q^{su} = (\mathcal{L}_\omega^{su} - Id)^{-1} \circ (-\tilde{\mathcal{E}}_{red,\omega}^{ss} Q^{su} + Q_+^{su} (\tilde{\mathcal{E}}_{red,\omega}^{us} Q^{su} + \tilde{\mathcal{E}}_{red,\omega}^{uu}) - \tilde{\mathcal{E}}_{red,\omega}^{su}) \circ (\mathcal{L}_\omega^u)^{-1}, \quad (2.15)$$

where  $Q_+ := Q(\theta + \omega)$ . By applying Neumann series reasoning on (2.14),

$$\|(\mathcal{L}_\omega^{su} - Id)^{-1}\|_\rho \leq \frac{1}{1 - \lambda^2}.$$

From now on, the right hand side of equation (2.15) will be considered as an operator  $T(Q^{su}) := T[Q^{su}]$  acting on  $Q^{su}$ . So equation (2.15) reads as a fixed point equation  $T(Q^{su}) = Q^{su}$ , which leads us back to the application of the fixed point Theorem 2.9. We will assume that  $Q^{su}$  is contained in a ball of radius  $\alpha$ . Again, the first step will be the estimation of  $\|T(0) - 0\|_\rho$ .

**Remark 2.13.** Keep in mind that when we specify that the map  $Q^{su} = 0$ , we are also saying that 0 is a matrix of the size of  $Q^{su}$ .

Observe that from estimate (2.10) we obtain estimates  $\|\tilde{\mathcal{E}}_{red,\omega}^{ss}\|_\rho \leq \tilde{\sigma}$ ,  $\|\tilde{\mathcal{E}}_{red,\omega}^{su}\|_\rho \leq \tilde{\sigma}$ ,  $\|\tilde{\mathcal{E}}_{red,\omega}^{us}\|_\rho \leq \tilde{\sigma}$  and  $\|\tilde{\mathcal{E}}_{red,\omega}^{uu}\|_\rho \leq \tilde{\sigma}$  because the norm of every block of the matrix cannot be bigger than the norm of the matrix itself given that we work with supremum norms.

We see then

$$\|T(0) - 0\|_\rho = \|T(0)\|_\rho \leq \|(\mathcal{L}_\omega^{su} - Id)^{-1}\|_\rho \|\tilde{\mathcal{E}}_{red,\omega}^{us}\|_\rho \|(\mathcal{L}_\omega^u)^{-1}\|_\rho \leq \frac{\lambda}{1 - \lambda^2} \tilde{\sigma} = \mu.$$

The next step is finding  $L(\alpha)$  such that

$$\|T(Q_2^{su}) - T(Q_1^{su})\|_\rho \leq L(\alpha) \|Q_2^{su} - Q_1^{su}\|_\rho.$$

For that, we proceed directly

$$\begin{aligned} & \|T(Q_2^{su}) - T(Q_1^{su})\|_\rho \leq \\ & \leq \|(\mathcal{L}_\omega^{su} - Id)^{-1} \circ (-\tilde{\mathcal{E}}_{red,\omega}^{ss} Q_2^{su} + Q_{+2}^{su} (\tilde{\mathcal{E}}_{red,\omega}^{us} Q_2^{su} + \tilde{\mathcal{E}}_{red,\omega}^{uu}) - \tilde{\mathcal{E}}_{red,\omega}^{su}) \circ (\mathcal{L}_\omega^u)^{-1} \\ & \quad - (\mathcal{L}_\omega^{su} - Id)^{-1} \circ (-\tilde{\mathcal{E}}_{red,\omega}^{ss} Q_1^{su} + Q_{+1}^{su} (\tilde{\mathcal{E}}_{red,\omega}^{us} Q_1^{su} + \tilde{\mathcal{E}}_{red,\omega}^{uu}) - \tilde{\mathcal{E}}_{red,\omega}^{su}) \circ (\mathcal{L}_\omega^u)^{-1}\|_\rho \\ & \leq \frac{\lambda}{1 - \lambda^2} \| -\tilde{\mathcal{E}}_{red,\omega}^{ss} (Q_2^{su} - Q_1^{su}) + (Q_{+2}^{su} - Q_{+1}^{su}) \tilde{\mathcal{E}}_{red,\omega}^{uu} + Q_{+2}^{su} \tilde{\mathcal{E}}_{red,\omega}^{us} Q_2^{su} \\ & \quad - Q_{+2}^{su} \tilde{\mathcal{E}}_{red,\omega}^{us} Q_1^{su} - Q_{+1}^{su} \tilde{\mathcal{E}}_{red,\omega}^{us} Q_1^{su} + Q_{+2}^{su} \tilde{\mathcal{E}}_{red,\omega}^{us} Q_1^{su} \|_\rho \\ & \leq \frac{\lambda}{1 - \lambda^2} (2\tilde{\sigma} + 2\alpha\tilde{\sigma}) \|Q_2^{su} - Q_1^{su}\|_\rho \leq 2\mu(1 + \alpha) \|Q_2^{su} - Q_1^{su}\|_\rho, \end{aligned}$$

where we have used that  $\|Q_{1,2}^{su}\|_\rho \leq \alpha$ . So  $L(\alpha) = 2\mu(1 + \alpha)$  and we just have to check the

fixed point theorem's condition:

$$\frac{\mu}{\alpha} + 2\mu(1 + \alpha) - 1 \leq 0 \iff \mu + (2\mu - 1)\alpha + 2\mu\alpha^2 \leq 0$$

Solving for  $\alpha$  we obtain

$$\alpha_{\pm} = \frac{(1 - 2\mu) \pm \sqrt{-4\mu^2 - 4\mu + 1}}{4\mu},$$

for these solutions to exist we need a non-negative discriminant, so it is required

$$-4\mu^2 - 4\mu + 1 \geq 0,$$

and for that,  $\mu$  needs to satisfy

$$\mu < \frac{\sqrt{2} - 1}{2} = \frac{1}{2 + 2\sqrt{2}}.$$

By hypothesis 8),  $\mu < \frac{1}{2+2\sqrt{2}}$ , which means that  $\alpha$  solutions exist for the inequation of the fixed point theorem, and therefore there exists a fixed point of the operator  $T(Q^{su})$  and hence exists  $Q^{su}$ , which is the correction matrix for approximately invariant subbundles, implying the existence of actually invariant subbundles.

Recall as well from Remark 2.10 that the estimate given by Theorem 2.9 cannot be further improved, meaning that the fixed point is bounded by the radius of the ball within which it is contained. More specifically, it will be bounded by  $\alpha_-$ .

$$\|Q^{su}\|_{\rho} \leq \alpha_- = \frac{(1 - 2\mu) - \sqrt{-4\mu^2 - 4\mu + 1}}{4\mu} = \frac{2\mu}{(1 - 2\mu) + \sqrt{-4\mu^2 - 4\mu + 1}},$$

which is the distance between the approximate invariant subbundles and the invariant ones.  $\square$



# Chapter 3

## Fourier Series

Fourier series are widely known for being an excellent tool for alternative function representation. The capability of expressing function values using Fourier coefficients can be of great use when it comes to computation. And that is exactly why we need them. In order to easily manipulate points on a grid as we will have to when dealing with operations over the torus, it will be convenient to use their Fourier coefficients so simple transformations can be applied over exponentials. Since a computer cannot work with continuous arrays, we will also introduce the discrete version of Fourier series and an algorithm for a faster execution of such calculations. The statements and results from this chapter have been adapted from [11] and [3].

### 3.1 The Fourier Transform and the Discrete Fourier Transform

For an analytic functions  $u : \mathbb{T}_\rho \rightarrow \mathbb{C}$ , we write its the Fourier expansion as

$$u(\theta) = \sum_{k \in \mathbb{Z}} \hat{u}_k e^{2\pi i k \theta}, \quad \hat{u}_k = \int_0^1 u(\theta) e^{-2\pi i k \theta} d\theta$$

and we note the average of  $u$  as  $\langle u \rangle = \hat{u}_0 = \int_0^1 u(\theta) d\theta$ . Notice that  $\hat{u}_k^* = \hat{u}_{-k}$ , where  $\hat{u}_k^*$  denotes the complex conjugate of  $\hat{u}_k$ .

Then we consider the Fourier norm

$$\|u\|_{F, \rho} = \sum_{k \in \mathbb{Z}} |\hat{u}_k| e^{2\pi |k| \rho}.$$

We observe that  $\|u\|_\rho \leq \|u\|_{F, \rho}$ ,  $\forall \rho > 0$ .

Now we are ready to introduce the Discrete Fourier Transform and its properties. We provide the definition of Fourier series given any function  $f : \mathbb{T} \rightarrow \mathbb{C}$ :

$$f(\theta) = \sum_{k \in \mathbb{Z}} \hat{f}_k e^{2\pi i k \theta}$$

where the Fourier coefficients are given by the Fourier Transform (FT)

$$\hat{f}_k = \int_0^1 f(\theta) e^{-2\pi i k \theta} d\theta. \quad (3.1)$$

We consider a sample of points on the regular grid of size  $N \in \mathbb{N}$ ,  $\theta_j := \frac{j}{N}$ , where  $0 \leq j < N$ . This defines a sampling  $\{f_j\}$ , with  $f_j = f(\theta_j)$  and a total number of points  $N$ .

The integrals in (3.1) are approximated using the trapezoidal rule on the regular grid, obtaining the Discrete Fourier Transform (DFT)

$$\tilde{f}_k = \frac{1}{N} \sum_{j=0}^{N-1} f_j e^{-2\pi i k \theta_j}.$$

**Remark 3.1.**  $\tilde{f}_k$  can be defined for all  $k \in \mathbb{Z}$ . Moreover, they are periodic with period  $N$ ,  $\tilde{f}_{k+N} = \tilde{f}_k$ .

The function  $f$  is approximated by the discrete Fourier approximation

$$\tilde{f}(\theta) = \sum_{k=-\lfloor \frac{N}{2} \rfloor}^{\lfloor \frac{N-1}{2} \rfloor} \tilde{f}_k e^{2\pi i k \theta}.$$

Along this section, we will use the standard notation  $[x] = \max\{j \in \mathbb{Z} : j \leq x\}$  for the integer part of  $x$ .

**Remark 3.2.** The DFT approximation  $\tilde{f}(\theta)$  interpolates the data on the grid. That is  $\forall j = 0, \dots, N-1$ ,  $\tilde{f}(\theta_j) = f(\theta_j)$ .

Notice that the stated process turns the sampling of points on the grid onto the Fourier coefficients for the DFT. The inverse process will get the Fourier coefficients for the DFT and turn them onto the values on the grid. This process is called the Inverse Discrete Fourier Transform (IDFT) and uses the following formula

$$f_j = \sum_{k=0}^{N-1} \tilde{f}_k e^{\frac{2\pi i}{N} j k}.$$

**Remark 3.3.** As we have previously stated, the Fourier coefficients are symmetrical, that is,  $\hat{f}_k^* = \hat{f}_{-k}$ , which holds for the DFT coefficients as well,  $\tilde{f}_k^* = \tilde{f}_{-k}$ . This presents a problem regarding the way we have defined the DFT. See that since we are treating the real analytic case, our function  $f$  evaluated over the points of the grid will acquire real values, but depending on the parity of the size of the grid,  $N$ , the discrete approximation will not. The reason behind this phenomenon lies on the fact that if  $N$  is odd, due to the coefficients' symmetry, the resulting function will remain real, but if  $N$  is even, then  $N-1$  is odd, which means that the term  $-\lfloor \frac{N}{2} \rfloor$  of the sum, called the Nyquist term, will be unpaired. The lack of its symmetrical pair results on a complex function whose derivative will have the imaginary

term  $i$ . This does not present a major issue since the Nyquist term will naturally be very small. Nonetheless, if it is desired to look for a way to express the function  $f$  in terms of its DFT without this little problem, one shall eliminate the Nyquist term, thus obtaining

$$p(\theta) = \sum_{k=-\lfloor \frac{N-1}{2} \rfloor}^{\lfloor \frac{N-1}{2} \rfloor} \tilde{f}_k e^{2\pi i k \theta}.$$

Although this solves the previous issue, it presents another one, the main reason why we are not taking  $p$  in our process. Since we have set the Nyquist term to 0, this approximation will not interpolate the data on the grid, which is a property of great use to us. Thus we will keep using  $\tilde{f}$ .

## 3.2 Error Estimates on Approximations

### 3.2.1 Analytic Periodic Functions

As we have seen, there are discrete ways of expressing a function in terms of a trigonometric polynomial. The DFT supposes a great advantage for computing Fourier series with a machine. But of course, the loss of exact information when interpolating between grid points produces an approximation error. Coming up next we present the error between DFT coefficients and FT coefficients and the error when approximating a function with the DFT approximation.

**Lemma 3.4.** *Fixed the grid size  $N \in \mathbb{N}$ , the coefficients of the DFT are obtained from the coefficients of the FT by*

$$\tilde{f}_k = \sum_{m \in \mathbb{Z}} \hat{f}_{k+Nm}.$$

*Proof.* The proof for the Lemma starts by substituting  $f_j$  by its aforementioned Fourier series expression

$$\tilde{f}_k = \frac{1}{N} \sum_{j=0}^{N-1} f_j e^{-2\pi i k \theta_j} = \frac{1}{N} \sum_{j=0}^{N-1} \sum_{l \in \mathbb{Z}} \hat{f}_l e^{2\pi i l \theta_j} e^{-2\pi i k \theta_j} = \sum_{l \in \mathbb{Z}} \hat{f}_l \left( \frac{1}{N} \sum_{j=0}^{N-1} e^{2\pi i (l-k) \frac{j}{N}} \right).$$

Notice that  $\frac{1}{N} \sum_{j=0}^{N-1} e^{2\pi i (l-k) \frac{j}{N}} = 1$  if  $l - k$  is a multiple of  $N$  since  $\frac{l-k}{N}, j \in \mathbb{Z}$  and then

$$e^{2\pi i (l-k) \frac{j}{N}} = 1 \text{ and } \frac{1}{N} \sum_{j=0}^{N-1} e^{2\pi i (l-k) \frac{j}{N}} = \frac{1}{N} \sum_{j=0}^{N-1} 1 = 1.$$

Let's see now the case where  $l - k$  is not a multiple of  $N$ .

$$\frac{1}{N} \sum_{j=0}^{N-1} e^{2\pi i (l-k) \frac{j}{N}} = \frac{1}{N} \sum_{j=0}^{N-1} (e^{2\pi i \frac{(l-k)}{N}})^j = \frac{1}{N} \frac{1 - (e^{2\pi i \frac{(l-k)}{N}})^N}{1 - e^{2\pi i \frac{(l-k)}{N}}} = \frac{1}{N} \frac{1 - e^{2\pi i (l-k)}}{1 - e^{2\pi i \frac{(l-k)}{N}}}.$$

Since  $l - k \in \mathbb{Z}$ ,  $e^{2\pi i (l-k)} = 1$  and  $1 - e^{2\pi i (l-k)} = 0$ . By hypothesis,  $l - k$  is not a multiple of  $N$ , which means that  $1 - e^{2\pi i \frac{(l-k)}{N}} \neq 0$ .

Wrapping up, we have

$$\frac{1}{N} \sum_{j=0}^{N-1} e^{2\pi i(l-k)\frac{j}{N}} = \begin{cases} 1 & \text{if } l-k \text{ is a multiple of } N \\ 0 & \text{otherwise} \end{cases}.$$

This means that the first sum will only have terms if  $l - k = Nm$  for  $m \in \mathbb{Z}$ , that is for the terms  $l = k + Nm$  and hence

$$\tilde{f}_k = \sum_{l \in \mathbb{Z}} \hat{f}_l \left( \frac{1}{N} \sum_{j=0}^{N-1} e^{2\pi i(l-k)\frac{j}{N}} \right) = \sum_{m \in \mathbb{Z}} \hat{f}_{k+Nm}.$$

□

**Proposition 3.5.** *Let  $f : \mathbb{T}_{\hat{\rho}} \rightarrow \mathbb{C}$  be a real analytic and bounded function in the complex strip  $\mathbb{T}_{\hat{\rho}}$  of size  $\hat{\rho} > 0$ . Let  $\tilde{f}$  be the discrete Fourier approximation of  $f$  in the regular grid of size  $N \in \mathbb{N}$  with Fourier coefficients  $\tilde{f}_k$ . Then for  $k = -\lfloor \frac{N}{2} \rfloor, \dots, \lfloor \frac{N-1}{2} \rfloor$ ,*

$$|\tilde{f}_k - \hat{f}_k| \leq S_N^*(k, \hat{\rho}) \cdot \|f\|_{\hat{\rho}}$$

where

$$S_N^*(k, \hat{\rho}) = \frac{e^{-2\pi\hat{\rho}N}}{1 - e^{-2\pi\hat{\rho}N}} \left( e^{-2\pi\hat{\rho}k} + e^{2\pi\hat{\rho}k} \right).$$

*Proof.* Let  $k \in \mathbb{Z}$ . From Lemma 3.4 and the fact that  $|\hat{f}_k| \leq e^{-2\pi|k|\hat{\rho}} \|f\|_{\hat{\rho}}$ , we obtain

$$\begin{aligned} |\tilde{f}_k - \hat{f}_k| &= \left| \sum_{m \in \mathbb{Z}} \hat{f}_{k+Nm} - \hat{f}_k \right| = \left| \sum_{m \in \mathbb{Z} \setminus \{0\}} \hat{f}_{k+Nm} \right| \leq \\ &\leq \sum_{m \in \mathbb{Z} \setminus \{0\}} |\hat{f}_{k+Nm}| \leq \sum_{m \in \mathbb{Z} \setminus \{0\}} e^{-2\pi\hat{\rho}|k+Nm|} \cdot \|f\|_{\hat{\rho}}. \end{aligned}$$

Then, we define

$$S_N^*(k, \hat{\rho}) = \sum_{m \in \mathbb{Z} \setminus \{0\}} e^{-2\pi\hat{\rho}|k+Nm|}$$

so we have  $|\tilde{f}_k - \hat{f}_k| \leq S_N^*(k, \hat{\rho}) \cdot \|f\|_{\hat{\rho}}$ . Notice that for  $k = -\lfloor \frac{N}{2} \rfloor, \dots, \lfloor \frac{N-1}{2} \rfloor$ , if  $m > 0$ ,  $k + Nm > 0$ , and if  $m < 0$ ,  $k + Nm < 0$ . We must find then a suitable expression for  $S_N^*(k, \hat{\rho})$ , so

$$\begin{aligned} S_N^*(k, \hat{\rho}) &= \sum_{m>0} e^{-2\pi\hat{\rho}(k+Nm)} + \sum_{m<0} e^{-2\pi\hat{\rho}(-k-Nm)} = e^{-2\pi\hat{\rho}k} \sum_{m>0} e^{-2\pi\hat{\rho}Nm} + e^{2\pi\hat{\rho}k} \sum_{m<0} e^{2\pi\hat{\rho}Nm} \\ &\leq e^{-2\pi\hat{\rho}k} \sum_{m>0} e^{-2\pi\hat{\rho}Nm} + e^{2\pi\hat{\rho}k} \sum_{m>0} e^{-2\pi\hat{\rho}Nm} = \frac{e^{-2\pi\hat{\rho}N}}{1 - e^{-2\pi\hat{\rho}N}} \left( e^{-2\pi\hat{\rho}k} + e^{2\pi\hat{\rho}k} \right). \end{aligned}$$

□

**Theorem 3.6.** *Let  $f : \mathbb{T}_{\hat{\rho}} \rightarrow \mathbb{C}$  be an analytic and bounded function in the complex strip  $\mathbb{T}_{\hat{\rho}}$  of size  $\hat{\rho} > 0$ . Let  $\tilde{f}$  be the discrete Fourier approximation of  $f$  in the regular grid of size  $N$  even. Then, for  $0 \leq \rho < \hat{\rho}$ , we have*

$$\|\tilde{f} - f\|_{\rho} \leq C_N(\rho, \hat{\rho}) \cdot \|f\|_{\hat{\rho}}$$

where

$$C_N(\rho, \hat{\rho}) = S_N^{*1}(\rho, \hat{\rho}) + S_N^{*2}(\rho, \hat{\rho}) + T_N(\rho, \hat{\rho})$$

with

$$\begin{aligned} S_N^{*1}(\rho, \hat{\rho}) &= \frac{e^{-2\pi\hat{\rho}N}}{1 - e^{-2\pi\hat{\rho}N}} \frac{e^{-2\pi(\hat{\rho}+\rho)} + 1}{e^{-2\pi(\hat{\rho}+\rho)} - 1} \left(1 - e^{\pi(\hat{\rho}+\rho)N}\right), \\ S_N^{*2}(\rho, \hat{\rho}) &= \frac{e^{-2\pi\hat{\rho}N}}{1 - e^{-2\pi\hat{\rho}N}} \frac{e^{2\pi(\hat{\rho}-\rho)} + 1}{e^{2\pi(\hat{\rho}-\rho)} - 1} \left(1 - e^{-\pi(\hat{\rho}-\rho)N}\right), \\ T_N(\rho, \hat{\rho}) &= \frac{e^{2\pi(\hat{\rho}-\rho)} + 1}{e^{2\pi(\hat{\rho}-\rho)} - 1} e^{-\pi(\hat{\rho}-\rho)N}. \end{aligned}$$

*Proof.* From the definition of the discrete Fourier approximation  $\tilde{f}$  of  $f$ , we have

$$\|\tilde{f} - f\|_{\rho} \leq \sum_{k=-\frac{N}{2}}^{\frac{N}{2}-1} |\tilde{f}_k - \hat{f}_k| e^{2\pi\rho|k|} + \sum_{k=-\infty}^{-\frac{N}{2}-1} |\hat{f}_k| e^{-2\pi\rho k} + \sum_{k=\frac{N}{2}}^{\infty} |\hat{f}_k| e^{2\pi\rho k}.$$

From Proposition 3.5 and the growth rate properties of the Fourier coefficients of an analytic function, we get

$$\|\tilde{f} - f\|_{\rho} \leq (S_N^*(\rho, \hat{\rho}) + T_N(\rho, \hat{\rho})) \cdot \|f\|_{\hat{\rho}}$$

where

$$S_N^*(\rho, \hat{\rho}) = \sum_{k=-\frac{N}{2}}^{\frac{N}{2}-1} S_N^*(k, \hat{\rho}) e^{2\pi\rho|k|}$$

and

$$T_N(\rho, \hat{\rho}) = \sum_{k=-\infty}^{-\frac{N}{2}-1} e^{2\pi(\hat{\rho}-\rho)k} + \sum_{k=\frac{N}{2}}^{\infty} e^{-2\pi(\hat{\rho}-\rho)k}.$$

Let's express  $T_N(\rho, \hat{\rho})$  in computable terms. Notice that

$$\begin{aligned} T_N(\rho, \hat{\rho}) &= e^{-2\pi(\hat{\rho}-\rho)k\frac{N}{2}} + 2 \sum_{k=\frac{N}{2}+1}^{\infty} e^{-2\pi(\hat{\rho}-\rho)k} = e^{-2\pi(\hat{\rho}-\rho)k\frac{N}{2}} + 2 \frac{e^{-2\pi(\hat{\rho}-\rho)(\frac{N}{2}+1)}}{1 - e^{-2\pi(\hat{\rho}-\rho)}} \\ &= e^{-\pi(\hat{\rho}-\rho)N} \frac{1 + e^{-2\pi(\hat{\rho}-\rho)}}{1 - e^{-2\pi(\hat{\rho}-\rho)}} = \frac{e^{2\pi(\hat{\rho}-\rho)} + 1}{e^{2\pi(\hat{\rho}-\rho)} - 1} e^{-\pi(\hat{\rho}-\rho)N}. \end{aligned}$$

Using the results obtained in Proposition 3.5 we compute

$$\begin{aligned} S_N^*(\rho, \hat{\rho}) &= \sum_{k=-\frac{N}{2}}^{\frac{N}{2}-1} S_N^*(k, \hat{\rho}) e^{2\pi\rho|k|} \leq \sum_{k=-\frac{N}{2}}^{\frac{N}{2}-1} \frac{e^{-2\pi\hat{\rho}N}}{1 - e^{-2\pi\hat{\rho}N}} \left( e^{-2\pi\hat{\rho}k} + e^{2\pi\hat{\rho}k} \right) e^{2\pi\rho|k|} \\ &= \frac{e^{-2\pi\hat{\rho}N}}{1 - e^{-2\pi\hat{\rho}N}} \sum_{k=-\frac{N}{2}}^{\frac{N}{2}-1} \left( e^{-2\pi\hat{\rho}k} + e^{2\pi\hat{\rho}k} \right) e^{2\pi\rho|k|}. \end{aligned}$$

Let's compute the last sum. It is equal to

$$\begin{aligned} &\left( e^{2\pi\hat{\rho}\frac{N}{2}} + e^{-2\pi\hat{\rho}\frac{N}{2}} \right) e^{2\pi\rho\frac{N}{2}} + \sum_{k=-\frac{N}{2}+1}^{\frac{N}{2}-1} \left( e^{-2\pi\hat{\rho}k} + e^{2\pi\hat{\rho}k} \right) e^{2\pi\rho|k|} \\ &= \left( e^{\pi(\hat{\rho}+\rho)N} + e^{-\pi(\hat{\rho}-\rho)N} \right) + 2 + 2 \sum_{k=1}^{\frac{N}{2}-1} \left( e^{-2\pi\hat{\rho}k} + e^{2\pi\hat{\rho}k} \right) e^{2\pi\rho k} \\ &= e^{\pi(\hat{\rho}+\rho)N} + e^{-\pi(\hat{\rho}-\rho)N} + 2 + 2e^{-2\pi(\hat{\rho}-\rho)} \frac{e^{-2\pi(\hat{\rho}-\rho)(\frac{N}{2}-1)} - 1}{e^{-2\pi(\hat{\rho}-\rho)} - 1} + 2e^{2\pi(\hat{\rho}+\rho)} \frac{e^{2\pi(\hat{\rho}+\rho)(\frac{N}{2}-1)} - 1}{e^{2\pi(\hat{\rho}+\rho)} - 1} \\ &= 2 + \frac{e^{-2\pi(\hat{\rho}-\rho)-\pi(\hat{\rho}-\rho)N} - e^{-\pi(\hat{\rho}-\rho)N} + 2e^{-\pi(\hat{\rho}-\rho)N} - 2e^{-2\pi(\hat{\rho}-\rho)} + e^{-\pi(\hat{\rho}-\rho)N}}{e^{-2\pi(\hat{\rho}-\rho)}} \\ &\quad + \frac{e^{2\pi(\hat{\rho}+\rho)+\pi(\hat{\rho}+\rho)N} - e^{\pi(\hat{\rho}+\rho)N} + 2e^{\pi(\hat{\rho}+\rho)N} - 2e^{2\pi(\hat{\rho}+\rho)}}{e^{2\pi(\hat{\rho}+\rho)}} \\ &= \frac{e^{-\pi(\hat{\rho}-\rho)N} (1 + e^{-2\pi(\hat{\rho}-\rho)}) - (1 + e^{-2\pi(\hat{\rho}-\rho)})}{e^{-2\pi(\hat{\rho}-\rho)} - 1} + \frac{e^{\pi(\hat{\rho}+\rho)N} (1 + e^{2\pi(\hat{\rho}+\rho)}) - (1 + e^{2\pi(\hat{\rho}+\rho)})}{e^{2\pi(\hat{\rho}+\rho)} - 1} \\ &= \left( 1 - e^{-\pi(\hat{\rho}-\rho)N} \right) \frac{1 + e^{-2\pi(\hat{\rho}-\rho)}}{1 - e^{-2\pi(\hat{\rho}-\rho)}} + \left( e^{\pi(\hat{\rho}+\rho)N} - 1 \right) \frac{1 + e^{-2\pi(\hat{\rho}+\rho)}}{1 - e^{-2\pi(\hat{\rho}+\rho)}} \\ &= \frac{e^{-2\pi(\hat{\rho}+\rho)} + 1}{e^{-2\pi(\hat{\rho}+\rho)} - 1} \left( 1 - e^{\pi(\hat{\rho}+\rho)N} \right) + \frac{e^{2\pi(\hat{\rho}-\rho)} + 1}{e^{2\pi(\hat{\rho}-\rho)} - 1} \left( 1 - e^{-\pi(\hat{\rho}-\rho)N} \right). \end{aligned}$$

Hence we have that

$$S_N^*(\rho, \hat{\rho}) = \frac{e^{-2\pi\hat{\rho}N}}{1 - e^{-2\pi\hat{\rho}N}} \left( \frac{e^{-2\pi(\hat{\rho}+\rho)} + 1}{e^{-2\pi(\hat{\rho}+\rho)} - 1} \left( 1 - e^{\pi(\hat{\rho}+\rho)N} \right) + \frac{e^{2\pi(\hat{\rho}-\rho)} + 1}{e^{2\pi(\hat{\rho}-\rho)} - 1} \left( 1 - e^{-\pi(\hat{\rho}-\rho)N} \right) \right).$$

Which finally gives us

$$\begin{aligned} S_N^{*1}(\rho, \hat{\rho}) &= \frac{e^{-2\pi\hat{\rho}N}}{1 - e^{-2\pi\hat{\rho}N}} \frac{e^{-2\pi(\hat{\rho}+\rho)} + 1}{e^{-2\pi(\hat{\rho}+\rho)} - 1} \left( 1 - e^{\pi(\hat{\rho}+\rho)N} \right), \\ S_N^{*2}(\rho, \hat{\rho}) &= \frac{e^{-2\pi\hat{\rho}N}}{1 - e^{-2\pi\hat{\rho}N}} \frac{e^{2\pi(\hat{\rho}-\rho)} + 1}{e^{2\pi(\hat{\rho}-\rho)} - 1} \left( 1 - e^{-\pi(\hat{\rho}-\rho)N} \right). \end{aligned}$$

□

**Remark 3.7.** We have proved the case in which  $N$  is even since in our implementation we will choose our  $N$  even. As we will soon see, the fact that  $N$  is even (and furthermore, a power of two) speeds the calculations up for a certain type of transform, the Fast Fourier Transform (FFT). The proof for the case in which  $N$  is odd can be found in [11], and a more general proof for a multi-dimensional scenario can be found in [3].

### 3.2.2 Matrices of Periodic Functions

In this section we will focus on the control of the propagation error when we perform matrix operations, mainly products and inverses. The procedures for other operations are analogous. The results hereby presented are no more than consequences of Theorem 3.6 from the previous section.

**Corollary 3.8.** *Let us consider two matrix functions  $A : \mathbb{T} \rightarrow \mathbb{C}^{m_1 \times m_2}$ , and  $B : \mathbb{T} \rightarrow \mathbb{C}^{m_2 \times m_3}$ , such that their entries are analytic and bounded functions in the complex strip  $\mathbb{T}_{\hat{\rho}}$  of size  $\hat{\rho} > 0$ . We denote by  $AB$  the product matrix and  $\widetilde{AB}$  the corresponding approximation given by DFT. Given a grid of size  $N \in \mathbb{N}$ , we evaluate  $A$  and  $B$  in the grid, and we interpolate the points  $AB(\theta_j) = A(\theta_j)B(\theta_j)$ . Then, we have*

$$\|AB - \widetilde{AB}\|_{\rho} \leq C_N(\rho, \hat{\rho}) \|A\|_{\hat{\rho}} \|B\|_{\hat{\rho}}$$

for every  $0 \leq \rho < \hat{\rho}$ .

**Corollary 3.9.** *Let us consider a matrix function  $A : \mathbb{T} \rightarrow \mathbb{C}^{m \times m}$  whose entries are analytic and bounded functions in the complex strip  $\mathbb{T}_{\hat{\rho}}$  of size  $\hat{\rho} > 0$ . Given a grid of size  $N \in \mathbb{N}$ , we evaluate  $A$  in the grid and compute the inverses  $X(\theta_j) = A(\theta_j)^{-1}$ . Then, if  $\widetilde{X}$  is the corresponding discrete Fourier approximation associated with the sample  $X(\theta_j)$ , the error  $E(\theta) = Id_m - A(\theta)\widetilde{X}(\theta)$  satisfies*

$$\|E\|_{\rho} \leq C_N(\rho, \hat{\rho}) \|A\|_{\hat{\rho}} \|\widetilde{X}\|_{\hat{\rho}}$$

for  $0 \leq \rho < \hat{\rho}$ . Moreover, if  $\|E\|_{\rho} < 1$ , there exists an analytic inverse  $A^{-1} : \mathbb{T} \rightarrow \mathbb{C}^{m \times m}$  satisfying

$$\|A^{-1} - \widetilde{X}\|_{\rho} \leq \frac{\|\widetilde{X}\|_{\hat{\rho}} \|E\|_{\rho}}{1 - \|E\|_{\rho}}.$$

*Proof.* To obtain the first inequality of the Corollary, we observe that if  $\widetilde{A\widetilde{X}}$  is the discrete Fourier approximation of  $A\widetilde{X}$ , then it turns out that

$$(A\widetilde{X})(\theta_j) = A(\theta_j)\widetilde{X}(\theta_j) = Id_m$$

for all points in the grid. This implies that  $\widetilde{A\widetilde{X}} = Id_m$ , and we end up with

$$\|E\|_{\rho} = \|Id_m - A\widetilde{X}\|_{\rho} = \|\widetilde{A\widetilde{X}} - A\widetilde{X}\|_{\rho}$$

and the inequality follows applying Corollary 3.8. The second inequality follows from the expression  $E = Id_m - A\tilde{X}$ , simply writing  $A^{-1} = \tilde{X}(Id_m - E)^{-1}$  and using a Neumann series argument. □

### 3.3 The Fast Fourier Transform

A Fast Fourier Transform (FFT) is an implementation algorithm for the Discrete Fourier Transform (DFT) but with a significant decrease of computational cost. Even though the number of operations of a regular DFT has a  $O(N^2)$  order, the number of operations for the FFT has a  $O(N \log N)$  order. There are several algorithms that are able to achieve such low computational cost, but the most common and used is the Cooley-Tukey FFT algorithm, which is the one we are going to explain in this section (as extracted from [7]).

The main idea of the Cooley-Tukey algorithm is to break down a DFT of any composite size  $N = N_1 N_2$  into many smaller DFTs of sizes  $N_1$  and  $N_2$ . This allows us to combine this algorithm with any other algorithm for the DFT, for instance algorithms that are able to handle large prime factors that cannot be decomposed by Cooley-Tukey.

The decomposition we are going to explain is the one used in the best known use of the Cooley-Tukey algorithm. It divides the transform into two pieces of size  $N/2$  at each step, which limits itself to values of  $N = 2^p$  for  $p \in \mathbb{N}$ . This is not a problem in general since the number of sample points  $N$  can usually be chosen freely. This decomposition is called the radix-2 case, and for other factorizations of  $N$  we call them the mixed-radix cases or split-radix.

The radix-2 decimation-in-time (DIT) FFT divides a DFT of size  $N$  into two interleaved DFTs of size  $N/2$  with each recursive stage.

The DFT is defined, as we have previously seen, by the formula

$$\tilde{f}_k = \frac{1}{N} \sum_{j=0}^{N-1} f_j e^{-\frac{2\pi i}{N} j k}.$$

The radix-2 DIT first computes the DFTs of the even-indexed inputs ( $f_{2m} = f_0, f_2, \dots, f_{N-2}$ ) and of the odd-indexed inputs ( $f_{2m+1} = f_1, f_3, \dots, f_{N-1}$ ), and then combines those two results to produce the DFT of the whole sequence. The algorithm rearranges the DFT of the function  $f_j$  into a sum over the even-numbered indices  $j = 2m$  and a sum over the odd-numbered indices  $j = 2m + 1$ .

$$\begin{aligned}
\tilde{f}_k &= \frac{1}{2} \left( \frac{1}{N/2} \sum_{m=0}^{N/2-1} f_{2m} e^{-\frac{2\pi i}{N}(2m)k} \right) + \frac{1}{2} \left( \frac{1}{N/2} \sum_{m=0}^{N/2-1} f_{2m+1} e^{-\frac{2\pi i}{N}(2m+1)k} \right) \\
&= \frac{1}{2} \left( \frac{1}{N/2} \sum_{m=0}^{N/2-1} f_{2m} e^{-\frac{2\pi i}{N/2}mk} \right) + \frac{1}{2} e^{-\frac{2\pi i}{N}k} \left( \frac{1}{N/2} \sum_{m=0}^{N/2-1} f_{2m+1} e^{-\frac{2\pi i}{N/2}mk} \right) \\
&= \frac{1}{2} E_k + \frac{1}{2} e^{-\frac{2\pi i}{N}k} O_k.
\end{aligned}$$

It is clear that the sums within the last two parentheses are the DFT of the even-indexed part  $f_{2m}$  and the DFT of odd-indexed part  $f_{2m+1}$  of the function  $f_j$ . We can denote the DFT of the even-indexed part  $f_{2m}$  by  $E_k$  and the DFT of the odd-indexed part by  $O_k$  and simplify the resulting expression.

Taking advantage of the periodicity of the DFT, we know that  $E_{k+\frac{N}{2}} = E_k$  and  $O_{k+\frac{N}{2}} = O_k$  if  $k < N/2$ . Thus, we can rewrite the previous equation as

$$\tilde{f}_k = \begin{cases} \frac{1}{2} E_k + \frac{1}{2} e^{-\frac{2\pi i}{N}k} O_k, & \text{for } 0 \leq k < N/2 \\ \frac{1}{2} E_{k-N/2} + \frac{1}{2} e^{-\frac{2\pi i}{N}k} O_{k-N/2}, & \text{for } N/2 \leq k < N. \end{cases}$$

Noticing that

$$e^{-\frac{2\pi i}{N}(k+N/2)} = e^{-\frac{2\pi i}{N}k - \pi i} = e^{-\pi i} e^{-\frac{2\pi i}{N}k} = -e^{-\frac{2\pi i}{N}k}$$

we can express  $\tilde{f}_k$  as

$$\begin{aligned}
\tilde{f}_k &= \frac{1}{2} E_k + \frac{1}{2} e^{-\frac{2\pi i}{N}k} O_k & \text{for } 0 \leq k < N/2, \\
\tilde{f}_{k+N/2} &= \frac{1}{2} E_k - \frac{1}{2} e^{-\frac{2\pi i}{N}k} O_k & \text{for } 0 \leq k < N/2.
\end{aligned}$$

Applying this method recursively, splitting into two half-size DFTs, gives a final output of a combination of  $E_k$  and  $e^{-\frac{2\pi i}{N}k} O_k$ , which is a very simple size-2 DFT. This procedure can reduce the overall runtime of the DFT, which is  $O(N^2)$ , to  $O(N \log N)$ , and moreover, increase the precision of the final results.

Notice that, even though we have explained the Cooley-Tukey algorithm to transform grid points into Fourier coefficients, the algorithm works as well for the inverse process. The only difference in the procedure is the disappearance of the  $1/N$  factor and the change of sign of the exponent of the complex exponential, given that the formula for the IDFT, as we stated previously, is

$$f_j = \sum_{k=0}^{N-1} \tilde{f}_k e^{\frac{2\pi i}{N}jk}.$$

Thus, the factor  $1/2$  preceding the sums also disappears, leaving us the formula

$$f_k = \sum_{m=0}^{N/2-1} \tilde{f}_{2m} e^{\frac{2\pi i}{N}(2m)k} + \sum_{m=0}^{N/2-1} \tilde{f}_{2m+1} e^{\frac{2\pi i}{N}(2m+1)k}.$$

Manipulating these terms in the same way we previously did, we obtain

$$f_k = \sum_{m=0}^{N/2-1} \tilde{f}_{2m} e^{\frac{2\pi i}{N/2}m k} + e^{\frac{2\pi i}{N}k} \sum_{m=0}^{N/2-1} \tilde{f}_{2m+1} e^{\frac{2\pi i}{N/2}m k} = \tilde{E}_k + e^{\frac{2\pi i}{N}k} \tilde{O}_k.$$

Again,  $\tilde{E}_{k+\frac{N}{2}} = \tilde{E}_k$  and  $\tilde{E}_{k+\frac{N}{2}} = \tilde{O}_k$  for  $k < N/2$ . We can now express  $f_k$  as

$$f_k = \begin{cases} \tilde{E}_k + e^{\frac{2\pi i}{N}k} \tilde{O}_k, & \text{for } 0 \leq k < N/2 \\ \tilde{E}_{k-N/2} + e^{\frac{2\pi i}{N}k} \tilde{O}_{k-N/2}, & \text{for } N/2 \leq k < N. \end{cases}$$

This time we have

$$e^{\frac{2\pi i}{N}(k+N/2)} = e^{\frac{2\pi i}{N}k + \pi i} = e^{\pi i} e^{\frac{2\pi i}{N}k} = -e^{\frac{2\pi i}{N}k}$$

Which finally gives us

$$\begin{aligned} f_k &= \tilde{E}_k + e^{\frac{2\pi i}{N}k} \tilde{O}_k & \text{for } 0 \leq k < N/2, \\ f_{k+N/2} &= \tilde{E}_k - e^{\frac{2\pi i}{N}k} \tilde{O}_k & \text{for } N/2 \leq k < N. \end{aligned}$$

## Chapter 4

# Computer Assisted Proof

In this section we will introduce the procedure for which invariant tori are validated with a computer. Such validation consists of a computer program in C code that receives a torus (among other inputs) and checks whether it fulfills the conditions of the validation Theorem 2.11. If so, the computer gives a green light for the affirmation of the existence of an invariant torus close to the approximately invariant one given in our input. During this validation process, the computer will have to handle error bounds (such as the invariance error bound or the reducibility error bound), which will possibly lead to the manipulation of very small numbers. In order to keep precision, we will use interval arithmetic so our bounds are precisely enclosed in a small range interval. This forces us to work with multi-precision and interval arithmetic packages, which are handled quite differently than regular double precision numbers.

The key point of the validation is the correspondence between Fourier coefficients and grid points of our torus. The ability to easily move from one space to the other using Fourier transforms (such as the FFT) will allow us to perform long or complicated calculations in a matter of just a multiplication by a constant (as in the case of the rotation) or other very simple and fast operations. Although this sounds very appealing, there is always a drawback. When performing certain operations on Fourier space, the correspondence with the grid points might be broken. Those situations may arise both when operating with matrices and when operating with vectors, and that is when we can make use of the results found in the dedicated Fourier chapter. In such cases one will have to proceed with care, handling properly the errors committed in those situations using high precision calculations.

In addition, a brief section on interval arithmetic is presented, so the reader can understand what is happening in the validation code when dealing with intervals.

Of course, an outline of the programming procedure is given at the end of the chapter so one can grasp the idea that the code is following.

## 4.1 Computation of Error Bounds

Given that we are working with quasi-periodically forced systems on complex environments, it is not straight-forward to make the computer perform some mathematical tasks, such as the calculation of the rotated torus on a complex environment of the grid. For such manipulations, Fourier transforms are commonly used, so it is easier to perform, following the same example, the rotation on the torus between the Fourier coefficients obtained from the points on the grid than applying the rotation directly on the grid points. Clearly there is a correspondence between grid points and Fourier coefficients given by the Fourier transform, but such relation can be broken when applying operations such matrix inversions or matrix products. In those cases, one has to proceed with caution, calculating the error produced in terms of Fourier transformations and taking them into account when bounding errors. And that is precisely what this section is all about, finding computable expressions for our one-dimensional objects so the invariance and reducibility errors can be properly bounded by a computer.

**Remark 4.1.** Keep in mind that under the same Finsler norm, the errors produced are the same even if changing the  $\theta$  support point of our torus. This means that in order to simplify calculations, for instance, we will take the invariance error as

$$E(\theta) = P_2(\theta + \omega)(F(K_0(\theta), \theta) - K_0(\theta + \omega))$$

instead of

$$E(\theta) = P_2(\theta)(F(K_0(\theta - \omega), \theta - \omega) - K_0(\theta)).$$

### 4.1.1 The Invariance Error Bound

Keeping the same notation as in the validation theorem for our analytic map  $F$  and our analytic approximately invariant torus  $K_0$ , we can write the error produced in the invariance equation as

$$E(\theta) = P_2(\theta + \omega)(F(K_0(\theta), \theta) - K_0(\theta + \omega)).$$

Notice that  $P_2$  will be one of our inputs, provided therefore in the shape of a matrix of periodic functions, that is, truncated Fourier series, the type of object with which we will usually operate.

$$\begin{aligned}
P_2(\theta) &= \begin{pmatrix} \sum_{k=-\lfloor \frac{N-1}{2} \rfloor}^{\lfloor \frac{N-1}{2} \rfloor} p_{1,1,k,2} e^{2\pi i k \theta} & \cdots & \sum_{k=-\lfloor \frac{N-1}{2} \rfloor}^{\lfloor \frac{N-1}{2} \rfloor} p_{1,n,k,2} e^{2\pi i k \theta} \\ \vdots & \ddots & \vdots \\ \sum_{k=-\lfloor \frac{N-1}{2} \rfloor}^{\lfloor \frac{N-1}{2} \rfloor} p_{n,1,k,2} e^{2\pi i k \theta} & \cdots & \sum_{k=-\lfloor \frac{N-1}{2} \rfloor}^{\lfloor \frac{N-1}{2} \rfloor} p_{n,n,k,2} e^{2\pi i k \theta} \end{pmatrix} \\
&= \sum_{k=-\lfloor \frac{N-1}{2} \rfloor}^{\lfloor \frac{N-1}{2} \rfloor} \begin{pmatrix} p_{1,1,k,2} & \cdots & p_{1,n,k,2} \\ \vdots & \ddots & \vdots \\ p_{n,1,k,2} & \cdots & p_{n,n,k,2} \end{pmatrix} e^{2\pi i k \theta}.
\end{aligned}$$

Since our theorem's main input object is the approximately invariant torus, we will take it also as a finite sum, and in case we pick  $N$  even, the Nyquist term will already be set to 0.

**Remark 4.2.** It is true that we have previously said that we have to take into account the error committed when we break the correspondence between grid points and Fourier coefficients, which is precisely what happens when we set the Nyquist term to 0. However, when doing so, we are just claiming that the object to be validated is the torus given in Fourier space with the Nyquist term set to 0. That means, that the previous torus evaluated on the grid is no longer our main object of study, and therefore no correspondence is broken.

Such torus will have the form

$$K_0(\theta) = \sum_{k=-\lfloor \frac{N}{2} \rfloor}^{\lfloor \frac{N-1}{2} \rfloor} \tilde{K}_{0,k} e^{2\pi i k \theta} = \sum_{k=-\lfloor \frac{N-1}{2} \rfloor}^{\lfloor \frac{N-1}{2} \rfloor} \tilde{K}_{0,k} e^{2\pi i k \theta}.$$

This expression is very useful since we can now easily obtain an analogous expression for  $K_0(\theta + \omega)$ ,

$$K_0(\theta + \omega) = \sum_{k=-\lfloor \frac{N-1}{2} \rfloor}^{\lfloor \frac{N-1}{2} \rfloor} (\tilde{K}_{0,k} e^{2\pi i k \omega}) e^{2\pi i k \theta}.$$

We should keep in mind that our main goal in this section is to find a computable value for the error bound of the invariance equation, which will lead us at some point to manipulate the function  $F(K_0(\theta), \theta)$  and its norm. Since the Fourier series of  $\varphi(\theta) = F(K_0(\theta), \theta)$  is an infinite sum, we would like to approximate it by a finite sum

$$\tilde{\varphi}(\theta) = \sum_{k=-\lfloor \frac{N}{2} \rfloor}^{\lfloor \frac{N-1}{2} \rfloor} \tilde{\varphi}_k e^{2\pi i k \theta}.$$

Then, we want to obtain a rigorous bound of  $\|\varphi(\theta) - \tilde{\varphi}(\theta)\|_\rho$ .

Recalling now the invariance error equation, by taking norms, separating the  $P_2(\theta + \omega)$  term and adding and subtracting  $\tilde{\varphi}(\theta)$  we see that,

$$\|E(\theta)\|_\rho \leq \|P_2(\theta + \omega)\|_\rho (\|F(K_0(\theta), \theta) - \tilde{\varphi}(\theta)\|_\rho + \|\tilde{\varphi}(\theta) - K_0(\theta + \omega)\|_\rho) .$$

For a given  $\hat{\rho} > \rho$  such that  $\{(K_0(\theta), \theta) \mid \theta \in \bar{\mathbb{T}}_{\hat{\rho}}\} \subset \mathcal{U}$ , where  $\mathcal{U}$  is the domain of  $F$ , using Theorem 3.6 we have

$$\|F(K_0(\theta), \theta) - \tilde{\varphi}(\theta)\|_\rho = \|\varphi(\theta) - \tilde{\varphi}(\theta)\|_\rho \leq C_N(\rho, \hat{\rho}) \|\varphi\|_{\hat{\rho}} \leq C_N(\rho, \hat{\rho}) \|F(K_0(\theta), \theta)\|_{\hat{\rho}} .$$

We have then left to calculate the second term of the sum, which follows

$$\begin{aligned} \|\tilde{\varphi}(\theta) - K_0(\theta + \omega)\|_\rho &= \left\| \sum_{k=-\lfloor \frac{N}{2} \rfloor}^{\lfloor \frac{N-1}{2} \rfloor} (\tilde{\varphi}_k - \tilde{K}_{0,k} e^{2\pi i k \omega}) e^{2\pi i k \theta} \right\|_\rho \\ &\leq \left\| \sum_{k=-\lfloor \frac{N}{2} \rfloor}^{\lfloor \frac{N-1}{2} \rfloor} (\tilde{\varphi}_k - \tilde{K}_{0,k} e^{2\pi i k \omega}) e^{2\pi i k \theta} \right\|_{F, \rho} \leq \tilde{\varepsilon} . \end{aligned}$$

Then we find

$$\|P_2(\theta + \omega)(F(K_0(\theta), \theta) - K_0(\theta + \omega))\|_\rho \leq \|P_2(\theta + \omega)\|_\rho (C_N(\rho, \hat{\rho}) \|F(K_0(\theta), \theta)\|_{\hat{\rho}} + \tilde{\varepsilon}) \leq \varepsilon ,$$

where  $\varepsilon$  is the invariance bound in Theorem 2.11, and  $C_N(\rho, \hat{\rho})$ , even though it depends on the system, is very small.

#### 4.1.2 The Reducibility Error Bound

The next bound to be computed is the reducibility error bound, where the reducibility error is given by

$$E_{red}(\theta) = P_2(\theta + \omega)M_0(\theta)P_1(\theta) - \Lambda(\theta) ,$$

with  $M_0(\theta) = DF(K_0(\theta), \theta)$ . Clearly, there are more objects in this equation than in the previous one, so we must know first how are we going to deal with each one of them.

Our first inputs will be, then, the matrix valued maps  $P_1, P_2 : \bar{\mathbb{T}}_\rho \rightarrow M_n(\mathbb{C})$ . Since we already showed  $P_2$ , we can directly say that  $P_1$  will have the same form

$$P_1(\theta) = \sum_{k=-\lfloor \frac{N-1}{2} \rfloor}^{\lfloor \frac{N-1}{2} \rfloor} \begin{pmatrix} p_{1,1,k,1} & \cdots & p_{1,n,k,1} \\ \vdots & \ddots & \vdots \\ p_{n,1,k,1} & \cdots & p_{n,n,k,1} \end{pmatrix} e^{2\pi i k \theta} .$$

Next we have our analytic block-diagonal matrix-valued map

$$\Lambda(\theta) = \begin{pmatrix} \Lambda^s(\theta) & 0 \\ 0 & \Lambda^u(\theta) \end{pmatrix}$$

where  $\Lambda^s : \bar{\mathbb{T}}_\rho \rightarrow M_{n_s}(\mathbb{C})$  and  $\Lambda^u : \bar{\mathbb{T}}_\rho \rightarrow M_{n_u}(\mathbb{C})$ , with  $n = n_s + n_u$  into which we want to reduce our system. Again, this can be expressed as

$$\Lambda(\theta) = \sum_{k=-\lfloor \frac{N-1}{2} \rfloor}^{\lfloor \frac{N-1}{2} \rfloor} \begin{pmatrix} \lambda_{1,1,k} & \cdots & \lambda_{1,n_s,k} & 0 & \cdots & 0 \\ \vdots & \ddots & \vdots & \vdots & \ddots & \vdots \\ \lambda_{n_s,1,k} & \cdots & \lambda_{n_s,n_s,k} & 0 & \cdots & 0 \\ 0 & \cdots & 0 & \lambda_{n_s+1,n_s+1,k} & \cdots & \lambda_{n_s+1,n,k} \\ \vdots & \ddots & \vdots & \vdots & \ddots & \vdots \\ 0 & \cdots & 0 & \lambda_{n,n_s+1,k} & \cdots & \lambda_{n,n,k} \end{pmatrix} e^{2\pi i k \theta}.$$

All in all, we can think as these inputs as matrices of Fourier coefficients that can be turned into points on the grid by an inverse DFT.

We need now to approximate  $M_0(\theta)$  with a DFT approximation with a sampling of  $N$  points over the regular grid, where we have our  $N$  fixed to a even number. Thus we will have

$$\widetilde{M}_0(\theta) = \sum_{k=-\lfloor \frac{N-1}{2} \rfloor}^{\lfloor \frac{N-1}{2} \rfloor} \begin{pmatrix} \widetilde{m}_{1,1,k} & \cdots & \widetilde{m}_{1,n,k} \\ \vdots & \ddots & \vdots \\ \widetilde{m}_{n,1,k} & \cdots & \widetilde{m}_{n,n,k} \end{pmatrix} e^{2\pi i k \theta}.$$

Recall that the validation theorem also talks about a constant  $\lambda$ , saying that there must be a  $\lambda$  such that  $\|\Lambda^s\|_\rho \leq \lambda < 1$  and  $\|(\Lambda^u)^{-1}\|_\rho \leq \lambda < 1$ . In order to verify such condition we will need to define the Fourier norm of a matrix. There are several ways of doing so, such as taking the maximum over  $\theta$  of the  $\|\cdot\|_\infty$  norm of the matrix, but we are taking a different one. Let  $A$  be an  $n \times n$  matrix depending on  $\theta$ , then

$$\|A\|_{F,\rho} = \max_{1 \leq i \leq n} \sum_{j=1}^n \|a_{ij}\|_{F,\rho}.$$

This norm still satisfies that  $\|A(\theta)\|_\rho \leq \|A(\theta)\|_{F,\rho}$ .

Now that we already have the necessary tools for bounding, we have to check if we can find a value  $\lambda < 1$  such that  $\|\Lambda^s\|_\rho \leq \|\Lambda^s\|_{F,\rho} \leq \lambda$ . If this value exists, we have to check the second hypothesis, which is  $\|(\Lambda^u)^{-1}\|_\rho \leq \lambda$ . The calculation of this norm is not as direct as the previous one. The fact that  $(\Lambda^u)^{-1}$  is the inverse of a matrix of Fourier series breaks the correspondence between grid points and Fourier coefficients, hence, we will have to proceed differently.

Notice that

$$\|(\Lambda^u)^{-1}\|_\rho \leq \|(\Lambda^u)^{-1} - \widetilde{(\Lambda^u)^{-1}}\|_\rho + \|\widetilde{(\Lambda^u)^{-1}}\|_\rho \leq \|(\Lambda^u)^{-1} - \widetilde{(\Lambda^u)^{-1}}\|_\rho + \|\widetilde{(\Lambda^u)^{-1}}\|_{F,\rho}.$$

We shall take the first term of the sum apart in order to apply Corollary 3.9, which handles the error while applying a DFT upon inverted matrices as long as the function entries of our

matrix can be analytically extended to a complex strip of width  $\hat{\rho}$ ,  $\mathbb{T}_{\hat{\rho}}$ , which holds true for our case since we are working with analytic functions.

$$\|(\Lambda^u)^{-1} - \widetilde{(\Lambda^u)^{-1}}\|_{\rho} \leq \frac{\|\widetilde{(\Lambda^u)^{-1}}\|_{\hat{\rho}} \|E_{f_{inv}}(\theta)\|_{\rho}}{1 - \|E_{f_{inv}}(\theta)\|_{\rho}}$$

where  $E_{f_{inv}}(\theta) = Id_{n_U} - \Lambda^u(\theta) (\widetilde{(\Lambda^u)^{-1}})^{-1}$  as used in Corollary 3.9, which also gave us a very useful result, that claimed

$$\|E_{f_{inv}}(\theta)\|_{\rho} \leq C_N(\rho, \hat{\rho}) \|\Lambda^u\|_{\hat{\rho}} \|\widetilde{(\Lambda^u)^{-1}}\|_{\hat{\rho}}.$$

Now we can finally write

$$\begin{aligned} \|(\Lambda^u)^{-1} - \widetilde{(\Lambda^u)^{-1}}\|_{\rho} &\leq \frac{\|\widetilde{(\Lambda^u)^{-1}}\|_{\hat{\rho}} C_N(\rho, \hat{\rho}) \|\Lambda^u\|_{\hat{\rho}} \|\widetilde{(\Lambda^u)^{-1}}\|_{\hat{\rho}}}{1 - C_N(\rho, \hat{\rho}) \|\Lambda^u\|_{\hat{\rho}} \|\widetilde{(\Lambda^u)^{-1}}\|_{\hat{\rho}}} \\ &\leq \frac{C_N(\rho, \hat{\rho}) \|\Lambda^u\|_{F, \hat{\rho}} \|\widetilde{(\Lambda^u)^{-1}}\|_{F, \hat{\rho}}^2}{1 - C_N(\rho, \hat{\rho}) \|\Lambda^u\|_{F, \hat{\rho}} \|\widetilde{(\Lambda^u)^{-1}}\|_{F, \hat{\rho}}}. \end{aligned}$$

The last inequality holds due to the fact that  $\Lambda^u$  is a matrix of Fourier series, which means that there is no error produced while turning back to the points of the grid and forth again to the Fourier series. However, as we have said before, this is not true for  $(\Lambda^u)^{-1}$  given that the inversion of the matrix breaks the direct and errorless correspondence between grid points and DFT coefficients.

Once we have expressed the desired norm in computable terms, is time now to check if  $\|(\Lambda^u)^{-1}\|_{\rho} \leq \lambda$ , that is, if

$$\|(\Lambda^u)^{-1}\|_{\rho} \leq \frac{C_N(\rho, \hat{\rho}) \|\Lambda^u\|_{F, \hat{\rho}} \|\widetilde{(\Lambda^u)^{-1}}\|_{F, \hat{\rho}}^2}{1 - C_N(\rho, \hat{\rho}) \|\Lambda^u\|_{F, \hat{\rho}} \|\widetilde{(\Lambda^u)^{-1}}\|_{F, \hat{\rho}}} + \|\widetilde{(\Lambda^u)^{-1}}\|_{F, \hat{\rho}} \leq \lambda.$$

In case this condition is not satisfied with the first  $\lambda$  we have picked, it may be interesting to play around with the  $\lambda$  value and try to find another  $\lambda' < 1$  such that satisfies both conditions. Or we can simply increase a bit the value of  $\lambda$  until the condition is satisfied.

Once the issue is settled and we have a suitable  $\lambda$ , the next step is to find the bound for the error. Recall that

$$E_{red}(\theta) = P_2(\theta + \omega)M_0(\theta)P_1(\theta) - \Lambda(\theta).$$

In order to calculate a suitable bound for  $\|E_{red}(\theta)\|$  we will have to manipulate some terms so we can apply Theorem 3.6 and Corollary 3.8.

$$\begin{aligned} \|E_{red}(\theta)\|_\rho &= \|P_2(\theta + \omega)M_0(\theta)P_1(\theta) - \Lambda(\theta)\|_\rho \\ &\leq \|P_2(\theta + \omega)M_0(\theta)P_1(\theta) - \widetilde{P_2(\theta + \omega)M_0(\theta)P_1(\theta)}\|_\rho \\ &\quad + \|\widetilde{P_2(\theta + \omega)M_0(\theta)P_1(\theta)} - \Lambda(\theta)\|_\rho \\ &\leq C_N(\rho, \hat{\rho})\|P_2(\theta + \omega)\|_{\hat{\rho}}\|M_0(\theta)\|_{\hat{\rho}}\|P_1(\theta)\|_{\hat{\rho}} + \|\widetilde{P_2(\theta + \omega)M_0(\theta)P_1(\theta)} - \Lambda(\theta)\|_\rho, \end{aligned}$$

where the last term remains the same since it is the norm of the difference of two matrices of trigonometric polynomials (given that  $\Lambda(\theta)$  is an input), which is a matrix of trigonometric polynomials. Furthermore, using the Fourier norm inequality we obtain

$$\|E_{red}(\theta)\|_\rho \leq C_N(\rho, \hat{\rho})\|P_2(\theta + \omega)\|_{F, \hat{\rho}}\|M_0(\theta)\|_{\hat{\rho}}\|P_1(\theta)\|_{F, \hat{\rho}} + \|\widetilde{P_2(\theta + \omega)M_0(\theta)P_1(\theta)} - \Lambda(\theta)\|_{F, \rho}.$$

**Remark 4.3.** In the example we will present in the following section,  $\Lambda$  will be constant.

### 4.1.3 The Invertibility Error Bound

Lastly, we seek a bound for the invertibility error. The invertibility error is the error produced when treating  $P_2(\theta)$  as the inverse of  $P_1(\theta)$ , that is

$$E_{inv}(\theta) = P_2(\theta)P_1(\theta) - Id.$$

By simply taking norms and applying the same procedures as before we obtain

$$\begin{aligned} \|E_{inv}(\theta)\|_\rho &\leq \|P_2(\theta)P_1(\theta) - \widetilde{P_2(\theta)P_1(\theta)}\|_\rho + \|\widetilde{P_2(\theta)P_1(\theta)} - Id\|_\rho \\ &\leq C_N(\rho, \hat{\rho})\|P_2(\theta)\|_{\hat{\rho}}\|P_1(\theta)\|_{\hat{\rho}} + \|\widetilde{P_2(\theta)P_1(\theta)} - Id\|_\rho \\ &\leq C_N(\rho, \hat{\rho})\|P_2(\theta)\|_{F, \hat{\rho}}\|P_1(\theta)\|_{F, \hat{\rho}} + \|\widetilde{P_2(\theta)P_1(\theta)} - Id\|_{F, \rho}. \end{aligned}$$

### 4.1.4 Norm of a Bilinear Form

The last bound to be computed is the one related to the second differential of  $F$ , which is  $b$ . Recall from Theorem 2.11, that we had the following condition:

For all points  $(x, \theta)$  in the strip

$$\bar{D}_\rho(K_0, r) = \{(x, \theta) \in \mathbb{C}^n \times \bar{\mathbb{T}}_\rho^d \mid x = K_0(\theta) + P_1(\theta)\xi, \xi \in \mathbb{C}^n, |\xi|_\theta \leq R\},$$

the bilinear maps over the rotation  $\omega$

$$B(x, \theta) = P_2(\theta + \omega)D_x^2 F(x, \theta)[P_1(\theta)\cdot, P_1(\theta)\cdot]$$

satisfy  $\|B(x, \theta)\| \leq b$  as a norm of a bilinear form.

It is natural, then, that we seek a computable way to find that  $b$ . For that we can simply start by

$$\|B(x, \theta)\| \leq \|P_2(\theta + \omega)\| \|D_x^2 F(x, \theta)\| \|P_1(\theta)\|^2$$

Notice that the only expression for which we don't yet have a computable expression is the second differential of  $F$ . Since it is only a specific case of a bilinear form, let's define the norm of a more general bilinear form that we will call  $H : \mathbb{C}^n \times \mathbb{C}^n \rightarrow \mathbb{C}^n$  such that it has  $m$  components. That is, we have

$$H = \begin{pmatrix} (H_{ij}^1) \\ \vdots \\ (H_{ij}^m) \end{pmatrix}_{i,j=1,\dots,n}, \quad v_s = \begin{pmatrix} v_s^1 \\ \vdots \\ v_s^n \end{pmatrix} \quad s = 1, 2$$

$$H^k(v_1, v_2) = \sum_{i,j=1}^n H_{ij}^k v_1^i v_2^j.$$

With this, we can define

$$\begin{aligned} \|H\|_\infty &= \max_{v_1, v_2 \in \mathbb{C}^n \setminus \{0\}} \frac{|H(v_1, v_2)|_\infty}{|v_1|_\infty |v_2|_\infty} = \max_{v_1, v_2 \in \mathbb{C}^n \setminus \{0\}} \max_{k=1,\dots,m} \frac{|H^k(v_1, v_2)|}{|v_1|_\infty |v_2|_\infty} \\ &\leq \max_{v_1, v_2 \in \mathbb{C}^n \setminus \{0\}} \frac{\max_{k=1,\dots,m} \sum_{i,j=1}^n |H_{ij}^k| |v_1^i| |v_2^j|}{|v_1|_\infty |v_2|_\infty} \leq \max_{k=1,\dots,m} \sum_{i,j=1}^n |H_{ij}^k|, \end{aligned}$$

where in the last inequality we have used that  $|v_s| \leq |v_s|_\infty$  for  $s = 1, 2$ .

With such result, we can state that the norm of  $B(x, \theta)$  can be bounded by

$$\|B(x, \theta)\| \leq \|P_2(\theta + \omega)\| \max_{(x, \theta) \in \bar{D}(K_0, R)} \|D_x^2 F(x, \theta)\|_\infty \|P_1(\theta)\|^2.$$

## 4.2 Intervalar Arithmetics

It is known that, although computers are great computing machines, they are not flawless. One of the most notable weaknesses they have is the incapability of representing certain numbers such as irrational numbers. Obviously, a computer only has a finite amount of memory to store floating-point numbers, which means that irrational numbers can only be represented up to a certain decimal, a truncation point (and not only irrationals, but also infinite decimal rationals). The error produced when truncating can be problematic in high precision calculations, such as in validated numerics, and that is why interval arithmetic is used. Instead of computing approximations of functions, the aim is to compute enclosures of functions. That is, in validated numerics one has to provide rigorous intervals for the coefficients of the approximations. Hence, the width of an enclosure gives a rigorous measurement of the quality of

the computation, so the first step to accomplish a validating program is to perform rigorous computations with intervals.

In rigorous computations, real numbers are substituted by intervals whose extrema are computer representable real numbers. In particular, when implementing interval operations in a computer, the result of an operation with intervals is an interval that includes the result. We must also be careful with this when retrieving the interval extrema after a calculation. The default rounding mode is usually set to round to the nearest floating-point value, but this is not the best method since it can leave our value of interest out of the interval when rounding. It is of more convenience to round the lower extrema towards  $-\infty$  and the upper extrema towards  $+\infty$  so the interval is just enlarged a bit (see [4, 8]). The package we will use for interval arithmetics is called MPFI, and will be implemented in C code. Let us formalize the expression of intervals a bit more.

From now on, we will denote intervals with boldface notation, such as  $\mathbf{a} = [\underline{a}, \bar{a}]$  where  $\underline{a}$  and  $\bar{a}$  are called the lower and upper endpoints of  $\mathbf{a}$ , respectively. The set of real intervals is denoted by  $\mathbb{IR}$ , in which one can define arithmetic operations. We emphasize that, although real interval addition and multiplication are both associative and commutative, they fail to satisfy distributive law. Let's dive then into the definitions of the basic arithmetic operations between intervals.

### 4.2.1 Basic Operations

Without going much into detail, we present here the form of basic operations between intervals, the ones that will be used in our computer program by the interval arithmetic package [8].

- Addition:  $\mathbf{x} + \mathbf{y} = [x, \bar{x}] + [y, \bar{y}] = [x + y, \bar{x} + \bar{y}]$ .
- Negation:  $-\mathbf{x} = -[x, \bar{x}] = [-\bar{x}, -x]$ .
- Subtraction:  $\mathbf{x} - \mathbf{y} = [x, \bar{x}] - [y, \bar{y}] = [x, \bar{x}] + [-\bar{y}, -y] = [x - \bar{y}, \bar{x} - y]$ .
- Multiplication:  $\mathbf{x} \cdot \mathbf{y} = [x, \bar{x}] \cdot [y, \bar{y}] = [\min\{xy, x\bar{y}, \bar{x}y, \bar{x}\bar{y}\}, \max\{xy, x\bar{y}, \bar{x}y, \bar{x}\bar{y}\}] = [xy, \bar{x}\bar{y}]$ .
- Reciprocal:  $1/\mathbf{x} = 1/[x, \bar{x}] = [1/\bar{x}, 1/x]$  if  $x > 0$  or  $\bar{x} < 0$ . Then we also have the cases  $1/[x, 0] \rightarrow [-\infty, 1/x]$  and  $1/[0, \bar{x}] \rightarrow [1/\bar{x}, \infty]$ .
- Division:  $\mathbf{x}/\mathbf{y} = [x, \bar{x}]/[y, \bar{y}] = [x, \bar{x}] \cdot 1/[y, \bar{y}] = [x/\bar{y}, \bar{x}/y]$ .
- Powers:

$$\mathbf{x}^n = [x, \bar{x}]^n = [x^n, \bar{x}^n], \text{ if } n = 2k + 1 \text{ for } k = 0, 1, \dots$$

$$\mathbf{x}^n = [x, \bar{x}]^n = \begin{cases} [x^n, \bar{x}^n], & x \geq 0, \text{ if } n = 2k, \text{ for } k = 1, 2, \dots \\ [\bar{x}^n, x^n], & \bar{x} < 0, \\ [0, \max\{x^n, \bar{x}^n\}], & \text{otherwise.} \end{cases}$$

- Absolute value:

$$|\mathbf{x}| = \begin{cases} [\min\{|\underline{x}|, |\bar{x}|\}, \max\{|\underline{x}|, |\bar{x}|\}] & \text{if } \underline{x}\bar{x} \geq 0, \\ [0, \max\{|\underline{x}|, |\bar{x}|\}] & \text{if } \underline{x}\bar{x} < 0. \end{cases}$$

Besides arithmetic operations, it is also useful to define equality and inequality operators.

- Equality:  $\mathbf{x} = \mathbf{y} \iff [\underline{x}, \bar{x}] = [\underline{y}, \bar{y}] \iff (\underline{x} = \underline{y}) \wedge (\bar{x} = \bar{y})$ .
- Inequality:  $\mathbf{x} \leq \mathbf{y} \iff [\underline{x}, \bar{x}] \leq [\underline{y}, \bar{y}] \iff (\underline{x} \leq \underline{y}) \wedge (\bar{x} \leq \bar{y})$ .
- Distance:  $\text{dist}(\mathbf{x}, \mathbf{y}) = \max\{|\underline{x} - \underline{y}|, |\bar{x} - \bar{y}|\}$ .
- Maximum:  $\max\{\mathbf{x}, \mathbf{y}\} = \max\{\bar{x}, \bar{y}\}$ .
- Minimum:  $\min\{\mathbf{x}, \mathbf{y}\} = \min\{\underline{x}, \underline{y}\}$ .

These are the basic manipulations between intervals that are performed when using an interval arithmetic package, such as the one we are using, the MPFI, and this is how we will have to deal with the expressions from the validation theorem, by manipulating intervals around the values we know instead of using actual numbers. The explanation for the programming procedure awaits in the following section.

### 4.3 Computer Validation

Now that we have the required tools, we can proceed and validate a torus. For starters, we will have to get an approximately invariant torus out of somewhere. For that, we will read the output file generated by the code presented in [11]. In such code a reducibility method algorithm is implemented in C in order to calculate a torus.

Since the reducibility method (explained as well in [11]) also updates  $P_1$  and  $\Lambda$  at each iteration, we will read from file  $K_0$ ,  $P_1$  and  $\Lambda$  and turn it to Fourier space via FFT. After this, we just have left to set the Nyquist term of every object to 0 before having the initial data fully prepared. Notice that in such data there is no  $P_2$ , so we will have to go back to grid space with  $P_1$ , invert it, and return to Fourier space. That should give us a good approximation for an inverse. The value of  $\omega$  in [11] was taken as the golden ratio  $\omega = \frac{\sqrt{5}-1}{2}$  (Diophantine irrational number) and so we will take it this time again, but enclosed within an interval.

Keep in mind that we are working in the complex field, but we also want to calculate with intervals instead of numbers. This means that we will have to create a new structure in our program, *complexi*, that represents complex intervals, that is, objects of the form  $[\underline{x}, \bar{x}] \times [\underline{y}, \bar{y}]$ , where  $[\underline{x}, \bar{x}]$  is the real part interval and  $[\underline{y}, \bar{y}]$  is the imaginary part interval. With this, all new functions have to be created so basic operations between complex intervals are covered. For this, we will use the MPFI package to, firstly set all intervals to work with a  $\sim 30$  digit

precision, and then create all the functions for complex intervals using the package's own interval operations functions applied to the real and imaginary parts. With the basic operations between complex intervals we can construct more intricate functions, such as the much needed FFT or other vectors and matrix operations.

Once all functions are created, the results found in Section 4.1 are applied using complex intervals so the constants  $\lambda, \varepsilon, \sigma$  and  $\tau$  from Theorem 2.11 are found (of course, in the form of a real interval, since they are norm bounds). Notice that we have to evaluate a  $\rho$ -norm of the non-truncated object  $F(K_0(\theta), \theta)$  and its differential. For that, we will have to evaluate each object (let's take  $F(K_0(\theta), \theta)$  as the example) over a complex neighborhood of our grid. Such new extended domain is made of the complex boxes  $C_j = \{\theta_j + \varphi \mid |\operatorname{Re} \varphi| \leq \frac{1}{2N}, |\operatorname{Im} \varphi| \leq \hat{\rho}\}$  (notice that the choice of  $\rho$  or  $\hat{\rho}$  will depend on the context). First we will have to calculate the image of such boxes through  $K$  before applying  $F$ . Thus, we first need to calculate  $K_0(\theta + \varphi)$ . Notice that this is no more than rotating the torus as we have done before, but this time the rotation is complex.

$$K_0(\theta + \varphi) = \sum_{k=-\lfloor \frac{N-1}{2} \rfloor}^{\lfloor \frac{N-1}{2} \rfloor} (\tilde{K}_{0,k} e^{2\pi i k \varphi}) e^{2\pi i k \theta} = \sum_{k=-\lfloor \frac{N-1}{2} \rfloor}^{\lfloor \frac{N-1}{2} \rfloor} \left( \frac{\tilde{K}_{0,k}}{e^{2\pi i k \operatorname{Im} \varphi}} e^{2\pi i k \operatorname{Re} \varphi} \right) e^{2\pi i k \theta}.$$

So we just have to change the Fourier coefficients and rotate by a factor of  $\operatorname{Re} \varphi$ . With this new torus, we can calculate  $F(K(C_j), C_j)$  for each  $j$  and its differential. We just have to find its supremum norm afterwards.

The procedure for calculating  $b$  is quite analogous. The only more problematic object is the norm of the second differential. Recall that the domain in which  $\|B(z, \theta)\| \leq b$  (adapted to our case, where  $z = (x, y)$ ) is

$$\bar{D}_\rho(K_0, R) = \{(z, \theta) \in \mathbb{C}^n \times \bar{\mathbb{T}}_\rho^d \mid z = K_0(\theta) + P_1(\theta)\xi, \xi \in \mathbb{C}^n, |\xi|_\theta \leq R\}.$$

Hence, our goal is to evaluate each of our second differential matrices (and picking the largest one) with  $z$ 's that belong to the space created by the sum of an extended torus and an extended  $P_1\xi$ . For that, we will need to extend both the torus and  $P_1$ . After performing the same operations as before, we go back to grid space with both  $K_0(C_j)$  and  $P_1(C_j)\xi$  for each  $j$  to add them together. Then we evaluate them on the norm of the second differential (taking the maximum between both components) and take the supremum for each  $C_j$ . The calculation of the remaining constants follows naturally.

### 4.3.1 Study Case: The Standard Map

Our case of study is the perturbed Standard Map since it is the one with which the approximate torus is computed. Thus,  $\hat{F}$  is  $(F, f) : \mathbb{C}^2 \times \mathbb{T}_\rho \rightarrow \mathbb{C}^2 \times \mathbb{T}_\rho$  given by

$$\begin{cases} f(\theta) = \theta + \omega \\ F^x(x, y) = x + y - \frac{\kappa}{2\pi} \sin(2\pi x) - \varepsilon \sin(2\pi\theta) \\ F^y(x, y) = y - \frac{\kappa}{2\pi} \sin(2\pi x) - \varepsilon \sin(2\pi\theta) \end{cases}$$

with differential matrix

$$D_{x,y}F(x, y) = \begin{pmatrix} 1 - \kappa \cos(2\pi x) & 1 \\ -\kappa \cos(2\pi x) & 1 \end{pmatrix}$$

and second differential matrices for components  $x$  and  $y$

$$D^2F^x(x, y) = \begin{pmatrix} 2\pi\kappa \sin(2\pi x) & 0 \\ 0 & 0 \end{pmatrix} \quad D^2F^y(x, y) = \begin{pmatrix} 2\pi\kappa \sin(2\pi x) & 0 \\ 0 & 0 \end{pmatrix}.$$

With this map, the approximate torus is calculated using the reducibility method within a continuation method for  $\varepsilon$ . Applying the previous explanation to this specific map will yield the necessary constants and error bounds for the validation (see the Annex for details on the implementation of the previous explanation to this case).

### 4.3.2 Results

In this section, some output examples of validations will be displayed. We have taken different inputs for different values of  $\varepsilon$  and checked the conditions for the torus to be validated.

We will start with the first case  $\varepsilon = 0.1$  (which is almost a planer torus) and play around with  $\rho$  and  $\hat{\rho}$  to see what happen to the errors and constants. We can start by setting  $\rho = 0$  so we first look at the real torus with  $R = 10^{-4}$ . For the calculation of Fourier norms we will use  $\hat{\rho} = 10^{-2}$ , but for the inflation of the torus we will use  $\hat{\rho} = 5 \cdot 10^{-3}$ .

CN(rho, rhohat): [6.8047018919335281312076456046925e-13,6.8047018919335281312076456070531e-13]

Invariance error: [1.5909644176201588172860064471273e-11,1.5932268362185730186487664094488e-11]

Lambda: [3.3828548368011231753495616835876e-1,3.3828548368011613854985332359308e-1]

Reducibility Error: [3.0953037229975405447470059225473e-9,3.0958269249002620014168739252433e-9]

Inversion Error: [9.2463408143891988645614886642009e-10,9.2463408143895368910319512333124e-10]

b: [2.8017225229974841450476962477150,3.4314984707078682189822147117411]

lambda + sigma + tau < 1

h: [1.0179917753413927022556095782971e-10,1.2485907231844659912024893932707e-10]



By looking at  $C_N(\rho, \hat{\rho})$  we can see the estimates are worse, and of course,  $\rho$  plays a crucial role in that since it gives the band for which the torus is real-analytic. Let's see what happens if we decrease the  $\hat{\rho}$  used for the norms to  $2 \cdot 10^{-3}$ , for instance.

CN(rho, rhohat): [1.7009250593058399876723639326190e1,1.7009250593058399876723639330356e1]

Invariance error: [1.2007445976031078103181698281255e1,1.2572979712920698955320340248740e1]

Lambda: [3.3828548367999999868516169954091e-1,3.3828548367999999868516169954092e-1]

Reducibility Error: [1.1305503181504561880506866617241e2,1.1307442014153522785221715120637e2]

Inversion Error: [3.4264225308153230639346240352168e1,3.4264225308153230639347506132225e1]

b: [2.8019370675805860925791246439299,3.4317663589204338906579305969056]

lambda + sigma + tau >= 1, condition not satisfied

h: [1.5638150541687520970518216456548e-3,2.0060747890028793391902878200682e-3]

h < 1/2

r0: [-1.1008592908211105868724739470982e-1,-6.3865611346287163627016135577732e-2]

r0 < R

mu: [-2.4596440744294486693543550197822,-2.4571379585268243467905628052118]

mu < 1/(1+sqrt(2))

The initial torus does not meet the requirements  
to ensure the existence of an invariant torus

Notice the big change in  $C_N(\rho, \hat{\rho})$ , which ultimately leads to the impossibility of validating the torus. This means that the values  $\rho, \hat{\rho}$  and also  $N$  are related to each other. A poor configuration of them can lead to big exponents in complex exponentials, which translates into large values of  $C_N(\rho, \hat{\rho})$ . Let's revert the value of the  $\hat{\rho}$  we just changed and increase the value of the  $\hat{\rho}$  for which we inflate the torus. Set  $\hat{\rho} = 10^{-2}$ .

CN(rho, rhohat): [1.7151174562071982359681427214174e-11,1.7151174562071982359681427219777e-11]

Invariance error: [1.1460988119269239890219488624462e-10,3.7366228296279814862444928125141e155]

Lambda: [3.3828548368568411773038311949549e-1,3.3828548368568793874528040059926e-1]

Reducibility Error: [2.3627902796587507103658356522390e-8,2.2981990896026450621867537082922e159]

Inversion Error: [2.3305297996373874253806384903207e-8,2.3305297996374717600595203447535e-8]

b: [0,1.8125957313665597697531662867201e168]

lambda + sigma + tau >= 1, condition not satisfied

```
h: [-@Inf@,@Inf@]
```

```
h >= 1/2, condition not satisfied
```

```
r0: [@NaN@,@NaN@]
```

```
r0 >= R, condition not satisfied
```

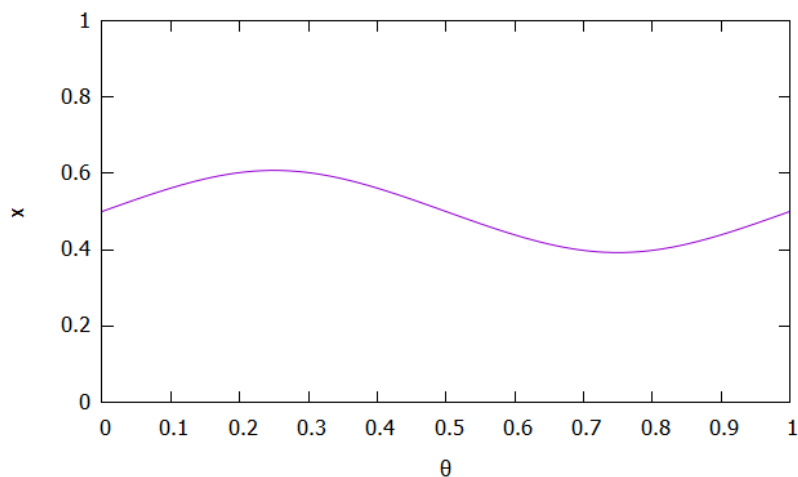
```
mu: [@NaN@,@NaN@]
```

```
mu >= 1/(1+sqrt(2)), condition not satisfied
```

The initial torus does not meet the requirements  
to ensure the existence of an invariant torus

The change in this case is even more drastic, we see that solutions explode by just tweaking  $\hat{\rho}$  a little bit. It is important then to play around and select the best values of  $\rho$  and  $\hat{\rho}$  so everything works properly.

Now we will show the bounds and constants for a couple more values of  $\varepsilon$  with the same  $\rho = 10^{-3}$ ,  $\hat{\rho} = 5 \cdot 10^{-3}$  for the inflation and  $\hat{\rho} = 10^{-2}$  for the norms values. Starting for instance with  $\varepsilon = 0.5$ . The x component of the initial torus has the following shape (taken from [11]):



```
CN(rho, rhohat): [1.7151174562071982359681427214174e-11,1.7151174562071982359681427219777e-11]
```

```
Invariance error: [1.3364537996428360704009295355594e-10,1.3665348908480223800232028358809e-10]
```

```
Lambda: [3.5717463727666573959231070015372e-1,3.5717463727666860535348366102287e-1]
```

```
Reducibility Error: [7.5676212897829297173314739964981e-8,7.6011799392034107526664262791188e-8]
```

```
Inversion Error: [2.2885536863654524298845311645552e-8,2.2885536863663332134927968855888e-8]
```





Reducibility Error: [2.4118312001358992063980495542665e11,3.0654258154845546997938811529493e239]

Inversion Error: [2.4118312001361417813578648336979e11,2.4118312001378599546280602547596e11]

b: [0,2.8294106485487984763006470336043e231]

$\lambda + \sigma + \tau \geq 1$ , condition not satisfied

h: [0,8.7605152205044994410718512354246e412]

$h \geq 1/2$ , condition not satisfied

r0: [NaN,NaN]

$r0 \geq R$ , condition not satisfied

mu: [NaN,NaN]

$\mu \geq 1/(1+\sqrt{2})$ , condition not satisfied

The initial torus does not meet the requirements  
to ensure the existence of an invariant torus

As we said before, the closer  $\varepsilon$  gets to the critical value  $\varepsilon \sim 1.2342$ , the harder it gets to validate the torus as seen in this last example. Even though  $\rho$  and  $\hat{\rho}$  can be adjusted to obtain better results, it is still hard to find the sweet spot to validate the torus.

One can go even a bit further and try validate tori within a continuation method for  $\omega$  or  $\varepsilon$ , or try figure out how the constants  $\rho$ ,  $\hat{\rho}$  and  $N$  depend on each other so one can choose optimally their values for a correct validation.

# Appendix

## Whiskers

In this appendix we want to show the bases of a possible future work encouraged by the validation process taken to term in the previous chapters. It is a topic that has been discussed during the research and writing processes but that was left as a possible future project should the first validation work succeed. Such topic is the study of the invariant manifolds known as whiskers.

When it comes to the study of quasi-periodically forced maps, there are two main interesting objects of study. One of them has been already addressed, and it is the existence of invariant tori under the quasi-periodic map. This has already been proven in the previous chapters through the validation theorem. The second one is the existence of asymptotic manifolds attached to our invariant torus. These manifolds, as we have already said, are usually called whiskers.

Since the proof of existence of such manifolds can be very complicated, we will present here just the main definitions and a computation algorithm for the easiest case, the one-dimensional and constant dynamics case. Keep in mind that our quasi-periodically forced map remains the same as before, where the dynamics on the torus is given by an ergodic rotation  $\omega \in \mathbb{R}^d$ . That is,  $k \cdot \omega \notin \mathbb{Z}, \forall k \in \mathbb{Z}^d \setminus \{0\}$ .

## Equations for Whiskers

In order to study whiskers of rank  $m$  attached to a torus, we seek maps  $W : \mathbb{C}^m \times \mathbb{T}_\rho^d \rightarrow \mathbb{C}^n$  and  $\Lambda : \mathbb{C}^m \times \mathbb{T}_\rho^d \rightarrow \mathbb{C}^m$  in such a way that

$$F(W(\eta, \theta), \theta) = W(\Lambda(\eta, \theta), \theta + \omega), \quad (4.1)$$

$$\Lambda(0, \theta) = 0. \quad (4.2)$$

Notice that equation (4.1) implies that the graph of  $W$

$$\mathcal{W} = \{(W(\eta, \theta), \theta) \mid \eta \in \mathbb{C}^m, \theta \in \mathbb{T}_\rho^d\}$$

is an  $m + d$  invariant manifold under  $\hat{F} = (F, f)$ . Recall that  $f(\theta) = \theta + \omega$ . It is useful to think of  $\mathcal{W}$  as a  $d$ -parameter family of  $m$ -dimensional manifolds

$$\mathcal{W}_\theta = \{(W(\eta, \theta), \theta) \mid \eta \in \mathbb{C}^m\},$$

with  $\theta \in \mathbb{T}_\rho^d$ . Notice also that the leaves  $\mathcal{W}_\theta$  are not invariant, since  $\hat{F}(\mathcal{W}_\theta) = \mathcal{W}_{\theta+\omega}$ .

We note that  $\Lambda$  is part of the unknowns that need to be computed, and corresponds to finding a representation of the dynamics on the invariant manifold. Given a point  $\eta$  belonging to a leaf  $\mathcal{W}_\theta$ ,  $\Lambda$  gives the dynamical displacement of such point on the same leaf.

**Remark 4.4.** Bear in mind that by choosing  $K(\theta) = W(0, \theta)$  we obtain a  $K$  which satisfies the invariance equation, so the manifold  $\mathcal{W}$  contains an invariant torus  $\mathcal{K}$ .

By taking derivatives on (4.1) with respect to  $\eta$ , and evaluating them at  $\eta = 0$ , we obtain the equation for the linearization of the whisker:

$$D_x F(W(0, \theta), \theta) D_\eta W(0, \theta) = D_\eta W(0, \theta + \omega) D_\eta \Lambda(0, \theta).$$

Hence, we obtain that the vector space based at  $K(\theta) = W(0, \theta)$  spanned by  $W_1(\theta) = D_\eta W(0, \theta)$  is mapped by  $D_x F(W(0, \theta), \theta)$  into the corresponding vector space based at  $K(\theta + \omega) = W(0, \theta + \omega)$  spanned by  $W_1(\theta + \omega) = D_\eta W(0, \theta + \omega)$  through the linear map  $\Lambda_1(\theta) = D_\eta \Lambda(0, \theta)$  [5].

Summing up, we obtain that  $W_1$  is an invariant subbundle of the cocycle. There may be, of course, several bundles invariant under linearization. For each of these invariant bundles, we can try to find an invariant manifold (whisker) tangent to it.

## One-dimensional Setting and Reducible Case

As we previously said, the matter of whiskers can get very complicated, so we will simplify our work gradually. For starters, we will work with rank-1 whiskers. That will be our first step towards simplification. In that case we would be looking for a manifold  $W : \mathbb{C} \times \mathbb{T}_\rho^d \rightarrow \mathbb{C}^n$  such that the invariance equation

$$F(W(s, \theta), \theta) = W(\lambda(\theta)s, \theta + \omega)$$

is satisfied, where  $s = \eta$  is a one-dimensional parameter and  $\lambda : \mathbb{T}_\rho^d \rightarrow \mathbb{C}$  a map such that  $\exists \lambda_s < 1, C > 0$  which satisfy

$$|\lambda(\theta + (k-1)\omega) \cdots \lambda(\theta + \omega) \lambda(\theta)| \leq C \cdot \lambda_s^k. \quad (4.3)$$

The second step for simplicity is to assume that the internal dynamics on the whisker is given by a multiplication by a constant. As said in section 1.2.3, in this case, the system is

reducible. We will also assume along this section that  $\omega \in \mathbb{R}^d$  is Diophantine. The definition of a Diophantine number is given as follows.

**Definition 4.5.** *Given  $\gamma > 0$  and  $\tau \geq d$ , we say that  $\omega \in \mathbb{R}^d$  is a  $(\gamma, \tau)$ -Diophantine vector of frequencies if*

$$|k \cdot \omega - m| \geq \frac{\gamma}{|k|_1^\tau}, \quad \forall k \in \mathbb{Z}^d \setminus \{0\}, m \in \mathbb{Z},$$

where  $|k|_1 = \sum_{i=1}^n |k_i|$ .

This basically means that  $\omega$  cannot be quickly approximated by rationals.

For our desired reduction, we have to express our  $\lambda(\theta)$  as a constant in our frame, to get so, we look for a function  $p : \mathbb{T}_\rho^d \rightarrow \mathbb{C} \setminus \{0\}$ . Specifically, we will take it as a positive function when applied to real torus.

$$p(\theta + \omega)^{-1} \lambda(\theta) p(\theta) = \lambda_0 \longrightarrow \lambda(\theta) p(\theta) = p(\theta + \omega) \lambda_0.$$

Considering the possibility of  $\lambda(\theta)$  being negative, we will take its absolute value when taking logarithms on both sides and  $\text{sign}(\lambda(\theta)) = \pm 1$  as the sign of  $\lambda(\theta)$ .

$$\begin{aligned} \log |\lambda(\theta)| + \log p(\theta) &= \log p(\theta + \omega) + \log |\lambda_0| \\ -\log p(\theta) + \log p(\theta + \omega) &= \log |\lambda(\theta)| - \log |\lambda_0|. \end{aligned}$$

Taking  $\xi(\theta) = \log p(\theta)$ ,  $\eta(\theta) = \log |\lambda(\theta)|$  and  $\eta_0 = \log |\lambda_0|$

$$\xi(\theta + \omega) - \xi(\theta) = \eta(\theta) - \eta_0. \quad (4.4)$$

Let's express  $\xi(\theta)$  and  $\eta(\theta)$  in terms of its Fourier series for a better manipulation of the expressions.

$$\begin{aligned} \xi(\theta) &= \sum_{k \in \mathbb{Z}} \hat{\xi}_k e^{2\pi i k \theta} \\ \eta(\theta) &= \sum_{k \in \mathbb{Z}} \hat{\eta}_k e^{2\pi i k \theta}. \end{aligned}$$

So, rewriting equation (4.4) in terms of Fourier series, we obtain

$$\sum_{k \in \mathbb{Z}} \left( \hat{\xi}_k e^{2\pi i k (\theta + \omega)} - \hat{\xi}_k e^{2\pi i k \theta} \right) = \sum_{k \neq 0} \hat{\xi}_k \left( e^{2\pi i k \omega} - 1 \right) e^{2\pi i k \theta} = \left( \sum_{k \neq 0} \hat{\eta}_k e^{2\pi i k \theta} \right) + \hat{\eta}_0 - \eta_0.$$

Equating Fourier coefficients we get

$$\begin{aligned} k \neq 0, \quad \hat{\xi}_k &= \frac{\hat{\eta}_k}{e^{2\pi i k \omega} - 1} \\ k = 0, \quad \hat{\eta}_0 &= \eta_0. \end{aligned}$$

Notice that, thanks to the fact that  $\omega$  is Diophantine (“very irrational”) the denominator of the coefficients in the  $k \neq 0$  case, will tend slower to 0, and therefore, the coefficients themselves will tend to infinity slower. With those expressions we can say now that  $p(\theta) = \exp \xi(\theta)$  and

$$\eta_0 = \hat{\eta}_0 = \int_{\theta \in \mathbb{T}_\rho^d} \log |\lambda(\theta)| \, d\theta \longrightarrow |\lambda_0| = \exp \int_{\theta \in \mathbb{T}_\rho^d} \log |\lambda(\theta)| \, d\theta .$$

And therefore,  $\lambda_0 = \text{sign}(\lambda(\theta)) \cdot |\lambda_0|$ .

## Computation of the Manifold

In this section we will specify an algorithm for the computation of whiskers of rank 1, which are parametrized by the map  $W(s, \theta)$ . Such map satisfies the invariance equation, assuming that the invariant bundles are of rank 1 and that  $\omega$  is Diophantine. For the first calculations we will assume the linear dynamics are uniform on the bundles and given by a map  $\lambda : \mathbb{T}_\rho^d \rightarrow \mathbb{C}$ . Nonetheless, assuming the dynamics are reduced to multiplication by a constant can simplify the calculations if the linear dynamics is hyperbolic and if the previous section’s conditions are fulfilled.

All in all, we are looking for a manifold  $W : \mathbb{C} \times \mathbb{T}_\rho^d \rightarrow \mathbb{C}^n$  and a map  $\lambda : \mathbb{T}_\rho^d \rightarrow \mathbb{C}$  satisfying condition (4.3), such that the invariance equation

$$F(W(s, \theta), \theta) = W(\lambda(\theta)s, \theta + \omega)$$

holds, with  $W_0(\theta) = W(0, \theta) = K(\theta)$ , that is, on the invariant torus. To do that, we will express  $W(s, \theta)$  in Fourier-Taylor series form, such that

$$W(s, \theta) = \sum_{k=0}^{\infty} W_k(\theta) s^k , \tag{4.5}$$

where  $W_k(\theta)$  are the Taylor coefficients of the series, which are also periodic functions (Fourier series) with respect to  $\theta$ . Notice that we already know that  $W_0(\theta) = K(\theta)$ . By differentiating the invariance equation with respect to  $s$  and taking  $s = 0$ , we have

$$D_x F(K(\theta), \theta) D_s W(0, \theta) = D_s W(0, \theta + \omega) \lambda(\theta) .$$

From here we get our second Taylor coefficient  $W_1(\theta) = D_s W(0, \theta)$ , which is a frame of an invariant bundle, turning the previous equation into

$$D_x F(K(\theta), \theta) W_1(\theta) = W_1(\theta + \omega) \lambda(\theta) .$$

At this point we will assume that we have calculated  $W_{<k}(s, \theta) = \sum_{r < k} W_r(\theta) s^r$  and we want to calculate  $W_k(\theta)$ . Substituting expression (4.5) into the invariance equation we have

$$F(W_{<k}(s, \theta) + W_k(\theta) s^k + \dots, \theta) = W_{<k}(\lambda(\theta)s, \theta + \omega) + W_k(\theta + \omega) \lambda(\theta)^k s^k + \dots$$

Taylor expanding the left hand side of the equation we have

$$\begin{aligned} F(W_{<k}(s, \theta) + W_k(\theta)s^k + \dots, \theta) &= F(W_{<k}(s, \theta), \theta) + D_x F(W_{<k}(s, \theta), \theta)(W_k(\theta)s^k + \dots) + \dots \\ &= [F(W_{<k}(s, \theta), \theta)]_{<k} + [F(W_{<k}(s, \theta), \theta)]_k s^k + \dots \\ &\quad + D_x F(K(\theta), \theta) W_k(\theta)s^k + \dots \end{aligned}$$

Recalling that  $D_x F(K(\theta), \theta) = M(\theta)$  and equating terms of the same order, we obtain

$$M(\theta)W_k(\theta)s^k - W_k(\theta + \omega)\lambda(\theta)^k s^k = - [F(W_{<k}(s, \theta), \theta)]_k s^k .$$

Thus we obtain the cohomology equation

$$M(\theta)W_k(\theta) - W_k(\theta + \omega)\lambda(\theta)^k = - [F(W_{<k}(s, \theta), \theta)]_k , \quad k \geq 2 .$$

Keep in mind that, for this equation to be solvable, the condition for

$$\lambda_0 = \exp \int_{\theta \in \mathbb{T}_p^d} \log |\lambda(\theta)| d\theta$$

to  $\lambda_0^l \notin \text{Spec}(\mathcal{M}_\omega)$  for  $l \geq 2$  must be satisfied (so  $\mathcal{M}_\omega - \lambda_0^l I$  is invertible), where  $\mathcal{M}_\omega$  is the transfer operator defined in Section 1.2.2. With that final expression we are now able to find the  $k$ -th term of the expansion, allowing us to fully calculate the object.

Notice that in order to prove the existence of  $W(s, \theta)$ , we should prove first that indeed the fact that  $\lambda_0^l \notin \text{Spec}(\mathcal{M}_\omega)$  for  $l \geq 2$  ensures the existence of solution of the cohomology equation. And secondly, we should prove that the series defining  $W(s, \theta)$  converges.

Such proof would require a lot of preparation work and, as said, it goes beyond the scope of this project. However, it is a very interesting topic worth considering for a future work, both of a theoretical nature and of a more validation focused approach.



# Conclusions

Certainly, skew-product systems are not unexplored territory although there is still a lot to learn. There are even several ways of proving the validation theorem even though we just have stated one. Nevertheless, although the approach that has been taken here has already been used for validations in KAM theory, the implementation to this very specific case can draw a path for other different and better computer assisted proofs to come. In the same way, regardless of the commonness and familiarity with Fourier transforms, the validation process using intervalar arithmetics and multi-precision can teach a lot about scientific coding that it might not be possible to learn somewhere else. The precision and care with which every computation has to be performed can be overwhelming at times but also very rewarding professional-wise.

As it has been already stated, this is just the beginning for what computer validations can become, by using its tools in other areas such as PDE's. But without leaving the topic of skew-product systems, we have also seen that we can move forward and see, for instance, how can whiskers be validated using similar procedures. As always in science and of course in mathematics, there is still a lot to progress and learn.



# Annex

```
1 #include <stdio.h>
2 #include <math.h>
3 #include <complex.h>
4 #include <stdlib.h>
5 #include <mpfi.h>
6 #include <mpfi_io.h>
7
8 typedef struct real {
9     mpfi_t real;
10 }real;
11
12 typedef struct complexi {
13     mpfi_t real;
14     mpfi_t imag;
15 }complexi;
16
17 real PI, DPI, one, two;
18 int prec = 100;
19 double rhod = 1.e-3, hatrhod = 5.e-3;
20
21 void comp_print (complexi x) {
22     /* Prints complex intervals */
23     mpfi_out_str(stdout, 10, 0, x.real);
24     printf(" x ");
25     mpfi_out_str(stdout, 10, 0, x.imag);
26     printf("\n\n");
27 }
28
29 void real_print (real x) {
30     /* Prints real intervals */
31     mpfi_out_str(stdout, 10, 0, x.real);
32     printf("\n\n");
33 }
34
35 complexi comp_init_c (complex x) {
36     /* Initializes a complex interval around a complex number */
37     complexi z;
38     mpfi_init2(z.real, prec);
39     mpfi_init2(z.imag, prec);
40     mpfi_set_d(z.real, creal(x));
41     mpfi_set_d(z.imag, cimag(x));
```

```
42
43     return z;
44 }
45
46 complexi comp_set_c (complex x) {
47     /* Sets a complex interval around a complex number */
48     complexi z;
49
50     z = comp_init_c(0);
51
52     mpfi_set_d(z.real, creal(x));
53     mpfi_set_d(z.imag, cimag(x));
54
55     return z;
56 }
57
58 void comp_clear (complexi x) {
59     /* Clears complex intervals */
60     mpfi_clear(x.real);
61     mpfi_clear(x.imag);
62 }
63
64 void allocm (complexi *m[2][2], unsigned N) {
65     /* Allocates a matrix of complex intervals */
66     int i, j;
67     for(i=0; i<2; i++)
68         for(j=0; j<2; j++)
69             m[i][j] = (complexi *) malloc(N*sizeof(complexi));
70 }
71
72 void allocv (complexi *v[2], unsigned N) {
73     /* Allocates a vector of complex intervals */
74     int i;
75     for(i=0; i<2; i++)
76         v[i] = (complexi *) malloc(N*sizeof(complexi));
77 }
78
79 void allocv_d (double *v[2], unsigned N) {
80     /* Allocates a vector of real numbers */
81     int i;
82     for(i=0; i<2; i++)
83         v[i] = (double *) malloc(N*sizeof(double));
84 }
85
86 void allocv_real (real *v[2], unsigned N) {
87     /* Allocates a vector of real numbers */
88     int i;
89     for(i=0; i<2; i++)
90         v[i] = (real *) malloc(N*sizeof(real));
91 }
92
93
```

```
94 void allocm_d (double *m[2][2], unsigned N) {
95     /* Allocates a matrix of complex intervals */
96     int i, j;
97     for(i=0; i<2; i++)
98         for(j=0; j<2; j++)
99             m[i][j] = (double *) malloc(N*sizeof(double));
100 }
101
102 void allocv_c (complex *v[2], unsigned N) {
103     /* Allocates a vector of complex numbers */
104     int i;
105     for(i=0; i<2; i++)
106         v[i] = (complex *) malloc(N*sizeof(complex));
107 }
108
109 void freev (complexi *v[2]) {
110     /* Frees the memory occupied by a vector */
111     int i;
112     for(i=0; i<2; i++)
113         free(v[i]);
114 }
115
116 void freem (complexi *m[2][2]) {
117     /* Frees the memory occupied by a matrix */
118     int i, j;
119     for(i=0; i<2; i++)
120         for(j=0; j<2; j++)
121             free(m[i][j]);
122 }
123
124 void comp_init_m (complexi *m[2][2], unsigned N) {
125     /* Initializes a matrix of complex intervals */
126     int i, j, k;
127     for(k=0; k<N; k++)
128         for(i=0; i<2; i++)
129             for(j=0; j<2; j++)
130                 m[i][j][k] = comp_init_c(0);
131 }
132
133 void comp_init_v (complexi *v[2], unsigned N) {
134     /* Initializes a vector of complex intervals */
135     int i, k;
136     for(k=0; k<N; k++)
137         for(i=0; i<2; i++)
138             v[i][k] = comp_init_c(0);
139 }
140
141 void real_init_v (real *v[2], unsigned N) {
142     /* Initializes a vector of complex intervals */
143     int i, k;
144     for(k=0; k<N; k++)
145         for(i=0; i<2; i++) {
```

```
146     mpfi_init2(v[i][k].real, prec);
147     mpfi_set_d(v[i][k].real, 0);
148 }
149 }
150
151 complexi comp_add (complexi x, complexi y) {
152     /* Sum of complex intervals */
153     complexi z;
154
155     z = comp_init_c(0);
156
157     mpfi_add(z.real, x.real, y.real);
158     mpfi_add(z.imag, x.imag, y.imag);
159
160     return z;
161 }
162
163 real real_add (real x, real y) {
164     /* Sum of real intervals */
165     real sum;
166
167     mpfi_init2(sum.real, prec);
168
169     mpfi_add(sum.real, x.real, y.real);
170
171     return sum;
172 }
173
174 complexi comp_sub (complexi x, complexi y) {
175     /* Subtraction of complex intervals */
176     complexi z;
177
178     z = comp_init_c(0);
179
180     mpfi_sub(z.real, x.real, y.real);
181     mpfi_sub(z.imag, x.imag, y.imag);
182
183     return z;
184 }
185
186 real real_sub (real x, real y) {
187     /* Subtraction of real intervals */
188     real sub;
189
190     mpfi_init2(sub.real, prec);
191
192     mpfi_sub(sub.real, x.real, y.real);
193
194     return sub;
195 }
196
197 complexi comp_mul (complexi x, complexi y) {
```

```
198  /* Product of complex intervals */
199  complexi z, r;
200
201  z = comp_init_c(0);
202      r = comp_init_c(0);
203
204      mpfi_mul(z.real, x.real, y.real);
205  mpfi_mul(z.imag, x.imag, y.imag);
206  mpfi_sub(r.real, z.real, z.imag);
207
208      mpfi_mul(z.real, x.real, y.imag);
209      mpfi_mul(z.imag, x.imag, y.real);
210      mpfi_add(r.imag, z.real, z.imag);
211
212  return r;
213 }
214
215 real real_mul (real x, real y) {
216  /* Multiplies real intervals */
217  real mul;
218
219  mpfi_init2(mul.real, prec);
220
221  mpfi_mul(mul.real, x.real, y.real);
222
223  return mul;
224 }
225
226 real real_sc_mul (double a, real x) {
227  /* Multiplies a real interval by a real scalar */
228  real mul;
229
230  mpfi_init2(mul.real, prec);
231
232  mpfi_mul_d(mul.real, x.real, a);
233
234  return mul;
235 }
236
237 real real_sc_div (double a, real x) {
238  /* Divides a real interval by a real scalar */
239  real div;
240
241  mpfi_init2(div.real, prec);
242
243  mpfi_d_div(div.real, a, x.real);
244
245  return div;
246 }
247
248 complexi comp_div (complexi x, complexi y) {
249  /* Division of complex intervals */
```

```

250     complexi z1, r;
251     real z2;
252
253     z1 = comp_init_c(0);
254     r = comp_init_c(0);
255     mpfi_init2(z2.real, prec);
256
257     /*Real numerator*/
258         mpfi_mul(z1.real, x.real, y.real);
259         mpfi_mul(z1.imag, x.imag, y.imag);
260         mpfi_add(r.real, z1.real, z1.imag);
261
262     /*Denominator*/
263     mpfi_mul(z1.real, y.real, y.real);
264     mpfi_mul(z1.imag, y.imag, y.imag);
265     mpfi_add(z2.real, z1.real, z1.imag);
266
267     /*Division of real part*/
268     mpfi_div(r.real, r.real, z2.real);
269
270     /*Imaginary numerator*/
271         mpfi_mul(z1.real, x.real, y.imag);
272         mpfi_mul(z1.imag, x.imag, y.real);
273         mpfi_sub(r.imag, z1.imag, z1.real);
274
275     /*Division of imagaginary part*/
276     mpfi_div(r.imag, r.imag, z2.real);
277
278     return r;
279 }
280
281 real real_div (real x, real y) {
282     /* Divides real intervals */
283     real div;
284
285     mpfi_init2(div.real, prec);
286
287     mpfi_div(div.real, x.real, y.real);
288
289     return div;
290 }
291
292 real real_sqrt (real x) {
293     /* Calculates the square root of a real interval */
294     real sqrt;
295
296     mpfi_init2(sqrt.real, prec);
297     mpfi_sqrt(sqrt.real, x.real);
298
299     return sqrt;
300 }
301

```

```
302 complexi comp_reali_mul (real a, complexi x) {
303     /* Multiplies a real interval by a complex interval as a scalar */
304     complexi z;
305
306     z = comp_init_c(0);
307
308     mpfi_mul(z.real, a.real, x.real);
309     mpfi_mul(z.imag, a.real, x.imag);
310
311     return z;
312 }
313
314 complexi comp_sc_mul (double a, complexi x) {
315     /* Multiplies a complex interval by a real scalar */
316     complexi z;
317     real y;
318
319     z = comp_init_c(0);
320
321     mpfi_init2(y.real, prec);
322     mpfi_set_d(y.real, a);
323
324     mpfi_mul(z.real, y.real, x.real);
325     mpfi_mul(z.imag, y.real, x.imag);
326
327     mpfi_clear(y.real);
328
329     return z;
330 }
331
332 complexi comp_abs (complexi x) {
333     /* Computes the absolute value of a complex interval interval-wise */
334     /* Caution: this is not the modulus of a complex interval */
335     complexi abs;
336
337     abs = comp_init_c(0);
338
339     mpfi_abs(abs.real, x.real);
340     mpfi_abs(abs.imag, x.imag);
341
342     return abs;
343 }
344
345 real real_abs (real x) {
346     /* Calculates the absolute value of a real interval */
347     real abs;
348
349     mpfi_init2(abs.real, prec);
350
351     mpfi_abs(abs.real, x.real);
352
353     return abs;
```

```
354 }
355
356 real comp_mod (complexi z) {
357     /* Calculates the modulus of a complex interval */
358     real mod;
359
360     mpfi_init2(mod.real, prec);
361
362     mpfi_hypot(mod.real, z.real, z.imag);
363
364     return mod;
365 }
366
367 complexi comp_sin (complexi x) {
368     /* Computes complex sine */
369     complexi z;
370     real a, b;
371
372     z = comp_init_c(0);
373
374     mpfi_init2(a.real, prec);
375     mpfi_init2(b.real, prec);
376
377     mpfi_sin(a.real, x.real);
378     mpfi_cosh(b.real, x.imag);
379     mpfi_mul(z.real, a.real, b.real);
380
381     mpfi_cos(a.real, x.real);
382     mpfi_sinh(b.real, x.imag);
383     mpfi_mul(z.imag, a.real, b.real);
384
385     mpfi_clear(a.real);
386     mpfi_clear(b.real);
387
388     return z;
389 }
390
391 complexi comp_cos (complexi x) {
392     /* Computes complex cosine */
393     complexi z;
394     real a, b, one;
395
396     mpfi_init2(one.real, prec);
397     mpfi_set_d(one.real, -1);
398     z = comp_init_c(0);
399
400     mpfi_init2(a.real, prec);
401     mpfi_init2(b.real, prec);
402
403     mpfi_cos(a.real, x.real);
404     mpfi_cosh(b.real, x.imag);
405     mpfi_mul(z.real, a.real, b.real);
```

```

406
407     mpfi_sin(a.real, x.real);
408     mpfi_sinh(b.real, x.imag);
409 mpfi_mul(b.real, one.real, b.real);
410     mpfi_mul(z.imag, a.real, b.real);
411
412     mpfi_clear(a.real);
413     mpfi_clear(b.real);
414 mpfi_clear(one.real);
415
416     return z;
417 }
418
419 real real_sin (real x) {
420     /* Calculates the sine of a real interval */
421     real sine;
422
423     mpfi_init2(sine.real, prec);
424
425     mpfi_sin(sine.real, x.real);
426
427     return sine;
428 }
429
430 real real_cos (real x) {
431     /* Calculates the cosine of a real interval */
432     real cosine;
433
434     mpfi_init2(cosine.real, prec);
435
436     mpfi_cos(cosine.real, x.real);
437
438     return cosine;
439 }
440
441 void matrixmult (complexi *z[2][2], complexi *x[2][2], complexi *y[2][2],
442     int N) {
443     /* Multiplies two matrices */
444     int i, j, k, l;
445     complexi p[2][2];
446     for(i=0; i<2; i++)
447         for(j=0; j<2; j++)
448             p[i][j] = comp_init_c(0);
449     for(k=0; k<N; k++) {
450         for(i=0; i<2; i++) {
451             for(j=0; j<2; j++) {
452                 p[i][j] = comp_set_c(0);
453                 for(l=0; l<2; l++){
454                     p[i][j] = comp_add(p[i][j], comp_mul(x[i
455 ] [l][k], y[l][j][k]));

```

```

456         }
457     }
458     for(i= 0; i<2; i++)
459         for(j= 0; j<2; j++)
460             z[i][j][k] = p[i][j];
461     }
462 }
463
464 void matrixvecmul (complexi *r[2], complexi *x[2][2], complexi *v[2], int N
465 ) {
466     /* Multiplies a matrix by a vector */
467     int i, j, k;
468     complexi p[2];
469     for(i=0; i<2; i++)
470         p[i] = comp_init_c(0);
471
472     for(k=0; k<N; k++) {
473         for(i=0; i<2; i++) {
474             p[i] = comp_set_c(0);
475             for(j=0; j<2; j++) {
476                 p[i] = comp_add(p[i], comp_mul(x[i][j][k],
477                     v[j][k]));
478             }
479         }
480         for(i=0; i<2; i++) {
481             r[i][k] = p[i];
482         }
483     }
484 }
485
486 void inverse (complexi *inv[2][2], complexi *a[2][2], int N) {
487     /* Inverts a matrix */
488     int k;
489     complexi det, adj[2][2];
490
491     det = comp_init_c(0);
492     adj[0][0] = comp_init_c(0);
493     adj[0][1] = comp_init_c(0);
494     adj[1][0] = comp_init_c(0);
495     adj[1][1] = comp_init_c(0);
496
497     for(k=0; k<N; k++) {
498         det = comp_sub(comp_mul(a[0][0][k], a[1][1][k]), comp_mul(a[0][1][k], a
499             [1][0][k]));
500         adj[0][0] = a[1][1][k];
501         adj[1][1] = a[0][0][k];
502         adj[0][1] = comp_sc_mul(-1, a[1][0][k]);
503         adj[1][0] = comp_sc_mul(-1, a[0][1][k]);
504         inv[0][0][k] = comp_div(adj[0][0], det);
505         inv[1][1][k] = comp_div(adj[1][1], det);
506         inv[1][0][k] = comp_div(adj[0][1], det);
507         inv[0][1][k] = comp_div(adj[1][0], det);

```

```
505     }
506 }
507
508 complexi comp_exp (real x) {
509     /* Calculates the complex exponential */
510     complexi compexp;
511
512     compexp = comp_init_c(0);
513
514     mpfi_cos(compexp.real, x.real);
515     mpfi_sin(compexp.imag, x.real);
516
517     return compexp;
518 }
519
520 real real_exp (real x) {
521     /* Calculates the real exponential */
522     real exp;
523
524     mpfi_init2(exp.real, prec);
525
526     mpfi_exp(exp.real, x.real);
527
528     return exp;
529 }
530
531 void dft (complexi *coef, complexi *grid, int N) {
532     /* Discrete Fourier Transform */
533     int j, k;
534     complexi sum, compexp;
535     compexp = comp_init_c(0);
536     for(k=0; k<N; k++){
537         sum = comp_init_c(0.);
538         for(j=0; j<N; j++) {
539             compexp = comp_exp(real_sc_mul(-2.0*k*j/N, PI)); /* Note: -2*k*j/N is
                    perfectly represented by the computer, but the product by PI is
                    not */
540             sum = comp_add(sum, comp_mul(grid[j], compexp));
541         }
542         coef[k] = comp_sc_mul(1./N, sum); /* Note: 1/N is perfectly
                    represented by the computer */
543         comp_clear(sum);
544     }
545     comp_clear(compexp);
546 }
547
548 void idft (complexi *grid, complexi *coef, int N) {
549     /* Inverse Discrete Fourier Transform */
550     int j, k;
551     complexi sum, compexp;
552     compexp = comp_init_c(0);
553     for(k=0; k<N; k++){
```

```

554         sum = comp_init_c(0.);
555         for(j=N/2; j<N; j++){
556             compexp = comp_exp(real_sc_mul(2.0*k*j/N, PI));
557             sum = comp_add(sum, comp_mul(coef[j], compexp));
558             compexp = comp_exp(real_sc_mul(2.0*k*(N-1-j)/N, PI));
559             sum = comp_add(sum, comp_mul(coef[N-1-j], compexp));
560         }
561         grid[k] = sum;
562         comp_clear(sum);
563     }
564     comp_clear(compexp);
565 }
566
567 void separate (complexi *a, int n) {
568     /* Copies all even elements to lower-half of a[]
569     and all odd elements to upper-half of a[] */
570     complexi b[n/2];
571     int i;
572     for(i=0; i<n/2; i++) {
573         b[i] = comp_init_c(0);
574         b[i] = a[i*2+1];
575     }
576     for(i=0; i<n/2; i++)
577         a[i] = a[i*2];
578     for(i=0; i<n/2; i++) {
579         a[i+n/2] = b[i];
580     }
581 }
582
583 void _fft (complexi *X, int N) {
584     /* Fast Fourier Transform */
585     int k;
586     complexi e, o, w;
587
588     e = comp_init_c(0);
589     o = comp_init_c(0);
590     w = comp_init_c(0);
591
592     if(N<2){
593
594     }else{
595         separate(X, N);
596         _fft(X, N/2);
597         _fft(X+N/2, N/2);
598         for(k=0; k<N/2; k++) {
599             e = X[k];
600             o = X[k+N/2];
601             w = comp_exp(real_sc_mul((-2.0*k)/N, PI));
602             X[k] = comp_add(comp_reali_mul(real_div(one, two), e), comp_mul(w,
                comp_reali_mul(real_div(one, two), o)));
603             X[k+N/2] = comp_sub(comp_reali_mul(real_div(one, two), e), comp_mul(w
                , comp_reali_mul(real_div(one, two), o)));

```

```

604     }
605 }
606 }
607
608 void fft (complexi *coef, complexi *grid, int N) {
609     /* Copies vectors and applies Fast Fourier Transform */
610     int k;
611     for (k=0; k<N; k++){
612         coef[k] = grid[k];
613     }
614     _fft(coef, N);
615 }
616
617 void _ifft (complexi *X, int N){
618     /* Inverse Fast Fourier Transform */
619     int k;
620     complexi e, o, w;
621
622     e = comp_init_c(0);
623     o = comp_init_c(0);
624     w = comp_init_c(0);
625
626     if(N<2){
627
628     }else{
629         separate(X, N);
630         _ifft(X, N/2);
631         _ifft(X+N/2, N/2);
632         for(k=0; k<N/2; k++) {
633             e = X[k];
634             o = X[k+N/2];
635             w = comp_exp(real_sc_mul((2.0*k)/N, PI));
636             X[k] = comp_add(e, comp_mul(w, o));
637             X[k+N/2] = comp_sub(e, comp_mul(w, o));
638         }
639     }
640 }
641
642 void ifft (complexi *grid, complexi *coef, int N){
643     /* Copies vectors and applies inverse Fast Fourier Transform */
644     int k;
645     for(k=0; k<N; k++){
646         grid[k] = coef[k];
647     }
648     _ifft(grid, N);
649 }
650
651 real real_sup (real x, real y) {
652     /* Finds the supremum of two real intervals */
653     real sup1, sup2;
654     mpfr_t sup1r, sup2r;
655     int n;

```

```

656
657 mpfr_init2(sup1r, prec);
658 mpfr_init2(sup2r, prec);
659
660     mpfi_init2(sup1.real, prec);
661     mpfi_init2(sup2.real, prec);
662
663     sup1 = real_abs(x);
664     sup2 = real_abs(y);
665
666 mpfi_get_right(sup1r, sup1.real);
667 mpfi_get_right(sup2r, sup2.real);
668
669 n = mpfr_cmp(sup1r, sup2r);
670
671     if(n < 0) {
672         return sup2;
673     } else {
674         return sup1;
675     }
676 }
677
678 void F (complexi *FK[2], complexi *K[2], real b, real e, int N) {
679     /* Calculates the image through the Standard Map */
680     int j;
681     real sin;
682     mpfi_init2(sin.real, prec);
683     complexi sine;
684     sine = comp_init_c(0);
685     for(j=0; j<N; j++){
686         sin = real_mul(e, real_sin(real_sc_mul((1.*j)/N, DPI)));
687         mpfi_set(sine.real, sin.real);
688         FK[1][j] = comp_sub(K[1][j], comp_add(comp_reali_mul(real_div(b, DPI),
689             comp_sin(comp_reali_mul(DPI, K[0][j]))), sine));
689         FK[0][j] = comp_add(K[0][j], FK[1][j]);
690     }
691 }
692
693 void Fbox (complexi *FK[2], complexi *K[2], real b, real e, int N) {
694     /* Calculates the image through the Standard Map */
695     int j;
696     complexi sine, theta[N];
697
698     for(j=0; j<N; j++) {
699         theta[j] = comp_init_c(0);
700         mpfi_interv_d(theta[j].real, (1.*j)/N-1./(2*N), (1.*j)/N+1./(2*N));
701         mpfi_interv_d(theta[j].imag, -hatrhod, hatrhod);
702     }
703
704     sine = comp_init_c(0);
705
706     for(j=0; j<N; j++){

```

```

707         sine = comp_reali_mul(e, comp_sin(comp_reali_mul(DPI, theta
708             [j]))));
709         FK[1][j] = comp_sub(K[1][j], comp_add(comp_reali_mul(
710             real_div(b, DPI), comp_sin(comp_reali_mul(DPI, K[0][j])
711             )), sine));
712         FK[0][j] = comp_add(K[0][j], FK[1][j]);
713     }
714 }
715
716 void difmatrix(complexi *dif[2][2], complexi *K[2], real b, int N){
717     /* Evaluates the differential matrix of the Standard Map over K */
718     int k;
719     for(k=0; k<N; k++){
720         dif[0][0][k] = comp_sub(comp_init_c(1), comp_reali_mul(b, comp_cos(
721             comp_reali_mul(DPI, K[0][k]))));
722         dif[0][1][k] = comp_init_c(1);
723         dif[1][1][k] = comp_init_c(1);
724         dif[1][0][k] = comp_reali_mul(real_sc_mul(-1, b), comp_cos(
725             comp_reali_mul(real_sc_mul(2.0, PI), K[0][k])));
726     }
727 }
728
729 real diff2norm (complexi *K[2], real b, int N){
730     /* Evaluates the second differential matrix of the Standard Map
731     over K */
732     int k;
733     real norm, sup;
734     mpfi_init2(norm.real, prec);
735     mpfi_init2(sup.real, prec);
736     mpfi_set_d(sup.real, 0);
737     for(k=0; k<N; k++){
738         norm = comp_mod(comp_reali_mul(real_mul(DPI, b), comp_sin(
739             comp_reali_mul(DPI, K[0][k]))));
740         sup = real_sup(sup, norm);
741     }
742     return sup;
743 }
744
745 real mu (real delta, int N) {
746     real a, b;
747     mpfi_init2(a.real, prec);
748     mpfi_init2(b.real, prec);
749     a = real_sc_mul(2.0, real_exp(real_mul(PI, delta)));
750     b = real_add(real_exp(real_sc_mul(2.0, real_mul(PI, delta))), one);
751     if(N%2 == 0) {
752         return one;
753     } else {
754         return real_div(a, b);
755     }
756 }

```

```

752 real CN (real rho, real hat, int N) {
753     /* Calculation of C_N Fourier error bound */
754     real S1, S2, T, a, b, c;
755
756     mpfi_init(S1.real);
757     mpfi_init(S2.real);
758     mpfi_init(T.real);
759     mpfi_init(a.real);
760     mpfi_init(b.real);
761     mpfi_init(c.real);
762
763     a = real_div(real_exp(real_sc_mul(-2.0*N, real_mul(PI, hat))), real_sub(
764         one, real_exp(real_sc_mul(-2.0*N, real_mul(PI, hat))));
765     b = real_div(real_add(real_exp(real_sc_mul(-2.0, real_mul(PI, real_add(
766         hat, rho)))), one), real_sub(real_exp(real_sc_mul(-2.0, real_mul(PI,
767         real_add(hat, rho))), one));
768     c = real_sub(one, real_mul(mu(real_sub(real_sc_mul(-1, hat), rho), N),
769         real_exp(real_sc_mul(N, real_mul(PI, real_add(hat, rho))))));
770     S1 = real_mul(a, b);
771     S1 = real_mul(S1, c);
772
773     b = real_div(real_add(real_exp(real_sc_mul(2.0, real_mul(PI, real_sub(hat
774         , rho)))), one), real_sub(real_exp(real_sc_mul(2.0, real_mul(PI,
775         real_sub(hat, rho))), one));
776     c = real_sub(one, real_mul(mu(real_sub(real_sc_mul(1, hat), rho), N),
777         real_exp(real_sc_mul(-N, real_mul(PI, real_sub(hat, rho))))));
778     S2 = real_mul(a, b);
779     S2 = real_mul(S2, c);
780
781     c = real_mul(mu(real_sub(real_sc_mul(1, hat), rho), N), real_exp(
782         real_sc_mul(-N, real_mul(PI, real_sub(hat, rho))));
783     T = real_mul(b, c);
784
785     return real_add(S1, real_add(S2, T));
786 }
787
788 void comp_add_v (complexi *s, complexi *x, complexi *y, int N) {
789     /* Sum of vectors */
790     int k;
791     for(k=0; k<N; k++)
792         s[k]= comp_add(x[k], y[k]);
793 }
794
795 void comp_sub_v (complexi *r, complexi *x, complexi *y, int N) {
796     /* Substraction of vectors */
797     int k;
798     for(k=0; k<N; k++)
799         r[k]= comp_sub(x[k], y[k]);
800 }
801
802 void comp_mul_v (complexi *m, complexi *x, complexi *y, int N) {
803     /* Product of vectors component-wise */

```

```

796     int k;
797     for(k=0; k<N; k++)
798         m[k]= comp_mul(x[k], y[k]);
799 }
800
801 void fourierrot(complexi *xrot, complexi *x, real om, int N){
802     /* Rotates the Fourier coefficients */
803     int k;
804     complexi compexp;
805     compexp = comp_init_c(0);
806     for(k=0; k<N/2; k++) {
807         compexp = comp_exp(real_sc_mul(k, real_mul(DPI, om)));
808         xrot[k] = comp_mul(x[k], compexp);
809     }
810     for(k=N/2; k<N; k++) {
811         compexp = comp_exp(real_sc_mul((k-N), real_mul(DPI, om)));
812         xrot[k] = comp_mul(x[k], compexp);
813     }
814 }
815
816 void fourierrot_c_m (complexi *frotx[2][2], complexi *fx[2][2], complexi
817     phi, int N) {
818     /* Rotates a matrix by a complex factor */
819     real aux;
820     complexi *mat[2][2];
821     int i;
822
823     allocm(mat, N);
824
825     comp_init_m(mat, N);
826
827     mpfi_init2(aux.real, prec);
828
829     mpfi_mul(aux.real, DPI.real, phi.imag);
830
831     for(i=0; i<N; i++) {
832         if(i < N/2) {
833             mat[0][0][i] = comp_reali_mul(real_div(one,
834                 real_exp(real_sc_mul(i, aux))), fx[0][0][i]);
835             mat[0][1][i] = comp_reali_mul(real_div(one,
836                 real_exp(real_sc_mul(i, aux))), fx[0][1][i]);
837             mat[1][0][i] = comp_reali_mul(real_div(one,
838                 real_exp(real_sc_mul(i, aux))), fx[1][0][i]);
839             mat[1][1][i] = comp_reali_mul(real_div(one,
840                 real_exp(real_sc_mul(i, aux))), fx[1][1][i]);
841         } else {
842             mat[0][0][i] = comp_reali_mul(real_div(one,
843                 real_exp(real_sc_mul((i-N), aux))), fx[0][0][i
844                 ]);
845             mat[0][1][i] = comp_reali_mul(real_div(one,
846                 real_exp(real_sc_mul((i-N), aux))), fx[0][1][i
847                 ]);

```

```

839         mat[1][0][i] = comp_reali_mul(real_div(one,
            real_exp(real_sc_mul((i-N), aux))), fx[1][0][i
            ]);
840         mat[1][1][i] = comp_reali_mul(real_div(one,
            real_exp(real_sc_mul((i-N), aux))), fx[1][1][i
            ]);
841     }
842 }
843 }
844
845     mpfi_set(aux.real, phi.real);
846
847     fourierrot(frotx[0][0], mat[0][0], aux, N);
848     fourierrot(frotx[0][1], mat[0][1], aux, N);
849     fourierrot(frotx[1][0], mat[1][0], aux, N);
850     fourierrot(frotx[1][1], mat[1][1], aux, N);
851 }
852
853 void fourierrot_c_v (complexi *frotx[2], complexi *fx[2], complexi phi, int
    N) {
854     /* Rotates a vector by a complex factor */
855     real aux;
856     complexi *vec[2];
857     int i;
858
859     allocv(vec, N);
860
861     comp_init_v(vec, N);
862
863     mpfi_init2(aux.real, prec);
864
865     mpfi_mul(aux.real, DPI.real, phi.imag);
866
867     for(i=0; i<N; i++) {
868         if(i < N/2) {
869             vec[0][i] = comp_reali_mul(real_div(one, real_exp(
                real_sc_mul(i, aux))), fx[0][i]);
870             vec[1][i] = comp_reali_mul(real_div(one, real_exp(
                real_sc_mul(i, aux))), fx[1][i]);
871         } else {
872             vec[0][i] = comp_reali_mul(real_div(one, real_exp(
                real_sc_mul((i-N), aux))), fx[0][i]);
873             vec[1][i] = comp_reali_mul(real_div(one, real_exp(
                real_sc_mul((i-N), aux))), fx[1][i]);
874
875         }
876     }
877
878     mpfi_set(aux.real, phi.real);
879
880     fourierrot(frotx[0], vec[0], aux, N);
881     fourierrot(frotx[1], vec[1], aux, N);

```

```

882
883 }
884
885
886 void matrixgf (complexi *coef[2][2], complexi *grid[2][2], int N) {
887     /* Transforms an array of matrices evaluated over a grid into
888        matrices of Fourier coefficients */
889     fft(coef[0][0], grid[0][0], N);
890     fft(coef[0][1], grid[0][1], N);
891     fft(coef[1][0], grid[1][0], N);
892     fft(coef[1][1], grid[1][1], N);
893 }
894
895 void matrixfg (complexi *grid[2][2], complexi *coef[2][2], int N) {
896     /* Transforms an array of matrices evaluated over a grid into
897        matrices of Fourier coefficients */
898     ifft(grid[0][0], coef[0][0], N);
899     ifft(grid[0][1], coef[0][1], N);
900     ifft(grid[1][0], coef[1][0], N);
901     ifft(grid[1][1], coef[1][1], N);
902 }
903
904 real fournorm (complexi *coef, real rho, int N) {
905     real sum;
906     int i;
907
908     mpfi_init2(sum.real, prec);
909     mpfi_set_d(sum.real, 0);
910
911     for(i=0; i<N; i++) {
912         if(i<N/2){
913             sum = real_add(sum, real_mul(real_exp(real_sc_mul(2.01*fabs(i),
914                 real_mul(PI, rho))), comp_mod(coef[i])));
915         } else {
916             sum = real_add(sum, real_mul(real_exp(real_sc_mul(2.01*fabs(i-N),
917                 real_mul(PI, rho))), comp_mod(coef[i])));
918         }
919     }
920 }
921
922 return sum;
923 }
924
925 real fournorm_v (complexi *x[2], real rho, int N) {
926     real a, b;
927     mpfi_init2(a.real, prec);
928     mpfi_init2(b.real, prec);
929     a = real_abs(fournorm(x[0], rho, N));
930     b = real_abs(fournorm(x[1], rho, N));
931
932     if(a.real <= b.real) {
933         return b;
934     } else {

```

```

930             return a;
931     }
932 }
933
934 real fournorm_m (complexi *x[2][2], real rho, int N) {
935     real sum1, sum2;
936
937     mpfi_init2(sum1.real, prec);
938     mpfi_init2(sum2.real, prec);
939
940     sum1 = real_add(fournorm(x[0][0], rho, N), fournorm(x[0][1], rho, N));
941     sum2 = real_add(fournorm(x[1][0], rho, N), fournorm(x[1][1], rho, N));
942
943     return real_sup(sum1, sum2);
944 }
945
946 real supnorm (complexi *x, int N) {
947     int i, n;
948     mpfr_t supr, modr;
949     real sup, mod;
950
951     mpfr_init2(supr, prec);
952     mpfr_init2(modr, prec);
953
954     mpfi_init2(sup.real, prec);
955     mpfi_set_d(sup.real, 0);
956     mpfi_init2(mod.real, prec);
957
958     for(i=0; i<N; i++) {
959         mod = comp_mod(x[i]);
960
961         mpfi_get_right(supr, sup.real);
962         mpfi_get_right(modr, mod.real);
963
964         n = mpfr_cmp(supr, modr);
965         if(n < 0) {
966             mpfi_set(sup.real, mod.real);
967         }
968     }
969     return sup;
970 }
971
972 real supnorm_v (complexi *x[2], int N) {
973     real sup1, sup2;
974     int n;
975     mpfr_t sup1r, sup2r;
976
977     mpfi_init2(sup1.real, prec);
978     mpfi_init2(sup2.real, prec);
979     mpfr_init2(sup1r, prec);
980     mpfr_init2(sup2r, prec);
981

```

```

982     sup1 = supnorm(x[0], N);
983     sup2 = supnorm(x[1], N);
984
985     mpfi_get_right(sup1r, sup1.real);
986     mpfi_get_right(sup2r, sup2.real);
987
988     n = mpfr_cmp(sup1r, sup2r);
989
990     if(n < 0) {
991         return sup2;
992     } else {
993         return sup1;
994     }
995 }
996
997 real supnorm_m (complexi *x[2][2], int N) {
998     real sum1, sum2;
999
1000     mpfi_init2(sum1.real, prec);
1001     mpfi_init2(sum2.real, prec);
1002
1003     sum1 = real_add(supnorm(x[0][0], N), supnorm(x[0][1], N));
1004     sum2 = real_add(supnorm(x[1][0], N), supnorm(x[1][1], N));
1005
1006     return real_sup(sum1, sum2);
1007 }
1008
1009 real comp_sup (complexi x, complexi y) {
1010     real sup1, sup2;
1011
1012     mpfi_init2(sup1.real, prec);
1013     mpfi_init2(sup2.real, prec);
1014
1015     sup1 = comp_mod(x);
1016     sup2 = comp_mod(y);
1017
1018     if(sup1.real <= sup2.real) {
1019         return sup2;
1020     } else {
1021         return sup1;
1022     }
1023 }
1024
1025 int main(){
1026     complexi *K[2], *diff[2][2], *fdiff[2][2], *frotdiff[2][2], *FK[2], *fFK
1027         [2], *fK[2], *frotK[2], *P1[2][2], *fP1[2][2], *frotP1[2][2], *fP2
1028         [2][2], *frotP2[2][2], *P2[2][2],
1029     *Lam[2][2], *fLam[2][2], *vec[2], *auxc[2], *fcopy[2][2], *Id[2][2], *
1030         fI[2][2], *xi[2], phi;
1031     int i, n, N, valh, valr0, valmu, vall;
1032     double *Kc[2], lam0, lam1, *P0[2][2], R = 1.e-4;
1033     FILE *torus;

```

```

1031  real b, e, om, rho, rhohat, inverr, rederr, finverr, fP1norm, fP2norm,
      fdiffnorm, tildeeps, sum[2], *aux[2],
1032      lambda, lams, lamu, lamuinv, lambdap, term1, term2, term3, five,
      kappa, hateps, beta, h, r0, r1, mu, Rinterv, hatlambda, alpha;
1033  mpfr_t bound1, bound2;
1034
1035  /* Initializes 1, 2 and 2*PI */
1036  mpfi_init2(one.real, prec);
1037  mpfi_set_str(one.real, "1", 10);
1038
1039  mpfi_init2(two.real, prec);
1040  mpfi_set_str(two.real, "2", 10);
1041
1042      mpfi_init2(PI.real, prec);
1043      mpfi_atan(PI.real, one.real);
1044
1045      mpfi_mul(PI.real, PI.real, two.real);
1046      mpfi_mul(PI.real, PI.real, two.real);
1047
1048  mpfi_init2(DPI.real, prec);
1049  mpfi_mul(DPI.real, PI.real, two.real);
1050
1051  /* Reads N */
1052      torus = fopen("K0.100000.txt", "r");
1053      if (!torus) {
1054          puts("File Error");
1055      }
1056
1057  fscanf(torus, "%d", &N);
1058  fclose(torus);
1059
1060  /* Allocates vectors */
1061  allocv(K, N);
1062  allocv(vec, N);
1063  allocv(auxc, N);
1064  allocv(fK, N);
1065  allocv(frotK, N);
1066  allocv(xi, N);
1067  allocv(fFK, N);
1068  allocv_real(aux, N);
1069  allocv_d(Kc, N);
1070  allocm_d(P0, N);
1071  allocv(FK, N);
1072  allocm(P1, N);
1073  allocm(fP1, N);
1074  allocm(fP2, N);
1075  allocm(frotP2, N);
1076  allocm(frotP1, N);
1077  allocm(P2, N);
1078  allocm(diff, N);
1079  allocm(fdiff, N);
1080  allocm(frotdiff, N);

```

```

1081     allocm(Lam, N);
1082     allocm(fLam, N);
1083     allocm(fcopy, N);
1084     allocm(Id, N);
1085     allocm(fI, N);
1086
1087     /* Reads grid input and initializes complex intervals */
1088     torus = fopen("KO.100000.txt", "r");
1089     for(i=0; i<N; i++) {
1090         fscanf(torus, "%*d %*f %lf %lf %lf %lf %lf %lf %lf %lf %*f %*f", &Kc
            [0][i], &Kc [1][i], &PO [0][0][i], &PO [0][1][i], &PO [1][0][i], &PO
            [1][1][i], &lam0, &lam1);
1091
1092         K[0][i] = comp_init_c(Kc [0][i]);
1093         K[1][i] = comp_init_c(Kc [1][i]);
1094
1095         P1 [0][0][i] = comp_init_c(PO [0][0][i]);
1096         P1 [0][1][i] = comp_init_c(PO [0][1][i]);
1097         P1 [1][0][i] = comp_init_c(PO [1][0][i]);
1098         P1 [1][1][i] = comp_init_c(PO [1][1][i]);
1099
1100         Lam [0][0][i] = comp_init_c(lam0);
1101         Lam [1][1][i] = comp_init_c(lam1);
1102         Lam [0][1][i] = comp_init_c(0);
1103         Lam [1][0][i] = comp_init_c(0);
1104
1105         Id [0][0][i] = comp_init_c(1);
1106         Id [1][1][i] = comp_init_c(1);
1107         Id [0][1][i] = comp_init_c(0);
1108         Id [1][0][i] = comp_init_c(0);
1109
1110     }
1111
1112     /* Initialize complex and real intervals */
1113     comp_init_v(FK, N);
1114     comp_init_v(fK, N);
1115     comp_init_v(vec, N);
1116     comp_init_v(auxc, N);
1117     comp_init_v(frotK, N);
1118     comp_init_v(fFK, N);
1119     real_init_v(aux, N);
1120     comp_init_m(fP1, N);
1121     comp_init_m(P2, N);
1122     comp_init_m(frotP2, N);
1123     comp_init_m(frotP1, N);
1124     comp_init_m(fP2, N);
1125     comp_init_m(diff, N);
1126     comp_init_m(fdiff, N);
1127     comp_init_m(frotdiff, N);
1128     comp_init_m(fLam, N);
1129     comp_init_m(fcopy, N);
1130     comp_init_m(fI, N);

```

```
1131   comp_init_v(xi, N);
1132   phi = comp_init_c(0);
1133
1134   mpfi_init2(b.real, prec);
1135
1136   mpfi_init2(kappa.real, prec);
1137   mpfi_set_str(kappa.real, "1.3", 10);
1138
1139   mpfi_init2(e.real, prec);
1140   mpfi_set_str(e.real, "0.10", 10);
1141
1142   mpfi_init2(five.real, prec);
1143   mpfi_set_str(five.real, "5", 10);
1144   mpfi_init2(om.real, prec);
1145   om = real_div(real_sub(real_sqrt(five), one), two);
1146
1147   mpfi_init2(rho.real, prec);
1148   mpfi_set_str(rho.real, "1.e-3", 10);
1149
1150   mpfi_init2(rhohat.real, prec);
1151   mpfi_set_str(rhohat.real, "1.e-2", 10);
1152
1153   mpfi_init2(sum[0].real, prec);
1154   mpfi_set_d(sum[0].real, 0);
1155
1156   mpfi_init2(sum[1].real, prec);
1157   mpfi_set_d(sum[1].real, 0);
1158
1159   mpfi_init2(inverr.real, prec);
1160   mpfi_init2(rederr.real, prec);
1161   mpfi_init2(finverr.real, prec);
1162   mpfi_init2(fP1norm.real, prec);
1163   mpfi_init2(fP2norm.real, prec);
1164   mpfi_init2(fdiffnorm.real, prec);
1165   mpfi_init2(tildeeps.real, prec);
1166   mpfi_init2(lams.real, prec);
1167   mpfi_init2(lamu.real, prec);
1168   mpfi_init2(lambdap.real, prec);
1169   mpfi_init2(lamuinv.real, prec);
1170   mpfi_init2(lambda.real, prec);
1171   mpfi_init2(hateps.real, prec);
1172   mpfi_init2(beta.real, prec);
1173   mpfi_init2(h.real, prec);
1174   mpfi_init2(r0.real, prec);
1175   mpfi_init2(r1.real, prec);
1176   mpfi_init2(mu.real, prec);
1177   mpfi_init2(term1.real, prec);
1178   mpfi_init2(term2.real, prec);
1179   mpfi_init2(term3.real, prec);
1180   mpfi_init2(Rinterv.real, prec);
1181   mpfi_set_str(Rinterv.real, "1.e-4", 10);
1182   mpfi_init2(hatlambda.real, prec);
```

```

1183     mpfi_init2(alpha.real, prec);
1184
1185     mpfr_init2(bound1, prec);
1186     mpfr_init2(bound2, prec);
1187
1188
1189     /* Invariance Error */
1190
1191     /* The inputs of the algorithm are in Fourier space, but given our input
1192        is in grid space
1193      * we will first transform them into Fourier series */
1194
1195     /* Since the eigenvalues are swapped, we change them back */
1196     for(i=0; i<N; i++) {
1197         fcopy[0][0][i] = Lam[0][0][i];
1198         Lam[0][0][i] = Lam[1][1][i];
1199         Lam[1][1][i] = fcopy[0][0][i];
1200     }
1201
1202     matrixgf(fP1, P1, N);
1203     matrixgf(fLam, Lam, N);
1204
1205     fft(fK[0], K[0], N);
1206     fft(fK[1], K[1], N);
1207
1208     /* We must set the Nyquist term to 0 */
1209     fP1[0][0][N/2] = comp_set_c(0);
1210     fP1[0][1][N/2] = comp_set_c(0);
1211     fP1[1][0][N/2] = comp_set_c(0);
1212     fP1[1][1][N/2] = comp_set_c(0);
1213
1214     fLam[0][0][N/2] = comp_set_c(0);
1215     fLam[0][1][N/2] = comp_set_c(0);
1216     fLam[1][0][N/2] = comp_set_c(0);
1217     fLam[1][1][N/2] = comp_set_c(0);
1218
1219     fK[0][N/2] = comp_set_c(0);
1220     fK[1][N/2] = comp_set_c(0);
1221
1222     /* We will take as the first P2 the inverse of P1, for that we will have
1223        to come back
1224      * to grid space and invert, since P2 is the approximate inverse by
1225        hypothesis, we
1226      * won't mind the inversion error produced by Fourier transforming */
1227     matrixfg(P1, fP1, N);
1228     inverse(P2, P1, N);
1229     matrixgf(fP2, P2, N);
1230
1231     fP2[0][0][N/2] = comp_set_c(0);
1232     fP2[0][1][N/2] = comp_set_c(0);
1233     fP2[1][0][N/2] = comp_set_c(0);

```

```

1232         fP2[1][1][N/2] = comp_set_c(0);
1233
1234     /* Rotate K and P2 in Fourier space */
1235     fourierrot(frotK[0], fK[0], om, N);
1236     fourierrot(frotK[1], fK[1], om, N);
1237
1238     fourierrot(frotP2[0][0], fP2[0][0], om, N);
1239     fourierrot(frotP2[0][1], fP2[0][1], om, N);
1240     fourierrot(frotP2[1][0], fP2[1][0], om, N);
1241     fourierrot(frotP2[1][1], fP2[1][1], om, N);
1242
1243     /* In order to operate on the grid, we must use our Fourier objects and
1244        transform them */
1244     ifft(K[0], fK[0], N);
1245     ifft(K[1], fK[1], N);
1246
1247     F(FK, K, kappa, e, N);
1248
1249     /* Save non-inflated K for next step */
1250     difmatrix(diff, K, kappa, N);
1251
1252     fft(fFK[0], FK[0], N);
1253     fft(fFK[1], FK[1], N);
1254
1255     for(i=0; i<N; i++) {
1256         auxc[0][i] = comp_sub(fFK[0][i], frotK[0][i]);
1257         auxc[1][i] = comp_sub(fFK[1][i], frotK[1][i]);
1258     }
1259
1260     tildeeps =ournorm_v(auxc, rho, N);
1261
1262     fP2norm =ournorm_m(frotP2, rho, N);
1263
1264     /* Inflate K so we can calculate the norm of FK */
1265     mpfi_interv_d(phi.real, (double) -1/(2*N), (double) 1/(2*N));
1266     mpfi_interv_d(phi.imag, -hatrhod, hatrhod);
1267
1268     fourierrot_c_v(frotK, fK, phi, N);
1269
1270     ifft(auxc[0], frotK[0], N);
1271     ifft(auxc[1], frotK[1], N);
1272
1273     /* Calculate the image through the standard map using complex boxes */
1274     Fbox(FK, auxc, kappa, e, N);
1275
1276     term1 =ournorm_v(FK, N);
1277
1278     inverr = real_add(real_mul(CN(rho, rhohat, N), term1), tildeeps);
1279
1280     inverr = real_mul(fP2norm, inverr);
1281
1282     printf("CN(rho, rhohat): ");

```

```

1283   real_print(CN(rho, rhohat, N));
1284
1285   printf("Invariance error: ");
1286   real_print(inverr);
1287
1288   /* Pick lambda so the norm of the stable block of Lamda and the norm of
1289      the inverse of the unstable
1290      * block are bounded by such lambda */
1290   for(i=0; i<N; i++) {
1291       fcopy[0][0][i] = fLam[0][0][i];
1292       fcopy[0][1][i] = fLam[0][1][i];
1293       fcopy[1][0][i] = fLam[1][0][i];
1294       fcopy[1][1][i] = fLam[1][1][i];
1295   }
1296
1297   lams =ournorm(fLam[0][0], rho, N);
1298   lamu =ournorm(fLam[1][1], rhohat, N);
1299   matrixfg(Lam, fLam, N);
1300   inverse(fcopy, Lam, N);
1301   matrixgf(fcopy, fcopy, N);
1302   lamuinv =ournorm(fcopy[1][1], rhohat, N);
1303   lambda = lams;
1304
1305   lambdap = real_add(real_div(real_mul(CN(rho, rhohat, N), real_mul(lamu,
1306       real_mul(lamuinv, lamuinv))), real_sub(one, real_mul(CN(rho, rhohat,
1307       N), real_mul(lamu, lamuinv)))), lamuinv);
1306
1307   mpfi_get_right(bound1, lambdap.real);
1308   mpfi_get_right(bound2, lambda.real);
1309   n = mpfr_cmp(bound1, bound2);
1310   if(n > 0) {
1311       lambda = lambdap;
1312   }
1313
1314   printf("Lambda: ");
1315   real_print(lambda);
1316
1317   /* Reducibility error */
1318   for(i=0; i<N; i++) {
1319       fcopy[0][0][i] = Lam[0][0][i];
1320       Lam[0][0][i] = Lam[1][1][i];
1321       Lam[1][1][i] = fcopy[0][0][i];
1322   }
1323
1324   /* Move to grid space to multiply the differential and P1 and come back
1325      to Fourier space */
1325   matrixgf(fLam, Lam, N);
1326       matrixfg(P2, frotP2, N);
1327       matrixmult(fcopy, diff, P1, N);
1328       matrixmult(fcopy, P2, fcopy, N);
1329       matrixgf(fcopy, fcopy, N);
1330

```

```

1331     for(i=0; i<N; i++) {
1332         fcopy[0][0][i] = comp_sub(fcopy[0][0][i], fLam[0][0][i]);
1333         fcopy[0][1][i] = comp_sub(fcopy[0][1][i], fLam[0][1][i]);
1334         fcopy[1][0][i] = comp_sub(fcopy[1][0][i], fLam[1][0][i]);
1335         fcopy[1][1][i] = comp_sub(fcopy[1][1][i], fLam[1][1][i]);
1336     }
1337
1338     term1 =ournorm_m(fcopy, rho, N);
1339
1340     /* Calculate differential with inflated torus with hatrho */
1341     difmatrix(diff, auxc, kappa, N);
1342
1343     fP2norm =ournorm_m(frotP2, rhohat, N);
1344     fP1norm =ournorm_m(fP1, rhohat, N);
1345     fdiffnorm = supnorm_m(diff, N);
1346
1347     term2 = real_mul(CN(rho, rhohat, N), real_mul(fP2norm, real_mul(fdiffnorm
1348         , fP1norm)));
1349
1350     rederr = real_add(term1, term2);
1351
1352     printf("Reducibility Error: ");
1353     real_print(rederr);
1354
1355     /* Inversion Error */
1356     inverse(P2, P1, N);
1357     matrixmult(fcopy, P2, P1, N);
1358     matrixgf(fcopy, fcopy, N);
1359     matrixgf(fI, Id, N);
1360
1361     for(i=0; i<N; i++) {
1362         fcopy[0][0][i] = comp_sub(fcopy[0][0][i], fI[0][0][i]);
1363         fcopy[1][1][i] = comp_sub(fcopy[1][1][i], fI[1][1][i]);
1364     }
1365
1366     term1 = real_mul(CN(rho, rhohat, N), real_mul(ournorm_m(fP2, rhohat, N),
1367         ournorm_m(fP1, rhohat, N)));
1368
1369     term2 =ournorm_m(fcopy, rho, N);
1370
1371     finverr = real_add(term1, term2);
1372
1373     printf("Inversion Error: ");
1374     real_print(finverr);
1375
1376     /* Norm of B */
1377     for(i=0; i<N; i++) {
1378         mpfi_interv_d(xi[0][i].real, -R, R);
1379         mpfi_interv_d(xi[0][i].imag, -R, R);
1380         mpfi_interv_d(xi[1][i].real, -R, R);
1381         mpfi_interv_d(xi[1][i].imag, -R, R);
1382     }

```

```

1381
1382  /* Extend each theta by 1/2N the real part, and rho the imaginary part */
1383  mpfi_interv_d(phi.real, (double) -1/(2*N), (double) 1/(2*N));
1384  mpfi_interv_d(phi.imag, -rhod, rhod);
1385
1386  fourierrot_c_v(frotK, fK, phi, N);
1387
1388  fourierrot_c_m(frotP1, fP1, phi, N);
1389
1390  /* Calculate z */
1391  matrixfg(fcopy, frotP1, N);
1392  matrixvecmul(vec, fcopy, xi, N);
1393  comp_add_v(auxc[0], vec[0], auxc[0], N);
1394  comp_add_v(auxc[1], vec[1], auxc[1], N);
1395
1396  /* Calculate the norm of the second differential */
1397  term2 = diff2norm(auxc, kappa, N);
1398
1399  matrixgf(fP2, P2, N);
1400  fourierrot(frotP2[0][0], fP2[0][0], om, N);
1401  fourierrot(frotP2[0][1], fP2[0][1], om, N);
1402  fourierrot(frotP2[1][0], fP2[1][0], om, N);
1403  fourierrot(frotP2[1][1], fP2[1][1], om, N);
1404  fP2norm =ournorm_m(frotP2, rho, N);
1405
1406  matrixgf(fP1, P1, N);
1407  fP1norm =ournorm_m(fP1, rho, N);
1408
1409  b = real_mul(fP2norm, real_mul(term2, real_mul(fP1norm, fP1norm)));
1410  printf("b: ");
1411  real_print(b);
1412
1413  /* Calculation of constants */
1414  term1 = real_add(lambda, real_add(rederr, finverr));
1415  mpfi_get_right(bound1, term1.real);
1416  mpfi_get_left(bound2, one.real);
1417  n = mpfr_cmp(bound1, bound2);
1418  if(n < 0) {
1419  printf("lambda + sigma + tau < 1\n\n");
1420  vall = 1;
1421  } else {
1422  printf("lambda + sigma + tau >= 1, condition not satisfied\n\n");
1423  }
1424
1425  hateps = real_div(inverr, real_sub(one, real_add(lambda, real_add(rederr,
    finverr))));
1426
1427  beta = real_div(b, real_sub(one, real_add(lambda, real_add(rederr,
    finverr))));
1428
1429  h = real_mul(hateps, beta);
1430

```

```

1431     printf("h: ");
1432     real_print(h);
1433
1434     mpfi_get_right(bound1, h.real);
1435     term1 = real_div(one, two);
1436     mpfi_get_left(bound2, term1.real);
1437     n = mpfr_cmp(bound1, bound2);
1438     if(n < 0) {
1439         printf("h < 1/2\n\n");
1440         valh = 1;
1441     } else {
1442         printf("h >= 1/2, condition not satisfied\n\n");
1443     }
1444
1445     r0 = real_mul(real_div(real_sub(one, real_sqrt(real_sub(one, real_mul(two
        , h)))), h), hateps);
1446
1447     printf("r0: ");
1448     real_print(r0);
1449     mpfi_get_right(bound1, r0.real);
1450     mpfi_get_left(bound2, term1.real);
1451     n = mpfr_cmp(bound1, bound2);
1452     if(n < 0) {
1453         printf("r0 < R\n\n");
1454         valr0 = 1;
1455     } else {
1456         printf("r0 >= R, condition not satisfied\n\n");
1457     }
1458
1459     hatlambda = supnorm_m(Lam, N);
1460     mu = real_mul(real_div(lambda, real_sub(one, real_mul(lambda, lambda))),
        real_mul(real_div(one, real_sub(one, finverr)), real_add(real_mul(b,
        r0), real_add(rederr, real_mul(hatlambda, finverr))));
1461     printf("mu: ");
1462     real_print(mu);
1463
1464     mpfi_get_right(bound1, mu.real);
1465     term1 = real_div(one, real_add(one, real_sqrt(two)));
1466     mpfi_get_left(bound2, term1.real);
1467     n = mpfr_cmp(bound1, bound2);
1468     if(n < 0) {
1469         printf("mu < 1/(1+sqrt(2))\n\n");
1470         valmu = 1;
1471     } else {
1472         printf("mu >= 1/(1+sqrt(2)), condition not satisfied\n\n");
1473     }
1474
1475     if((vall == 1) && (valh == 1) && (valr0 == 1) && (valmu == 1)) {
1476         printf("\nCongratulations, there exists a hyperbolic invariant torus
            with invariant subbundles. \nMoreover, it is unique within a radius
            ");

```

```

1477     r1 = real_mul(real_div(real_add(one, real_sqrt(real_sub(one, real_mul(
1478         two, h))))), h), hateps);
1478     mpfi_get_left(bound1, r1.real);
1479     mpfi_get_left(bound2, Rinterv.real);
1480     n = mpfr_cmp(bound1, bound2);
1481     if(n < 0) {
1482         mpfr_out_str(stdout, 10, 0, bound1, MPFR_RNDD);
1483     } else {
1484         mpfr_out_str(stdout, 10, 0, bound2, MPFR_RNDD);
1485     }
1486     printf("\n and it is contained within a radius ");
1487     mpfi_get_right(bound1, r0.real);
1488     mpfr_out_str(stdout, 10, 0, bound1, MPFR_RNDD);
1489     printf(".\n What's more, the distance between approximately invariant
1490         bundles \nand the invariant bundles is smaller than ");
1490
1491     term1 = real_sub(one, real_mul(two, mu));
1492
1493     term2 = real_sqrt(real_sub(real_sub(one, real_mul(real_mul(two, two),
1494         mu)), real_mul(real_mul(two, two), real_mul(mu, mu))));
1494
1495     term3 = real_mul(two, mu);
1496
1497     alpha = real_div(term3, real_add(term1, term2));
1498
1499     mpfi_get_right(bound1, alpha.real);
1500
1501     mpfr_out_str(stdout, 10, 0, bound1, MPFR_RNDD);
1502
1503     printf("\n");
1504 } else {
1505     printf("The initial torus does not meet the requirements \nto ensure
1506         the existence of an invariant torus\n");
1506 }
1507
1508     freev(K);
1509         freev(vec);
1510         freev(auxc);
1511         freev(fK);
1512         freev(frotK);
1513         freev(xi);
1514         freev(fFK);
1515     freev(FK);
1516     freem(P1);
1517         freem(fP1);
1518         freem(fP2);
1519         freem(frotP2);
1520         freem(frotP1);
1521         freem(P2);
1522         freem(diff);
1523         freem(fdiff);
1524         freem(frotdiff);

```

```
1525         freem(Lam);
1526         freem(fLam);
1527         freem(fcopy);
1528         freem(Id);
1529         freem(fI);
1530
1531     return 0;
1532 }
```

# Bibliography

- [1] Marta Canadell and Àlex Haro. Computation of quasiperiodic normally hyperbolic invariant tori: rigorous results. *Journal of Nonlinear Science*, 27(6):1869–1904, 2017.
- [2] Rafael De La Llave and Rafael Obaya. Regularity of the composition operator in spaces of hölder functions. *Discrete and Continuous Dynamical Systems*, 5:157–184, 1999.
- [3] J-Ll Figueras, Alex Haro, and Alejandro Luque. Rigorous computer-assisted application of kam theory: a modern approach. *Foundations of Computational Mathematics*, 17(5):1123–1193, 2017.
- [4] Alex Haro, Marta Canadell, Jordi-Lluis Figueras, Alejandro Luque, and Josep-Maria Mondelo. The parameterization method for invariant manifolds. *Appl. Math. Sci*, 195, 2016.
- [5] Alex Haro and Rafael de la Llave. A parameterization method for the computation of invariant tori and their whiskers in quasi-periodic maps: numerical algorithms. *Discrete and Continuous Dynamical Systems Series B*, 6(6):1261, 2006.
- [6] Dale Husemoller. *Fibre bundles*, volume 5. Springer, 1966.
- [7] Jake VanderPlas. Understanding the FFT Algorithm. <https://jakevdp.github.io/blog/2013/08/28/understanding-the-fft/>. [Accessed November 26, 2019].
- [8] Ronald T Kneusel. *Numbers and computers*, volume 2. Springer, 2017.
- [9] Rowland, Todd. "Fiber Bundle." From MathWorld—A Wolfram Web Resource. <http://mathworld.wolfram.com/FiberBundle.html>. [Accessed October 5, 2019].
- [10] Rowland, Todd. "Vector Bundle." From MathWorld—A Wolfram Web Resource, created by Eric W. Weisstein. <http://mathworld.wolfram.com/FiberBundle.html>. [Accessed October 5, 2019].
- [11] Eric Sandín Vidal. Quasi-periodic solutions in quasi-periodic systems via fourier transforms. <http://hdl.handle.net/2445/127600>, 2018.
- [12] Silly rabbit at the English Wikipedia. Bundle section. [https://en.wikipedia.org/wiki/File:Bundle\\_section.svg](https://en.wikipedia.org/wiki/File:Bundle_section.svg). [Accessed October 5, 2019].
- [13] Dirk Werner. *Funktionalanalysis*. Springer, 2006.